

Role of Ceramidase in Regulating Hepatic Lipid Metabolism and Whole Body Insulin Sensitivity

APPROVED BY SUPERVISORY COMMITTEE

Philipp E. Scherer, Ph.D.

Perry Bickel, M.D.

William L. Holland, Ph.D.

Jay D. Horton

Joel M. Goodman, Ph.D.

DEDICATION

To my parents Lijun Xia and Zhimin Liang
And my sister Jessica and our dog Toby

Role of Ceramidase in Regulating Hepatic Lipid Metabolism and Whole
Body Insulin Sensitivity

by

Jonathan Y. Xia

DISSERTATION

Presented to the Faculty of the Graduate School of Biomedical Sciences

The University of Texas Southwestern Medical Center at Dallas

In Partial Fulfillment of the Requirements

For the Degree of

DOCTOR OF PHILOSOPHY

The University of Texas Southwestern Medical Center at Dallas

Dallas, Texas

May, 2017

Copyright

by

Jonathan Y. Xia, 2017

All Rights Reserved

ACKNOWLEDGMENTS

I would like to express my sincere and unconditional gratitude to the many people who have made my research training possible, first among them my mentor, Dr. Philipp Scherer, whose patience, generosity, and enthusiasm I hope to emulate in my future career. I am deeply thankful for the opportunity to have trained in such an independent environment and greatly appreciate the time and resources Dr. Scherer invested in my training, and for the many hours I spent in his office discussing, writing, and re-writing our work. I would also like to thank Dr. William Holland for not only providing his intellectual input and technical guidance but also giving his support and friendship during my time in lab.

I thank my committee members Dr. Perry Bickel, Dr. Jay Horton, Dr. William Holland, and Dr. Joel Goodman for challenging me and for the animated and helpful discussions we had during my committee meetings.

The research I performed during my training could not have been accomplished without an immensely helpful network of collaborators. I would like to thank Xiaoli Lin and Estelle Anuwe of the UT Southwestern Metabolic Core for their help in phenotypic characterization of the mice; Dr. Ruth Gordillo and Mackenzie Pearson for providing lipid quantifications through mass spectrometry; Dr. John Shelton for his help in the histology core; Dr. Christine Kusminski for her help in mitochondrial experiments.

I would like to extend a special thank you to Thomas Morely, a fellow MD/PhD student in the lab for answering my technical questions, giving intellectual input, as well as providing support, friendship, and beer tastings.

I am grateful to my colleagues in the lab, past and present, for providing lively discussion during lab meetings and a good lab environment. In particular, I would like to thank Dr. Joseph Rutkowski for answering my never-ending series of questions and always helping me maintain perspective in my projects.

My training would not have been possible without the generous support of the Ruth L. Kirschstein Individual Predoctoral Fellowship for Dual Degree Candidates, afforded to me by the National Institute of Diabetes and Digestive and Kidney Diseases of the National Institutes of Health.

Finally, I would like to thank my family for their constant support and encouragement, particularly from my parents, Lijun and Zhimin, whose love and sacrifice are unparalleled.

Role of Ceramidase in Regulating Hepatic Lipid Metabolism and Whole Body Insulin Sensitivity

Jonathan Y. Xia

The University of Texas Southwestern Medical Center at Dallas, 2017

Philipp E. Scherer, Ph.D.

Concomitant with the rise in obesity, the prevalence of non-alcoholic fatty liver disease (NAFLD), a newly emerging obesity-related disorder, has also been rising steadily. NAFLD is a chronic liver disease that ranges histologically from simple steatosis in its mildest form to non-alcoholic steatohepatitis (NASH) in the more severe form, which is characterized by hepatocyte inflammation and fibrosis. In recent years, sphingolipids have garnered increasing attention for their role in the development of diabetes and metabolic syndrome. Specifically, the accumulation of ceramides in liver was shown to be associated with both hepatic insulin resistance and NAFLD. We recently demonstrated that the adipose-derived secretory factor adiponectin promotes an increase in ceramide catabolism, which is dependent on adiponectin receptors 1 and

2. The associated ceramidase activity promotes ceramide degradation and generation of sphingosine 1-phosphate (S1P). To further investigate the tissue-specific effects of the receptor associated ceramidase activity, we have developed transgenic mice that inducibly express adiponectin receptors 1 and 2 under the control of a tetracycline response element. Hepatic overexpression of adiponectin receptors improved whole body glucose metabolism and prevented hepatic steatosis. Furthermore, we found that catabolism of hepatic ceramides improved insulin signaling in the adipocyte, which suggests the existence of a “cross-talk” between liver and adipose tissue.

TABLE OF CONTENTS

PRIOR PUBLICATIONS	XII
LIST OF FIGURES	XII
LIST OF TABLES	XIV
LIST OF ABBREVIATIONS	XV
CHAPTER 1: Introduction	1
1:1 Lipid induced insulin resistance	1
Role of adipocytes in metabolism	1
Ectopic lipid accumulation	2
References	5
1:2 The adipokine/ceramide axis: key aspects of insulin sensitization	7
Synthesis of ceramides and sphingosine-1-phosphate	7
Sphingolipid synthesis and metabolism	8
Plasma ceramides and insulin resistance	9
Role of sphingolipids in macrophages	11
Role of sphingolipids in hepatocytes	18
Role of sphingolipids in Adipocytes	24
Role of sphingolipids in beta cells	25
Role of sphingolipids in the heart	26
How do leptin, adiponectin, and FGF21 alter sphingolipids	27
"Healthy" adipose tissue rescues systemic ceramide accumulation	29
Concluding remarks	30
References	32
CHAPTER 2: Targeted Induction of ceramide degradation leads to improved systemic metabolism and reduced hepatic steatosis	42
Abstract	43
Introduction	44
Results	46
Discussion	63
Author Contributions	68
Acknowledgements	69

References	70
Methods	75
Figures	81
Supplemental Figures	88
Table	Error! Bookmark not defined.
CHAPTER 3: Inducible overexpression of adiponectin receptors highlight the roles of adiponectin induced ceramidase signaling in lipid and glucose homeostasis	
Abstract	95
Introduction	96
Results	98
Discussion	101
Methods	110
Author Contributions	114
Acknowledgements	119
References	120
Figures	121
Supplemental Figures	124
CHAPTER 4: Conclusions and Future Direction	
Conclusions.....	129
Future Directions	131
Figures	135
	142

PRIOR PUBLICATIONS

Morley TS, Xia JY, Schere PE. 2015. Selective Enhancement of Insulin Sensitivity in the Mature Adipocyte is Sufficient for Systemic Metabolic Improvements.
Nature Communications, In press.

Xia JY, Holland WL, Kusminksi CM, Sun K, Sharma AX, Pearson MJ, Sifuentes AJ, Gordillo R, Scherer PE. 2015. Targeted Induction of Ceramide Degradation Reveals Roles for Ceramides in Non Alcoholic Fatty Liver Disease and Glucose Metabolism in Mice.
Cell Metabolism, In press.

Rutkowski JM, Halberg N, Wang QA, Holland WL, Xia JY, and Scherer PE. 2014.
Differential transendothelial transport of adiponectin complexes.
Cardiovascular Diabetology, (1):47. PMID: 24552349

Xia JY, Morely TS, Scherer PE. The adipokine/ceramide axis: Key aspects of insulin sensitization.
Biochemie, 2013 Aug 20. doi:pii: S0300-9084(13)00283-6.
10.1016/j.biochi.2013.08.013. PMID: 23969158

Ju T, Lanneau GS, Gautam T, Wang Y, Xia B, Stowell SR, Willard MT, Wang W, **Xia JY**, Zuna RE, Laszik Z, Benbrook DM, Hanigan MH, Cummings RD. Human Tumor Antigens Tn and Sialyl Tn Arise from Mutations in Cosmc.
Cancer Research, 68[6], 1636-1646. PMID: 18339842

LIST OF FIGURES

CHAPTER 1

Figure 1: Ceramide synthesis pathway	40
Figure 2: Ceramide target tissues	41

CHAPTER 2

Figure 1: Inducible liver-specific overexpression of acid ceramidase results in significantly reduced C16 ceramide species in the liver and improved total body glucose homeostasis and insulin sensitivity under HFD feeding	81
Figure 2: Liver specific overexpression of acid ceramidase significantly reduced hepatic lipid accumulation and improves adipose tissue metabolic health	82
Figure 3: Inducible adipose specific overexpression of acid ceramidase results reduced in ceramide species in the adipose and improved total body glucose homeostasis and insulin sensitivity under HFD feeding	83
Figure 4: Adipose specific overexpression of acid ceramidase significantly reduces hepatic lipid accumulation and improves adipose tissue metabolic health when challenged with HD	84
Figure 5: Induction of acid ceramidase significantly improves insulin signaling and rescues hepatic steatosis in mice with diet induced obesity	85
Figure 6: Ceramides facilitate lipid uptake by mechanisms involving activation of PKC-zeta and CD36	86
Supplement Figure 1 in support of Fig. 1	88
Supplement Figure 2 in support of Fig. 2	89
Supplement Figure 3 in support of Fig. 3	90
Supplement Figure 4 in support of Fig. 4	91
Supplement Figure 5 in support of Fig. 6	92

CHAPTER THREE

Figure 1: Inducible adipose specific overexpression of AdipoR2 result in systemic improvements in glucose and lipid homeostasis	125
---	-----

Figure 2: Inducible liver specific overexpression of either AdipoR1 or AdipoR2 results in significantly reduced C16 ceramide species in the liver and improved total body glucose homeostasis and reduced lipid accumulation under HFD feeding. 126

Figure 3: The metabolic improvements of adiponectin receptor overexpression in the liver are adiponectin dependant 127

Figure 4: Overexpression of adiponectin receptors, but no acid ceramidase rescues glucose homeostasis in ob/ob mice 128

Supplemental Figure 1 in support of Fig. 1 129

Supplemental Figure 2 in support of Fig. 2 130

CONCLUSIONS AND FUTURE DIRECTION

Figure 1: Hepato-adipo axis of sphingolipid metabolism..... 142

Figure 2: Overexpression of acid ceramidase in glial cells reduces wight gain and improves glucose homeostasis in mice fed HFD 143

LIST OF TABLES

CHAPTER TWO

Table 1: Metabolic data before and during hyperinsulinemic-euglycemic clamp study in WT and AC transgenics	87
Supplemental Table 1: List of qPCR primers used.....	93

LIST OF ABBREVIATIONS

APN – adiponectin
AdipoR – adiponectin receptor
Alb- albumin
AMPK – AMP-activated protein kinase
BAT- brown adipose tissue
C1P – ceramide-1-phosphate
DAG – diacylglycerol
DIO – diet induced obesity
Dox- doxycycline
FFAs- free fatty acids
FGF21- fibroblast growth factor 21
GFAP- glial fibrillary acidic protein
gWAT- gonadal white adipose tissue
het- heterozygous
HFD – high fat diet
HFD-dox – high fat diet with dox
ITT- insulin tolerance test
KO- knockout
mWAT- mesenteric white adipose tissue
mCSF – macrophage colony stimulating factor
NSMase – neutral sphingomyelinase
OGTT- oral glucose tolerance test
LDL – low density lipoprotein
PKC – protein kinase C
PPAR γ – peroxisome proliferator activated receptor
ROS – reactive oxygen species
rtTA- reverse tetracycline transactivator
S1P- sphingosine-1-phosphate
STZ- streptozotocin
SPT – serine palmitoyl-CoA transferase
sWAT- subcutaneous white adipose tissue
TG- triglyceride
TNF- α – tumor necrosis factor alpha
TLR4 – toll like receptor 4
TRE- tetracycline response element
TZD- thiazolidinediones
VLDL –very low density lipoprotein
WT- wildtype

Chapter 1

INTRODUCTION

(The following section contains parts of a manuscript published in *Biochimie* 2014 PMID: 23969158).

1:1 Lipid Induced Insulin Resistance

Individuals with a history of diabetes present with an elevated risk for a number of complications, including hypertension, micro- as well as macrovascular complications, and metabolic syndrome. A major mediator of diabetes, with its associated dysregulation in carbohydrate and lipid metabolism, is the resistance to the actions of the hormone insulin in tissues such as liver, muscle and adipose tissue, with a concomitant unopposed action of glucagon. Here, we review studies in rodents and humans that have influenced our current understanding of the link between ectopic lipid accumulation and insulin resistance.

Role of adipocytes in metabolism

The understanding of adipose tissue function has changed dramatically in the past century. Initially, adipose tissue was thought simply as lipid droplet containing connective tissue that had no role in systemic metabolism. This idea eventually progressed with the discovery that adipocytes was a source of circulating fatty acids during fasting and its lipid droplets were a site of calorie storage. Furthermore, in the 1980s and 1990s, concomitant with the discovery of serum factors such as leptin, TNF- α , and adiponectin, adipose tissue was found to secrete a wide array of unique factors, adipokines, which allow it to act on target organs in an autocrine, paracrine, and endocrine manner (1).

Thus, although it was once viewed simply as a passive reservoir for energy storage, adipose tissue is now recognized as a dynamic endocrine organ that plays an important role in nutrient homeostasis (2). As obesity ascends to epidemic levels in the United States, understanding obesity in terms of adipose tissue dysfunction becomes increasingly important.

Ectopic lipid accumulation

In normal cellular metabolic operations, there is a balance between the production of lipids and their breakdown, either via oxidation or transport. In times of overnutrition, excess calories are stored in white adipocytes. In addition to providing storage space for surplus calories, white adipocytes also minimize lipid accumulation in non-adipose tissues. Adipocytes can facilitate this process through the secretion of the hormone leptin, which can both regulate food intake and enhance the oxidation of excess lipids that may spill into non-adipose tissues. Furthermore, another adipocytes secreted hormone, adiponectin (APN), may also increase fatty acid oxidation in tissues (3, 4). However, too much caloric excess will overburden these compensatory mechanisms and result in a spillover of lipids into non-adipose tissues such as the liver and skeletal muscle. This spillover of lipids in non-adipose tissues is termed “ectopic lipid accumulation,” which can result in a variety of cellular dysfunctions, including insulin resistance (5).

The notion that lipids can cause insulin resistance was first established in the early 1960s when Randle and colleagues demonstrated an inhibitory effect of free fatty acids on glucose uptake in the perfused rat heart (6). Subsequent *in vivo* studies showed that rats infused with lipids for 3-6 hours, to raise plasma FFA concentrations, exhibited reductions in insulin-stimulated glucose transport in muscle, one of the main insulin

responsive tissues, due to decreased insulin signaling (7). These findings were recapitulated in human clinical studies where a lipid infusion in healthy human subjects was capable of inducing insulin resistance and inhibition of whole-body glucose disposal (8). These lipid infusion studies not only showed that lipids can induce insulin resistance in both rodents and humans but also raised the question of whether circulating plasma lipids or lipid accumulation within insulin responsive tissues as the major driver of insulin resistance. Findings in non-obese, non-diabetic human adults found that intramuscular triglyceride content was a strong predictor of muscle insulin resistance compared to serum fatty acids (9). Furthermore, several human studies also demonstrated a strong association between hepatic triglyceride content and hepatic insulin resistance (10). Thus, these studies show that the accumulation of lipid species in insulin responsive tissues is capable of blunting insulin signaling within the tissues and cause metabolic dysfunction.

Previous studies have already correlated intracellular triglyceride content to insulin resistance. Recent findings suggest that other intracellular lipids, mainly diacylglycerol(DAG) and ceramides, play a more major role in mediating insulin resistance at the molecular level (11, 12). In rodents, a high fat diet (HFD) has been shown to increase the concentration of DAG in muscles. Intracellularly, DAGs have been shown to activate novel protein kinase C (PKC) isoforms to impair activation of the insulin receptor (5). A recent study by Holland *et al* showed that rats infused with either lard oil, which is high in saturated fatty acids, or soy oil, which is primarily unsaturated fatty acids, had increased skeletal muscle DAG content along with reduced skeletal muscle glucose uptake, and reduced Akt phosphorylation, a mediator of insulin

intracellular action (13). However, only infusion of lard oil increased intramuscular ceramide content. Interestingly, when intracellular ceramide accumulation was blocked by treatment with myriocin, an inhibitor of *de novo* ceramide synthesis, glucose uptake and Akt phosphorylation were normalized in the lard-infused rats, but not in the soy-infused mice. This study not only showed that saturated and unsaturated fats have differential mechanisms of promoting insulin resistance, but also demonstrated that intracellular accumulation of ceramides can indeed induce insulin resistance in insulin responsive tissues. Thus, the discrepancies between studies that correlate insulin resistance to ceramide accumulation post-lipid infusion and those that do not may be attributed to the ratio of saturated to unsaturated fatty acids in the lipid infusion. Furthermore, since plasma free fatty acids in humans are a mixture of both unsaturated and saturated fatty acids, both mediators probably play a role in mediating peripheral insulin resistance. Foods such as butter, cream, and red meats—all rich in saturated fat but not unsaturated fat—have become a common staple in our Western diet (14). Ceramides are therefore likely to play a more important and clinically relevant role in individuals developing diet-induced obesity in developed nations than previously thought.

References

1. Rosen ED, Spiegelman BM. What we talk about when we talk about fat. *Cell*. 2014;156(1-2):20-44. doi: 10.1016/j.cell.2013.12.012. PubMed PMID: 24439368; PubMed Central PMCID: PMC3934003.
2. Kershaw EE, Flier JS. Adipose tissue as an endocrine organ. *The Journal of clinical endocrinology and metabolism*. 2004;89(6):2548-56. doi: 10.1210/jc.2004-0395. PubMed PMID: 15181022.
3. Unger RH. Longevity, lipotoxicity and leptin: the adipocyte defense against feasting and famine. *Biochimie*. 2005;87(1):57-64. doi: 10.1016/j.biochi.2004.11.014. PubMed PMID: 15733738.
4. Tomas E, Tsao TS, Saha AK, Murrey HE, Zhang Cc C, Itani SI, Lodish HF, Ruderman NB. Enhanced muscle fat oxidation and glucose transport by ACRP30 globular domain: acetyl-CoA carboxylase inhibition and AMP-activated protein kinase activation. *Proceedings of the National Academy of Sciences of the United States of America*. 2002;99(25):16309-13. doi: 10.1073/pnas.222657499. PubMed PMID: 12456889; PubMed Central PMCID: PMC138607.
5. Samuel VT, Shulman GI. Mechanisms for insulin resistance: common threads and missing links. *Cell*. 2012;148(5):852-71. doi: 10.1016/j.cell.2012.02.017. PubMed PMID: 22385956; PubMed Central PMCID: PMC3294420.
6. Randle PJ, Newsholme EA, Garland PB. Regulation of glucose uptake by muscle. 8. Effects of fatty acids, ketone bodies and pyruvate, and of alloxan-diabetes and starvation, on the uptake and metabolic fate of glucose in rat heart and diaphragm muscles. *The Biochemical journal*. 1964;93(3):652-65. PubMed PMID: 4220952; PubMed Central PMCID: PMC1214024.
7. Griffin ME, Marcucci MJ, Cline GW, Bell K, Barucci N, Lee D, Goodyear LJ, Kraegen EW, White MF, Shulman GI. Free fatty acid-induced insulin resistance is associated with activation of protein kinase C theta and alterations in the insulin signaling cascade. *Diabetes*. 1999;48(6):1270-4. PubMed PMID: 10342815.
8. Roden M, Price TB, Perseghin G, Petersen KF, Rothman DL, Cline GW, Shulman GI. Mechanism of free fatty acid-induced insulin resistance in humans. *The Journal of clinical investigation*. 1996;97(12):2859-65. doi: 10.1172/JCI118742. PubMed PMID: 8675698; PubMed Central PMCID: PMC507380.
9. Krssak M, Falk Petersen K, Dresner A, DiPietro L, Vogel SM, Rothman DL, Roden M, Shulman GI. Intramyocellular lipid concentrations are correlated with insulin sensitivity in humans: a ¹H NMR spectroscopy study. *Diabetologia*. 1999;42(1):113-6. doi: 10.1007/s001250051123. PubMed PMID: 10027589.
10. Pagadala M, Kasumov T, McCullough AJ, Zein NN, Kirwan JP. Role of ceramides in nonalcoholic fatty liver disease. *Trends in endocrinology and metabolism: TEM*. 2012;23(8):365-71. doi: 10.1016/j.tem.2012.04.005. PubMed PMID: 22609053; PubMed Central PMCID: PMC3408814.
11. Petersen KF, Shulman GI. Etiology of insulin resistance. *Am J Med*. 2006;119(5 Suppl 1):S10-6. Epub 2006/03/28. doi: 10.1016/j.amjmed.2006.01.009. PubMed PMID: 16563942; PubMed Central PMCID: PMC2995525.
12. Jornayvaz FR, Shulman GI. Diacylglycerol activation of protein kinase Cepsilon and hepatic insulin resistance. *Cell Metab*. 2012;15(5):574-84. Epub 2012/05/09. doi: 10.1016/j.cmet.2012.03.005. PubMed PMID: 22560210; PubMed Central PMCID: PMC3353749.

13. Holland WL, Brozinick JT, Wang LP, Hawkins ED, Sargent KM, Liu Y, Narra K, Hoehn KL, Knotts TA, Siesky A, Nelson DH, Karathanasis SK, Fontenot GK, Birnbaum MJ, Summers SA. Inhibition of ceramide synthesis ameliorates glucocorticoid-, saturated-fat-, and obesity-induced insulin resistance. *Cell metabolism*. 2007;5(3):167-79. doi: 10.1016/j.cmet.2007.01.002. PubMed PMID: 17339025.
14. Jaworowska A, Blackham T, Davies IG, Stevenson L. Nutritional challenges and health implications of takeaway and fast food. *Nutr Rev*. 2013;71(5):310-8. Epub 2013/04/18. doi: 10.1111/nure.12031. PubMed PMID: 23590707.

1:2 The Adipokine/Ceramide Axis: Key Aspects of Insulin Sensitization

Until recently, sphingolipid physiology was primarily the domain of oncologists and immunologists. However, mounting evidence implicates ceramides and their derivatives in various aspects of metabolism via directly impacting the insulin receptor as well as modulating critical target cell survival and proliferation (1). This esoteric and rather heterogeneous class of lipids is composed of a sphingosine backbone conjugated to a fatty acid derivative. A number of physiological effects have been attributed to this diverse class of sphingolipids ubiquitously present in all cell types. The cellular sphingolipid biosynthetic and degradative machineries are quite active and subject to multiple levels of regulation by cell type- and nutritional status-specific events, altogether providing a pathway that experiences a high flux through its intermediates. This makes it challenging to predict what intermediate metabolites will actually accumulate in a specific cell or in plasma upon genetic or pharmacological inhibition of the key regulatory components.

Synthesis of Ceramides and Sphingosine 1-phosphate

Ceramides are typically generated via 3 different pathways (**Fig. 1**). *De novo* synthesis occurs via the addition of a serine moiety to a palmitoyl-CoA. This reaction is catalyzed by the enzymes serine palmitoyl transferase-1 or -2 and results in the production of 3-ketosphinganine. Via the addition of another fatty acyl-CoA and a desaturation reaction by dihydroceramide desaturase, the final product, ceramide is produced. Depending on the fatty-acyl CoA moieties used, these lipids can have a diverse range of sizes, though commonly C16 through C24 ceramides are the most

biologically relevant. The alternative pathway is the direct generation of ceramide via the cleavage of sphingomyelin by sphingomyelinase. From here, ceramides can be phosphorylated by ceramide kinase, or degraded via ceramidase activity to sphingosine. Sphingosine kinase is then able to phosphorylate this molecule to generate sphingosine-1-phosphate (S1P). The degradation of S1P is subsequently controlled by S1P-lyase, which irreversibly cleaves and destroys it. Finally, the third pathway, the so-called “salvage pathway”, is able to produce ceramides from the direct breakdown of sphingolipids to sphingosine, which can be converted to ceramides by the enzyme ceramide synthase. Alterations in the enzymatic activity in any of these steps can drastically alter the intracellular levels of these lipid moieties; a process which can be favorable or deadly for a cell, depending on the physiological conditions (2). Given that three separate pathways can be active in parallel, inhibition of any one of them may have profound consequences for cellular physiology, or only a marginal effect, depending on the specific cell type, developmental stage and nutritional setting.

Sphingolipid Synthesis and Metabolism

Ceramides are important members of the sphingolipid family and are essential building blocks for the structure of the phospholipid bilayer that constitutes the cell membrane. Other than structural roles, ceramides also play a part in cell signaling, inflammation, and apoptosis. In the cell, ceramides are synthesized through the three different pathways that we outlined above. The *de novo* pathway of ceramide generation occurs in the endoplasmic reticulum and is composed of four sequential enzymatic reactions and regulated by its rate-limiting enzyme, serine palmitoyl-CoA transferase (SPT) (3). Once generated, ceramides are the common precursor to an

array of complex sphingolipids and they can also be glucosylated, deacylated, and phosphorylated to produce a variety of downstream metabolites and signaling molecules.

The *de novo* pathway can be induced by an increase in dietary serine, oxidative stress, and oxidized LDLs (3). Furthermore, SPT has a high specificity for its substrate, palmitoyl-CoA, the saturated fatty acid that is required for formation of the sphingoid backbone of ceramides. Thus, a diet that is high in saturated fat can effectively drive *de novo* ceramide synthesis and promote ceramide accumulation in peripheral tissues (4). In 2002, Chang et al showed that gram negative bacterial infection (via lipopolysaccharide) and induction of inflammatory cytokines such as TNF α and IL-1 can both increase the mRNA expression and activity of SPT in macrophages and ultimately drive *de novo* ceramide synthesis (5). Considering that expanding fat pads secrete a wide variety of inflammatory cytokines, including TNF α and IL-1, dysfunctional and inflamed fat pads are likely to contribute to the accumulation of ceramides in tissues (6).

Independent of the *de novo* synthesis pathway, ceramides are also generated by neutral sphingomyelinase (N-SMase)-catalyzed hydrolysis of sphingomyelin in cell membranes. Studies have shown that inflammation can induce N-SMase activity and drive ceramide synthesis (7, 8).

Plasma Ceramides and Insulin Resistance

Human and murine plasma is a rich source of ceramides, typically reported to circulate in the low micromolar range (0.5-10 μ M) (9-11). The most abundant of the plasma ceramides are those with long chain fatty acyl groups including C24:0, C24:1

and C22:0 (10). 75% of these ceramides are contained in VLDL and LDL particles, with the rest partitioning into HDL particles, with the distribution of the varying ceramide species remaining consistent between the different lipoprotein particles, with few exceptions (12). While the association with lipoproteins is well established, we cannot rule out other mechanisms of transport, such as serum albumin or via packaging into exosomes (13). Due to their stable association with lipoproteins, one could postulate that the primary source of circulating ceramides is hepatic in origin. This hypothesis was supported by isolating hepatocytes from obese mice and confirming that these cells secrete a significantly greater amount of ceramide compared to lean controls (14). This question as to what plasma ceramide levels really reflect is far from being resolved. For the moment, plasma ceramides primarily serve as useful biomarkers for metabolic dysfunction, and future work will need to establish specific biological functions for individual sphingolipid subspecies.

Many clinical studies have reported elevated circulating ceramides in patients with type 2 diabetes, and further that these levels correlate with the severity of insulin resistance (10, 14, 15). These correlative studies are supported by *in vivo* evidence showing that LDL particles containing ceramide were capable of inducing insulin resistance when infused into lean mice (14). Insulin-stimulated glucose uptake was reduced in L6 myotubes exposed to the same LDL containing ceramides (14). This data supports a possible role of liver derived ceramides contained in LDL particles as a mediator of systemic insulin resistance.

Other studies have shown that total ceramide levels highly correlate with a number of parameters involved in insulin resistance. Elevated ceramides correlate with

both elevated circulating TNF α and interleukin-6 (10, 16). Furthermore, following gastric bypass surgery, plasma ceramides levels decreased, as did circulating levels of TNF α . These reductions were correlated with a dramatic improvement in insulin sensitivity in these patients (17). Together these studies help to link circulating ceramides, inflammation and the subsequent insulin resistance in a number of different states of obesity and type 2 diabetes.

Role of Sphingolipids in Macrophages

Ceramides

Macrophages are primarily known for their role in the innate immune system, highly important for controlling infections and repairing damaged tissue. Macrophage infiltration into adipose tissue during states of obesity plays a primary driving force for the insulin resistant state of this overly expanded adipose tissue (18-21). As obesity progresses, macrophages turn from an alternatively activated anti-inflammatory phenotype (M2), to a more classically activated pro-inflammatory phenotype (M1) (22). M1 macrophages produce a number of pro-inflammatory cytokines, including TNF α , a factor that can increase ceramide levels in several tissues. As Ceramide and its degradation product sphingosine-1-phosphate (S1P), have been implicated in altering sensitivity to insulin as well as mediating processes such as apoptosis, it is of great importance to determine the significance of these lipids on the macrophage population. The role and function of ceramides in macrophages has therefore been explored in great detail over the last decade. Primary reports on experiments with macrophages showed that cultured macrophages (the "Raw264" cell line) are able to ramp up ceramide production upon exposure to lipopolysaccharide (23). However, this claim has

recently been challenged by a group who showed that LPS alone was unable to induce this increase in ceramide production in bone marrow derived macrophages (BMDMs). Rather, LPS could act in concert with palmitate exposure to create a synergistic increase in C16 ceramides (24). Both groups are in agreement that LPS -mediated increases in ceramide content are dependent on TLR-4 receptor and mediated by *de novo* synthesis pathways. However, differences between the two groups were manifest in that the former group shows that TLR-4 mediated activation of NF- κ B leads to increased SPT1 (serine palmitoyl transferase) production, while the latter group refutes this claim. They show that upon LPS stimulation of bone marrow-derived macrophages, expression of SPT1 does not change at the RNA level (based on RT-QPCR), while SPT2 is elevated, though only slightly. They further substantiate this claim by demonstrating that the *de novo* synthesis pathway is the predominant mediator of ceramide production. Additional evidence for this mechanism relates to the fact that a dramatic rise in 3-ketosphinganine, the immediate downstream product of the condensation reaction performed by SPT1/2, is present (24). Differences in the findings between these two groups may be based on cell-intrinsic properties, while the former used the cultured myoblast cell line C2C12 and cultured macrophages, the latter used primary macrophages. If the SPT pathway is already saturated in the primary isolates, the expression may be rendered less responsive to treatment with LPS. Notwithstanding the details, a fairly large body of literature implicates ceramides as mediators of a number of key physiological processes within the macrophage (25).

Recent work has shown that ceramides may be critically important in the activation of PI3-kinase by TLR-4 in macrophages (26, 27). A short-term challenge of

macrophages with LPS results in a burst of ceramide production occurring via the sphingomyelinase degradation pathway. This burst of ceramide production occurs within 30 seconds, but is normalized within 30 minutes following the initial stimulation. The PI3-kinase pathway is of critical importance for signaling during macrophage activation through signal transduction components, including but not limited to Akt, mTOR and NF- κ B. These observations highlight the pivotal role of LPS-mediated ceramide production for LPS mediated PI3-kinase activation (26, 27). Ceramide generation by LPS stimulation is highly apoptotic under conditions in which the PI3-kinase pathway is inhibited with the small molecule inhibitor LY294002. However, many groups have shown that in other cell types, ceramides inhibit the activity of PI3-kinase. Therefore, the authors suggest that this may be a macrophage, or even alveolar macrophage-specific finding.

Ceramide-1-phosphate in macrophages

Another important component in this signaling cascade is the phosphorylation of ceramide. Ceramide-1 phosphate is generated via the phosphorylation of ceramide by ceramide kinase. Ceramide-1-phosphate (C-1-P) is capable of stimulating cell division in bone marrow-derived macrophages in mice (28, 29). Withdrawal of serum from mouse BMDM cultures results in cell death, and that this process correlates with an elevation in sphingomyelinase activity. This activation is further characterized by a concomitant accumulation of ceramide with a corresponding decrease in C-1-P. These authors go on to show that C-1-P improves the viability of these cells following serum withdrawal by preventing activation of caspase-9. More importantly however, they show that C-1-P can inhibit acid sphingomyelinase directly, and hypothesize that this may be

the direct mechanism for the prevention of the rise in ceramides and improved cell viability (28).

C-1-P is further able to activate PI3 kinase, and that this results in downstream activation of the MAPK/JNK pathway, though p38 MAPK was not involved in this process (29). This activity leads to activation of NF- κ B. All of these findings were underscored by the observation that C-1-P levels rise in macrophages following macrophage colony-stimulating factor (mCSF) treatment, which ultimately results in cell division (29). This provides compelling evidence that C-1-P can activate the PI3-kinase pathway, leading to cell cycle progression, though no mechanism for this activation has been offered thus far. This remains a question of great interest in the context of the observation that C-1-P and ceramide both activate the PI3-kinase pathway (29, 30). A strong possibility is that these components may feed into the sphingosine-1-phosphate pathway, S-1-P representing a lipid mediator which activates specific receptors of the G protein coupled receptor upstream of the PI3-kinase pathway.

Sphingosine-1 Phosphate

Sphingosine-1-phosphate is generated by sphingosine kinase-mediated phosphorylation of sphingosine, which is a lipid metabolite generated from the breakdown of ceramides by ceramidase. S1P can signal through any one of its 5 receptors identified so far, all of which are GPCRs, each signaling through a variety of G proteins including G_i , G_s and G_y . These receptors play a diverse role in cellular homeostasis with knockout animals of the individual receptors showing a wide variety of phenotypes. S1P receptor 1 knockout mice are not viable as a result of an extreme

vascular instability phenotype (31). Receptor -2 and -3 knockouts are viable, however S1P receptor-2 knockouts present with seizures and deafness in certain genetic backgrounds, while S1P receptor-3 knockouts present with reduced viability though with an enhanced sepsis outcome (31). The S1PR4 and S1PR5 receptor knockout mice have no obvious phenotype that has been described so far. Of interest clinically is the pharmacologic agonist FTY720, an immunosuppressive drug used in the treatment of multiple sclerosis and transplant rejection. This drug binds with high affinity to all of the S1P receptors and is proposed to cause receptor down-modulation and internalization upon binding. So even though it acts as a strong agonist initially, the associated down-regulation of the S1P receptors is functionally equivalent to antagonist action. Systemically, this results in the sequestration of lymphocytes within lymph organs (32).

S1P and the macrophage

Clearly, S1P is an important regulator of immune function. Macrophage treatment with LPS skews the macrophage phenotype toward a pro-inflammatory state, characterized by expression of iNOS and increased secretion of TNF α and macrophage chemoattractant protein 1 (MCP-1). Various groups have shown that co-treatment of macrophages with LPS and S1P inhibits this phenotypic switch and clamps macrophages in a more anti-inflammatory state characterized by expression of arginase 1 (33). Furthermore, treatment with a highly specific S1P receptor 1 agonist (SEW2871) resulted in a similar anti-inflammatory response, while the specific antagonist VPC44116 was capable of inhibiting this phenotypic switch (33). S1P receptor 2 deficient macrophages showed a blunted response to LPS, but respond similarly to SEW2871 treatment. These changes were all shown to be dependent on the NF- κ B, a

transcription factor whose activation through LPS increases production of inflammatory mediators in the macrophage such as TNF α . S1P inhibits this pathway, as does SEW2871, and this phenomenon critically depends on receptor 1 (33).

S1P receptor response in atherosclerosis models

S1P levels in the blood positively correlate with HDL levels, and therefore it was suggested that S1P may play an important role in atherosclerotic lesions. The S1P receptor 3 deficient, whole body knockout mouse displays changes in the atherosclerotic plaque formation on the ApoE^{-/-} background (34). These lesions were not smaller in volume, yet contained significantly fewer macrophages than the wild type lesions (34). Bone marrow transplantation to an ApoE-deficient mouse from a S1P-R3 knockout mouse again demonstrated reduced macrophage infiltration of the plaques; however this effect diminished compared to the whole body knockout, leading various groups to hypothesize that S1PR3 may play an important role in the endothelial response during atherosclerotic development (34). Another paper, though later retracted for different reasons, showed similar findings in the S1P-R2 deficient mouse on an ApoE^{-/-} background (35). Surprisingly, no findings have been reported on S1PR1's role in the atherosclerotic progression; however FTY720, the agonist which down-modulates receptors, has been shown to decrease atherosclerotic lesion development in ApoE-deficient mice (36).

Excessive signaling of S1P

Sphingosine-1-phosphate is degraded by sphingosine lyase (SGPL). The SGPL knockout mouse presents with profound lymphopenia and neutrophilia and typically dies

around week 4. In this mouse, serum S1P levels are highly elevated, as are the levels of circulating ceramide (37). Furthermore, these mice are acutely inflamed, presenting with elevated C-reactive protein (CRP), TNF α and IL-6. Furthermore, an injection of LPS into these mice was lethal to the knockouts, while this was not the case in wildtype controls. Intraperitoneal injection of thioglycolate shows neutrophil and macrophage trafficking defects, and that there is a lack of L-selectin on the neutrophils in the knockouts (37). A bone marrow transplant from SGPL mice into wild type mice recapitulates the findings from the knockout mouse. In the S1P-R4 knockout background, SGPL deficient mice normalize their neutrophil and cytokine levels and aberrant S1P-R4 signaling may be a primary defect resulting in this extreme phenotype of the mice. Finally, they show that G-CSF and IL-17 are elevated in the SGPL null mice, and that this causes increased neutrophil production. This results from a defect in neutrophil egress from the blood, an event which regulates the secretion of Granulocyte colony-stimulating factor (G-CSF) and down regulates further production of these cytokines. Therefore, it is the lack of L-selectin on neutrophils which results in an inability of macrophages to egress from the blood, causing apparently uncontrolled expression of G-CSF, thereby driving the neutrophilia phenotype. Interestingly the findings presented in this SGPL mouse are reminiscent of the findings in the treatment of wildtype mice with FTY720 which also results in severe lymphopenia.

FTY720 and mucosal immunity

As describe above, FTY720 is an immunosuppressant and works as an agonist of all the S1P receptors. Its true mechanism of action is due to its extremely high affinity for its receptors, which are effectively internalized and not recycled (32). Clinically, this

drug's resulting immunosuppressive effects are attributed to lymphocyte sequestration in lymphoid organs, thereby achieving excellent anti-inflammatory effects. However, similar to many other anti-inflammatory and immune-suppressive drugs, a significant increase in number of infections per patient has been reported upon long-term treatment with FTY720 (32). To investigate the role this compound has on gut mucosal immunity, a fluorescent enteric pathogen known as *Citrobacter Rodentium* was used. *C. Rodentium* is easily cleared by wild type, drug-naive mice within 14 days. However, FTY720 exposure significantly impaired the ability to clear the infection. 14 days *post* infection, the treated mice still displayed significant colonization of their colons, ceca and spleens, whereas in the untreated group, no pathogen colonization could be detected. Further, mucosal thickening and epithelial hyperplasia was apparent in the colons of treated mice. This was associated with a significant increase in number of neutrophils present in and around these tissues. IL6 and TNF α were elevated compared to vehicle on day 14 *post* infection, indicating a systemic inflammatory response despite anti-inflammatory treatment. These results indicate that FTY720 works effectively in the clinic for its intended purpose. Nevertheless, excessive S1P receptor signaling and down modulation of the receptors may have significant negative side effects on individuals and the treatment response must therefore be monitored carefully.

Role of Sphingolipids in Hepatocytes

Concomitant with the rise in obesity, the prevalence of non-alcoholic fatty liver disease (NAFLD), a newly emerging obesity-related disorder, has also been rising steadily (38). NAFLD is a chronic liver disease that ranges histologically from simple steatosis in its mildest form to nonalcoholic steatohepatitis (NASH) in the more severe

form, which is characterized by hepatocyte inflammation and fibrosis. Furthermore, NASH can potentially develop into cirrhosis and hepatocellular carcinoma in extreme cases (38). Recent data from the National Health and Nutrition Examination Survey has estimated that NAFLD may affect up to 30% of the general population and 80% of obese and diabetic individuals, making it the most common liver dysfunction in the United States (39, 40).

Due to its increasing prevalence and detrimental health consequences the need to identify the mechanisms that mediate the pathogenesis and progression of NAFLD has become increasingly important. In 1998, Day et al proposed the “two-hit” hypothesis for the pathogenesis of NAFLD. According to these authors, hepatic lipid accumulation or steatosis represents the “first hit,” which makes the liver vulnerable to various additional insults that can ultimately result in the inflammation, fibrosis, and cell death observed in NASH, and this concept was further elaborated on by others (41, 42). Concurrently, Unger *et al.* introduced the notion of lipotoxicity, which demonstrated that accumulation of lipids, especially saturated fatty acids, in non-adipose tissue leads to cell dysfunction and death (43). These two concepts were further elaborated on in 2005 when Yamazaki et al identified that the deposition of lipids in the liver, especially triacylglycerol, as an essential step on the path to the development of NAFLD (44), though a much more nuanced understanding of the relationship of hepatic lipid accumulation, NAFLD and insulin resistance has emerged (45). In addition, additional evidence implicates sphingolipids and their derivatives as important players in NAFLD and its progression to NASH (46).

Ceramides and the liver

Even though ceramide synthesis is ubiquitous in all tissues in the body, many recent *in vitro* and *in vivo* studies suggest that the liver is an important site for ceramide production. Nikolova *et al* showed that treatment of hepatocytes with pro-inflammatory cytokines including TNF α and IL-1 β , and strong pro-inflammatory compounds such as lipopolysaccharide (LPS) can all trigger rapid turnover of sphingomyelin and intracellular ceramides (47). The rapid turnover of sphingomyelin and ceramides is attributed to the inflammation-mediated induction of N-SMase. However, inflammation induced activation of the *de novo* ceramide synthesis should not be ruled out as a contributor. As early as 1998, Memon *et al* confirmed this *in vivo* by administering LPS in Syrian hamsters, which resulted in a 2-fold increase of hepatic SPT mRNA and activity within 16 hours. Hepatic sphingomyelin and ceramides also showed a 2.5-fold increase under these conditions (48). These studies suggest that infection and the resulting inflammation regulate hepatic ceramide accumulation at the transcriptional level.

LPS induces inflammation by activating Toll-like receptors (TLRs), specifically TLR4. These receptors are essential for mounting inflammatory responses in innate immunity. In addition, studies have shown that saturated fatty acids can serve as agonists for TLR4 (49-51). Furthermore, studies exposing H4IIE rat liver hepatoma cells to saturated fatty acids (such as palmitate) resulted in significant accumulation of ceramides in the cells (52). Holland *et al* showed that TLR4 is an upstream signaling component required for saturated fatty acid-induced ceramide biosynthesis in liver by both *in vitro* and *in vivo* studies (53). This further affirmed the notion that TLR4 is a major player in hepatic ceramide production. In addition, this study also revealed that TLR4 activation by saturated fatty acids can induce insulin resistance. Thus, these

findings not only established a plausible mechanism of how saturated fatty acids induce ceramide synthesis but also linked dysregulation of fatty acid metabolism to hepatic ceramide accumulation.

Ceramides and hepatic dysfunction

Liver dysfunction prompts ceramide levels in both liver and plasma to increase correspondingly. Ichi and colleagues induced hepatic necrosis by administering carbon tetrachloride to mice, a potent pro-fibrotic agent and detected a significant increase in both hepatic and plasma ceramide concentrations (54). Obese mice with hepatic steatosis also have increased hepatic ceramide content (55).

A major contributor in the development of hepatic steatosis is the upregulation of peripheral tissue lipolysis, primarily in adipose tissue, leading to an increased delivery of free fatty acids (FFAs) to the liver (41, 56). Once in the liver, the FFAs are converted into triglycerides, diacylglycerol, and ceramides or oxidized in the mitochondria to ultimately maintain proper systemic carbohydrate homeostasis (57). Triglycerides are exported from the liver as VLDL. When the net influx of FFAs is greater than the secretion of triglycerides or oxidation, lipids such as triglyceride and ceramides accumulate in the liver resulting in steatosis (41). Obesity-associated insulin resistance prompts an increased rate of FFA influx into liver is increased, thereby resulting in NAFLD.

Additional evidence for the importance of ceramides in mediating the development of hepatic steatosis has recently emerged. In 2007, Holland *et al* showed that blocking *de novo* ceramide synthesis using myriocin, an SPT inhibitor, reduced

macrovesicular hepatic steatosis, hepatic triglyceride content, and SOCS-3 expression, a cytokine mediated gene that is generally seen upregulated in NAFLD (58). In parallel, mice in this study also showed improved insulin sensitivity as judged by restored Akt signaling, and this was seen in liver and muscle (58). Studies like these lend support to the notion that ceramides promote insulin resistance and they are indeed directly involved in the development of NAFLD. Nevertheless, it is still not clear whether ceramide accumulation directly mediates hepatic steatosis or rather is the result of ceramide-induced insulin resistance.

Another aspect of the role of ceramides in the pathogenesis of NAFLD arises from studies involving adiponectin and its role in NAFLD. Adiponectin is an adipocyte-derived secretory protein that has been widely studied for its insulin sensitizing, anti-inflammatory, and anti-apoptotic effects on a number of cell types (59, 60). In 2002, a study by Yamauchi *et al* found that adiponectin exerts a hepatoprotective role by decreasing FFA influx, *de novo* lipogenesis, and increasing hepatic FFA β -oxidation (61). Additional studies showed that adiponectin improved insulin sensitivity, thereby leading to reduced hepatic gluconeogenesis (62, 63). The mechanisms underlying these effects exerted by adiponectin have been a topic of ongoing research. In 2011, we found that the adiponectin receptors (AdipoR1 & R2) potently mediate ceramidase activity, thereby leading to an enhanced break-down of ceramides, in an adiponectin ligand-dependent manner (64). Data from this study showed that adiponectin injections can potently reduce hepatic ceramides *in vivo*. Furthermore, mice with hepatic overexpression of AdipoR1 and R2 through adenoviral infection have significantly improved insulin sensitivity and reduced hepatocyte apoptosis when challenged with a

high fat diet (64). Similarly, clinical studies have shown that patients with advanced steatosis have reduced expression of hepatic AdipoR2 (65). Considering that the liver is a major target organ of adiponectin action (66), the beneficial metabolic effects of adiponectin have been linked to the lowering of intracellular ceramides. Furthermore, these studies not only confirm that hepatic ceramides are important in the development of NAFLD, but also suggests that they play a more important role as causative factors for the induction of insulin resistance and inflammation that ultimately results in the progression to NASH.

Ceramides and progression to NASH

Insulin resistance and inflammation are known contributors to NAFLD's progression to NASH. Ceramides contribute to systemic insulin resistance by impairing insulin sensitivity in skeletal muscle and liver (58), and are likely to exert similar effects in other tissues as well. At the molecular level, ceramides disrupt the insulin-signaling cascade at the level of Akt activation (67, 68). The resulting insulin resistance promotes lipolysis and increased FFA delivery to liver, thus increasing hepatic lipid accumulation (57). Ceramides also interact with TNF α signaling in the liver to increase mitochondrial generation of reactive oxygen species (ROS), resulting in apoptosis and recruitment of inflammatory cells leading to worsening of hepatic inflammation (69). In addition, the pro-inflammatory cytokine IL-1 is increased in NASH and also induces ceramide synthesis (1). Ceramides have also been shown to induce the pro-inflammatory transcription factor nuclear factor kappa light chain enhancer of activated B cells (NF- κ B). Therefore, once its production is induced by cytokines, ceramides can sustain and amplify inflammation through this positive feedback system (70). Considering its role in

both insulin resistance and inflammation, it seems like ceramide accumulation may provide the important “second hit” in the development towards full-blown NASH.

Role of Sphingolipids in Adipocytes

Once viewed simply as a passive reservoir for triglycerides, adipose tissue is now recognized as an active endocrine organ that plays a central role in the pathogenesis of obesity associated insulin resistance (71). Although skeletal muscle is the major tissue responsible for peripheral glucose uptake, adipose tissue also expresses the insulin receptor and is responsible for clearing a portion of plasma glucose (72). Early work on insulin resistance in adipose tissue showed that the cytokine TNF α , which is upregulated in adipose tissue during obesity, is able to induce insulin resistance by attenuating insulin signaling at the level of insulin receptor and by suppressing the expression of the insulin responsive glucose transporter GLUT4 (73, 74). The mechanism by which TNF α induces these effects is not clear. In 1996, Long et al. demonstrated that TNF α mediates ceramide biosynthesis through the sphingomyelin pathway in 3T3-L1 adipocytes. The resulting rise in intracellular ceramide levels is concomitant with a 60% decrease of GLUT4 mRNA content. Furthermore, treatment of 3T3-L1 adipocytes with C8-ceramide, a membrane-permeable short chain analogue of ceramide, also decreased GLUT4 mRNA content, suggesting that a ceramide initiated signal transduction pathway exists in adipocytes and plays a role in facilitating TNF- α 's control on GLUT4 expression (75). Studies in 3T3-L1 adipocytes have shown that TNF-alpha can also cause insulin resistance by increasing the sphingolipid ganglioside GM3, which can attenuate insulin signaling at the level of the insulin receptor (76). Clinical studies in humans have linked sphingolipid

content in adipose tissue to systemic metabolic health. In 2007, Kolak *et al* showed that obese individuals with liver steatosis had increased inflammation, ceramide content, and sphingomyelinase activity in adipose tissue compared to their counterparts without liver steatosis (77). Thus, it is evident that a strong link exists between adipose sphingolipids, inflammation, and insulin resistance, and adipose tissue plays an integral role in this process.

Role of Sphingolipids in β -cells

Early indications that ceramides played a significant role came from studies of ZDF rats, a rodent model of β -cell failure. These animals present early in life with β -cell hyperplasia followed by subsequent failure. Elevated circulating triglycerides in these rats leads to inappropriate deposition of lipids in β -cells, and this accumulation causes elevated ceramide content in islets (43). These ceramides lead to β -cell death, and inhibition of the ceramide synthase with fumonisin B rescues cultured ZDF islets from this lipid mediated apoptosis (43). Follow up studies revealed that these ceramides are generated via the *de novo* synthesis pathway, and that inhibition of the rate limiting enzyme in this pathway is sufficient to reduce ceramide accumulation and apoptosis of the islets *in vivo* (78). Consistent with a role of ceramides in β -cell death are additional recent observations from our laboratory. These results show that the adipokine adiponectin is can rescue β -cells from apoptosis *in vivo* via its ability to decrease intracellular ceramides (64).

In light of the compelling evidence arguing that ceramides are toxic to the β -cells, a mechanism for this action has been sought in recent years. A common theme

emerging from these studies is that ceramides are capable of causing endoplasmic reticulum stress, and that this is partly responsible for the death of β -cells. Consistent with this theme is that reduction of ceramides in an insulin secreting β -cell line results in decreased ER stress while improving cell survival (79). Another aspect of ceramide action relates to the fact that they can alter mitochondrial function, and β -cells have a very limited tolerance with respect to altered mitochondrial function. This is further highlighted by the treatment of INS-1 cells with a cell permeable ceramide. This markedly reduces the mitochondrial membrane potential, leading to a concomitant increase in cytosolic cytochrome *c* (80, 81). While the direct effects of ceramides on mitochondrial membrane integrity are still subject to discussions, this remains a plausible mechanism which has been better defined in other organs, such as the heart.

Role of sphingolipids in the heart

The mammalian heart is a highly aerobic organ deriving approximately 60% of its energy from the direct utilization of lipids via oxidative phosphorylation. Although the heart is well equipped to handle lipids, states of excess lipid deposition occur under conditions of insulin resistance and type 2 diabetes and are linked to diastolic dysfunction in both human and rodent studies (82, 83). Key mediators of the dysfunction in the heart under these conditions are thought to be ceramides. *In vitro* studies have shown that short and long chain ceramides can inhibit mitochondrial respiration (84). This effect is produced via a membrane dependent inhibition of mitochondrial complexes I and III (84). Similar to the situation in β -cells, short chain cell permeable ceramides are directly toxic to isolated rat cardiac myocytes via induction of apoptotic cell death (85). From these results, we can see that ceramides are directly

toxic to cardiomyocytes, in large part via inhibition of mitochondrial respiration. However, most studies were performed on isolated cells and mitochondria. The role *in vivo* role of ceramides in whole animal cardiac physiology remains less well defined.

Lipoprotein lipase is an enzyme on the surface of cells which mediates the cleavage of fatty acyl groups from circulating lipoprotein particles, thereby stimulating uptake of these lipids into proximal tissues. Overexpression of lipoprotein lipase in the heart results in lipid accumulation and cardiac dysfunction as characterized by left ventricular dilation (LVD) and decreased contractility (86). Treatment with myriocin, an inhibitor of the *de novo* ceramide synthesis pathway, corrected both LVD and the loss of contractility, further highlighting the importance of ceramides in diastolic dysfunction during lipid overload in the heart (86).

With respect to acute cell injury, ceramides are greatly elevated during ischemic cardiac cell death *in vivo* (85). Recent evidence implicates adiponectin as a potent cardioprotective factor through its activation of cellular ceramidases (64). Overexpression of adiponectin prevents cardiac cell death upon induction of apoptosis *in vivo*, while loss of adiponectin enhances cardiac damage and increases mortality (64). These studies build upon previously published experiments that highlight adiponectin knockout mice as more susceptible to cardiac ischemic death, though a ceramide-dependent mechanism was not tested (87). Altogether, these studies put ceramides at the center of cardiac health and fitness and emphasize the importance of lipid homeostasis in the mammalian heart.

How do leptin, adiponectin and FGF21 alter sphingolipids

Adipose tissue secretes a wide array of unique factors, adipokines, which have been widely discussed in the literature with respect to their function as regulators of whole body metabolism and insulin sensitivity (71). Among these adipokines, leptin is one of the most active regulators of body weight and food intake. Dysregulation of leptin usually results in obesity and eventually insulin resistance and type 2 diabetes (88-91). Rats treated with leptin display systemic improvements in insulin sensitivity and suppress *de novo* ceramide synthesis (43, 92). More recently, Bonzon-Kulichenko *et al.* have demonstrated that central leptin infusion in the hypothalamus in mice reduces total ceramide content in WAT via action through the autonomic nervous system. Central leptin represses serine palmitoyl transferase (SPT), the rate-limiting enzyme of ceramide production in WAT by 30%. Furthermore, the reduction of ceramides in WAT coincides with improved systemic insulin sensitivity; suggesting that reduction of WAT ceramides contributes to improvements in systemic insulin sensitivity (93). As discussed in the various sections above on adiponectin action in specific target tissues, adiponectin exerts its beneficial metabolic effects by lowering cellular ceramide levels. Furthermore, adiponectin is potently anti-apoptotic in the context of cardiomyocytes and pancreatic β -cells *in vivo* through the lowering of cellular ceramides. The adiponectin receptors, AdipR1 and AdipoR2 exhibit ceramidase activity in an adiponectin dependent manner (64). Whether the receptors themselves contain the ceramidase activity or they sequester or induce a ceramidase upon activation is still unclear. FGF21 has been the target of much interest (94). Expressed primarily in the liver upon prolonged fasting, it can also be synthesized in other tissues. In a similar

fashion as adiponectin, FGF21 mediates potent beneficial effects on carbohydrate and lipid metabolism (95) and effectively lowers ceramides (96). These effects critically rely on FGF21's ability to stimulate adiponectin release from the adipocyte. Thiazolidinediones (TZDs), agonists for the nuclear receptor PPAR γ , are potent inducers of FGF21 and adiponectin, and in turn lower plasma ceramide levels as well. Based on our own work and that of others, we propose a model in which there is a linear relationship between TZD exposure, leading to the induction of FGF21, which in turn triggers increased release of adiponectin from adipocytes, resulting in a systemic lowering of ceramides (96, 97).

These observations highlight the dual role of the adipocyte, both as a source of lipotoxic fatty acids as well as a source for potentially anti-lipotoxic adipokines that include, but may not be limited to, leptin, adiponectin and FGF21 that exert protective roles for susceptible cell types, both during times of maximal FFA release from the adipocyte during fasting as well in the postprandial state.

“Healthy” adipose tissue rescues systemic ceramide accumulation

In the past, we have generated several mouse models that display the ability to massively expand their subcutaneous adipose tissue. We define “healthy” tissue as a tissue that can undergo a very high level of expansion without the usual side effects of obesity, i.e. adipose tissue displaying increased levels of adipogenesis, effective recruitment of precursor cells, proper angiogenesis, lack of hypoxia and fibrosis, with limited infiltration of immune cells and subsequent inflammation (98). We have achieved that by either local overexpression of adiponectin (99) or overexpression of the

mitochondrial protein mitoNEET (100). In both cases, systemic insulin sensitivity is fully preserved, and minimal ectopic lipids accumulate under those conditions. This highlights the powerful effects that adipose tissue can exert as a “metabolic sink” for excess lipids, which can effectively be neutralized in subcutaneous adipose tissue rather than being deposited ectopically in other tissues, where they give rise to ceramides.

Concluding remarks

Lipids are a highly heterogeneous class of bioactive molecules that play diverse functions within the cell. Here, we have outlined the important functions of metabolites of the ceramide and sphingosine pathways with respect to cellular and systemic metabolic function (**Fig. 2**). The involvement of ceramides in the development of diabetes and metabolic syndrome is an emerging field in metabolism research. While the liver is an important site of ceramide synthesis, it is clear that the manipulation of the sphingolipid pathways in other tissues, particularly the adipocyte, may also potentially affect the systemic sphingolipid pool. The accumulation of ceramides in the liver can potentially promote hepatic steatosis and further its development into steatohepatitis. This finding suggests that the “cross-talk” between adipose tissue and liver may be important in the development of liver dysfunction and other metabolic impairments. Sphingolipid metabolism is a potent upstream mediator of the insulin sensitizing and anti-inflammatory effects of the key known adipokines, such as leptin, adiponectin and FGF21. One of the key challenges in the field in the future remains to build a better understanding of the actions of these adipokines on their key target tissues and how that translates into measurements of individual sphingolipid subspecies in plasma. This

also entails a better understanding of what distinct physiological role the many different subspecies play at the level of the individual target cells, which - though currently a daunting task - will unquestionably contribute in major ways towards an improved holistic understanding of metabolic dysfunction.

References

1. Holland WL, Summers SA. Sphingolipids, insulin resistance, and metabolic disease: new insights from in vivo manipulation of sphingolipid metabolism. *Endocr Rev.* 2008;29(4):381-402. Epub 2008/05/03. doi: er.2007-0025 [pii]10.1210/er.2007-0025. PubMed PMID: 18451260.
2. Holland WL, Knotts TA, Chavez JA, Wang LP, Hoehn KL, Summers SA. Lipid mediators of insulin resistance. *Nutr Rev.* 2007;65(6 Pt 2):S39-46. Epub 2007/07/04. PubMed PMID: 17605313.
3. Gault CR, Obeid LM, Hannun YA. An overview of sphingolipid metabolism: from synthesis to breakdown. *Advances in experimental medicine and biology.* 2010;688:1-23. Epub 2010/10/06. PubMed PMID: 20919643; PubMed Central PMCID: PMC3069696.
4. Frangioudakis G, Garrard J, Raddatz K, Nadler JL, Mitchell TW, Schmitz-Peiffer C. Saturated- and n-6 polyunsaturated-fat diets each induce ceramide accumulation in mouse skeletal muscle: reversal and improvement of glucose tolerance by lipid metabolism inhibitors. *Endocrinology.* 2010;151(9):4187-96. Epub 2010/07/28. doi: 10.1210/en.2010-0250. PubMed PMID: 20660065; PubMed Central PMCID: PMC2940499.
5. Chang YT, Choi J, Ding S, Prieschl EE, Baumruker T, Lee JM, Chung SK, Schultz PG. The synthesis and biological characterization of a ceramide library. *Journal of the American Chemical Society.* 2002;124(9):1856-7. Epub 2002/02/28. PubMed PMID: 11866590.
6. Uysal KT, Wiesbrock SM, Marino MW, Hotamisligil GS. Protection from obesity-induced insulin resistance in mice lacking TNF-alpha function. *Nature.* 1997;389(6651):610-4. Epub 1997/10/23 22:33. doi: 10.1038/39335. PubMed PMID: 9335502.
7. Clarke CJ, Snook CF, Tani M, Matmati N, Marchesini N, Hannun YA. The extended family of neutral sphingomyelinases. *Biochemistry.* 2006;45(38):11247-56. Epub 2006/09/20. doi: 10.1021/bi061307z. PubMed PMID: 16981685.
8. Clarke CJ, Hannun YA. Neutral sphingomyelinases and nSMase2: bridging the gaps. *Biochim Biophys Acta.* 2006;1758(12):1893-901. Epub 2006/08/30. doi: 10.1016/j.bbamem.2006.06.025. PubMed PMID: 16938269.
9. Kirwan JP. Plasma ceramides target skeletal muscle in type 2 diabetes. *Diabetes.* 2013;62(2):352-4. Epub 2013/01/26. doi: 10.2337/db12-1427. PubMed PMID: 23349544; PubMed Central PMCID: PMC3554378.
10. Haus JM, Kashyap SR, Kasumov T, Zhang R, Kelly KR, Defronzo RA, Kirwan JP. Plasma ceramides are elevated in obese subjects with type 2 diabetes and correlate with the severity of insulin resistance. *Diabetes.* 2009;58(2):337-43. doi: 10.2337/db08-1228. PubMed PMID: 19008343; PubMed Central PMCID: PMC2628606.
11. Brozinick JT, Hawkins E, Hoang Bui H, Kuo MS, Tan B, Kievit P, Grove K. Plasma sphingolipids are biomarkers of metabolic syndrome in non-human primates maintained on a Western-style diet. *Int J Obes (Lond).* 2012. Epub 2012/12/05. doi: 10.1038/ijo.2012.191. PubMed PMID: 23207405.
12. Wiesner P, Leidl K, Boettcher A, Schmitz G, Liebisch G. Lipid profiling of FPLC-separated lipoprotein fractions by electrospray ionization tandem mass spectrometry. *Journal of lipid research.* 2009;50(3):574-85. doi: 10.1194/jlr.D800028-JLR200. PubMed PMID: 18832345.
13. Wang G, Dinkins M, He Q, Zhu G, Poirier C, Campbell A, Mayer-Proschel M, Bieberich E. Astrocytes secrete exosomes enriched with proapoptotic ceramide and prostate apoptosis response 4 (PAR-4): potential mechanism of apoptosis induction in Alzheimer

- disease (AD). *J Biol Chem.* 2012;287(25):21384-95. Epub 2012/04/26. doi: 10.1074/jbc.M112.340513. PubMed PMID: 22532571; PubMed Central PMCID: PMC3375560.
14. Boon J, Hoy AJ, Stark R, Brown RD, Meex RC, Henstridge DC, Schenk S, Meikle PJ, Horowitz JF, Kingwell BA, Bruce CR, Watt MJ. Ceramides contained in LDL are elevated in type 2 diabetes and promote inflammation and skeletal muscle insulin resistance. *Diabetes.* 2013;62(2):401-10. Epub 2012/11/10. doi: 10.2337/db12-0686. PubMed PMID: 23139352; PubMed Central PMCID: PMC3554351.
 15. Lopez X, Goldfine AB, Holland WL, Gordillo R, Scherer PE. Plasma ceramides are elevated in female children and adolescents with type 2 diabetes. *Journal of pediatric endocrinology & metabolism : JPEM.* 2013:1-4. Epub 2013/04/25. doi: 10.1515/jpem-2012-0407. PubMed PMID: 23612696.
 16. de Mello VD, Lankinen M, Schwab U, Kolehmainen M, Lehto S, Seppanen-Laakso T, Oresic M, Pulkkinen L, Uusitupa M, Erkkila AT. Link between plasma ceramides, inflammation and insulin resistance: association with serum IL-6 concentration in patients with coronary heart disease. *Diabetologia.* 2009;52(12):2612-5. Epub 2009/08/12. doi: 10.1007/s00125-009-1482-9. PubMed PMID: 19669729.
 17. Huang CK, Goel R, Chang PC, Lo CH, Shabbir A. Single-incision transumbilical (SITU) surgery after SITU laparoscopic Roux-en-Y gastric bypass. *Journal of laparoendoscopic & advanced surgical techniques Part A.* 2012;22(8):764-7. Epub 2012/09/20. doi: 10.1089/lap.2011.0434. PubMed PMID: 22989038.
 18. Wellen KE, Hotamisligil GS. Obesity-induced inflammatory changes in adipose tissue. *J Clin Invest.* 2003;112(12):1785-8. PubMed PMID: 14679172.
 19. Xu H, Barnes GT, Yang Q, Tan G, Yang D, Chou CJ, Sole J, Nichols A, Ross JS, Tartaglia LA, Chen H. Chronic inflammation in fat plays a crucial role in the development of obesity-related insulin resistance. *J Clin Invest.* 2003;112(12):1821-30. PubMed PMID: 14679177.
 20. Berg AH, Scherer PE. Adipose tissue, inflammation, and cardiovascular disease. *Circ Res.* 2005;96(9):939-49. PubMed PMID: 15890981.
 21. Asterholm IW, McDonald J, Blanchard PG, Sinha M, Xiao Q, Mistry J, Rutkowski JM, Deshaies Y, Brekken RA, Scherer PE. Lack of "immunological fitness" during fasting in metabolically challenged animals. *J Lipid Res.* 2012;53(7):1254-67. Epub 2012/04/17. doi: 10.1194/jlr.M021725. PubMed PMID: 22504909; PubMed Central PMCID: PMC3371237.
 22. Lumeng CN, Deyoung SM, Bodzin JL, Saltiel AR. Increased inflammatory properties of adipose tissue macrophages recruited during diet-induced obesity. *Diabetes.* 2007;56(1):16-23. Epub 2006/12/29. doi: 10.2337/db06-1076. PubMed PMID: 17192460.
 23. Chang ZQ, Lee SY, Kim HJ, Kim JR, Kim SJ, Hong IK, Oh BC, Choi CS, Goldberg IJ, Park TS. Endotoxin activates de novo sphingolipid biosynthesis via nuclear factor kappa B-mediated upregulation of Sptlc2. *Prostaglandins & other lipid mediators.* 2011;94(1-2):44-52. Epub 2010/12/21. doi: 10.1016/j.prostaglandins.2010.12.003. PubMed PMID: 21167294; PubMed Central PMCID: PMC3366150.
 24. Schilling JD, Machkovech HM, He L, Sidhu R, Fujiwara H, Weber K, Ory DS, Schaffer JE. Palmitate and lipopolysaccharide trigger synergistic ceramide production in primary macrophages. *J Biol Chem.* 2013;288(5):2923-32. Epub 2012/12/20. doi: 10.1074/jbc.M112.419978. PubMed PMID: 23250746; PubMed Central PMCID: PMC3561515.
 25. Levi M, Meijler MM, Gomez-Munoz A, Zor T. Distinct receptor-mediated activities in macrophages for natural ceramide-1-phosphate (C1P) and for phospho-ceramide

- analogue-1 (PCERA-1). *Mol Cell Endocrinol.* 2010;314(2):248-55. Epub 2009/05/27. doi: 10.1016/j.mce.2009.05.007. PubMed PMID: 19467294.
26. Ojaniemi M, Glumoff V, Harju K, Liljeroos M, Vuori K, Hallman M. Phosphatidylinositol 3-kinase is involved in Toll-like receptor 4-mediated cytokine expression in mouse macrophages. *European journal of immunology.* 2003;33(3):597-605. Epub 2003/03/05. doi: 10.1002/eji.200323376. PubMed PMID: 12616480.
 27. Fallah MP, Chelvarajan RL, Garvy BA, Bondada S. Role of phosphoinositide 3-kinase-Akt signaling pathway in the age-related cytokine dysregulation in splenic macrophages stimulated via TLR-2 or TLR-4 receptors. *Mechanisms of ageing and development.* 2011;132(6-7):274-86. Epub 2011/06/08. doi: 10.1016/j.mad.2011.05.003. PubMed PMID: 21645538; PubMed Central PMCID: PMC3155631.
 28. Gomez-Munoz A, Kong JY, Salh B, Steinbrecher UP. Ceramide-1-phosphate blocks apoptosis through inhibition of acid sphingomyelinase in macrophages. *J Lipid Res.* 2004;45(1):99-105. Epub 2003/10/03. doi: 10.1194/jlr.M300158-JLR200. PubMed PMID: 14523050.
 29. Gangoiti P, Granado MH, Wang SW, Kong JY, Steinbrecher UP, Gomez-Munoz A. Ceramide 1-phosphate stimulates macrophage proliferation through activation of the PI3-kinase/PKB, JNK and ERK1/2 pathways. *Cellular signalling.* 2008;20(4):726-36. Epub 2008/02/01. doi: 10.1016/j.cellsig.2007.12.008. PubMed PMID: 18234473.
 30. Monick MM, Mallampalli RK, Carter AB, Flaherty DM, McCoy D, Robeff PK, Peterson MW, Hunninghake GW. Ceramide regulates lipopolysaccharide-induced phosphatidylinositol 3-kinase and Akt activity in human alveolar macrophages. *J Immunol.* 2001;167(10):5977-85. Epub 2001/11/08. PubMed PMID: 11698477.
 31. Rosen H, Gonzalez-Cabrera PJ, Sanna MG, Brown S. Sphingosine 1-phosphate receptor signaling. *Annu Rev Biochem.* 2009;78:743-68. Epub 2009/02/24. doi: 10.1146/annurev.biochem.78.072407.103733. PubMed PMID: 19231986.
 32. Murphy CT, Hall LJ, Hurley G, Quinlan A, MacSharry J, Shanahan F, Nally K, Melgar S. The sphingosine-1-phosphate analogue FTY720 impairs mucosal immunity and clearance of the enteric pathogen *Citrobacter rodentium*. *Infect Immun.* 2012;80(8):2712-23. Epub 2012/05/23. doi: 10.1128/IAI.06319-11. PubMed PMID: 22615252; PubMed Central PMCID: PMC3434556.
 33. Hughes JE, Srinivasan S, Lynch KR, Proia RL, Ferdek P, Hedrick CC. Sphingosine-1-phosphate induces an antiinflammatory phenotype in macrophages. *Circ Res.* 2008;102(8):950-8. Epub 2008/03/08. doi: 10.1161/CIRCRESAHA.107.170779. PubMed PMID: 18323526; PubMed Central PMCID: PMC2875063.
 34. Keul P, Lucke S, von Wnuck Lipinski K, Bode C, Graler M, Heusch G, Levkau B. Sphingosine-1-phosphate receptor 3 promotes recruitment of monocyte/macrophages in inflammation and atherosclerosis. *Circ Res.* 2011;108(3):314-23. Epub 2010/12/18. doi: 10.1161/CIRCRESAHA.110.235028. PubMed PMID: 21164103.
 35. Wang F, Okamoto Y, Inoki I, Yoshioka K, Du W, Qi X, Takuwa N, Gonda K, Yamamoto Y, Ohkawa R, Nishiuchi T, Sugimoto N, Yatomi Y, Mitsumori K, Asano M, Kinoshita M, Takuwa Y. Sphingosine-1-phosphate receptor-2 deficiency leads to inhibition of macrophage proinflammatory activities and atherosclerosis in apoE-deficient mice. *J Clin Invest.* 2010;120(11):3979-95. Epub 2010/10/28. doi: 10.1172/JCI42315. PubMed PMID: 20978351; PubMed Central PMCID: PMC2964972.
 36. Nofer JR, Bot M, Brodde M, Taylor PJ, Salm P, Brinkmann V, van Berkel T, Assmann G, Biessen EA. FTY720, a synthetic sphingosine 1 phosphate analogue, inhibits development of atherosclerosis in low-density lipoprotein receptor-deficient mice. *Circulation.* 2007;115(4):501-8. Epub 2007/01/24. doi: 10.1161/CIRCULATIONAHA.106.641407. PubMed PMID: 17242282.

37. Allende ML, Bektas M, Lee BG, Bonifacino E, Kang J, Tuymetova G, Chen W, Saba JD, Proia RL. Sphingosine-1-phosphate lyase deficiency produces a pro-inflammatory response while impairing neutrophil trafficking. *J Biol Chem*. 2011;286(9):7348-58. Epub 2010/12/22. doi: 10.1074/jbc.M110.171819. PubMed PMID: 21173151; PubMed Central PMCID: PMC3044991.
38. Kim CH, Younossi ZM. Nonalcoholic fatty liver disease: a manifestation of the metabolic syndrome. *Cleveland Clinic journal of medicine*. 2008;75(10):721-8. Epub 2008/10/23. PubMed PMID: 18939388.
39. Wieckowska A, McCullough AJ, Feldstein AE. Noninvasive diagnosis and monitoring of nonalcoholic steatohepatitis: present and future. *Hepatology*. 2007;46(2):582-9. Epub 2007/07/31. doi: 10.1002/hep.21768. PubMed PMID: 17661414.
40. McCullough AJ. Pathophysiology of nonalcoholic steatohepatitis. *Journal of clinical gastroenterology*. 2006;40 Suppl 1:S17-29. Epub 2006/03/17. doi: DOI: 10.1097/01.mcg.0000168645.86658.22. PubMed PMID: 16540762.
41. Gentile CL, Pagliassotti MJ. The role of fatty acids in the development and progression of nonalcoholic fatty liver disease. *The Journal of nutritional biochemistry*. 2008;19(9):567-76. Epub 2008/04/24. doi: 10.1016/j.jnutbio.2007.10.001. PubMed PMID: 18430557; PubMed Central PMCID: PMC2551556.
42. Day CP, James OF. Steatohepatitis: a tale of two "hits"? *Gastroenterology*. 1998;114(4):842-5. Epub 1998/04/18. PubMed PMID: 9547102.
43. Shimabukuro M, Zhou YT, Levi M, Unger RH. Fatty acid-induced beta cell apoptosis: a link between obesity and diabetes. *Proceedings of the National Academy of Sciences of the United States of America*. 1998;95(5):2498-502. PubMed PMID: 9482914; PubMed Central PMCID: PMC19389.
44. Yamazaki T, Sasaki E, Kakinuma C, Yano T, Miura S, Ezaki O. Increased very low density lipoprotein secretion and gonadal fat mass in mice overexpressing liver DGAT1. *The Journal of biological chemistry*. 2005;280(22):21506-14. doi: 10.1074/jbc.M412989200. PubMed PMID: 15797871.
45. Cohen JC, Horton JD, Hobbs HH. Human fatty liver disease: old questions and new insights. *Science*. 2011;332(6037):1519-23. Epub 2011/06/28. doi: 10.1126/science.1204265. PubMed PMID: 21700865; PubMed Central PMCID: PMC3229276.
46. Pagadala M, Kasumov T, McCullough AJ, Zein NN, Kirwan JP. Role of ceramides in nonalcoholic fatty liver disease. *Trends in endocrinology and metabolism: TEM*. 2012;23(8):365-71. doi: 10.1016/j.tem.2012.04.005. PubMed PMID: 22609053; PubMed Central PMCID: PMC3408814.
47. Nikolova-Karakashian M, Karakashian A, Rutkute K. Role of neutral sphingomyelinases in aging and inflammation. *Sub-cellular biochemistry*. 2008;49:469-86. Epub 2008/08/30. doi: 10.1007/978-1-4020-8831-5_18. PubMed PMID: 18751923.
48. Memon RA, Holleran WM, Moser AH, Seki T, Uchida Y, Fuller J, Shigenaga JK, Grunfeld C, Feingold KR. Endotoxin and cytokines increase hepatic sphingolipid biosynthesis and produce lipoproteins enriched in ceramides and sphingomyelin. *Arterioscler Thromb Vasc Biol*. 1998;18(8):1257-65. Epub 1998/08/26. PubMed PMID: 9714132.
49. Shi H, Kokoeva MV, Inouye K, Tzameli I, Yin H, Flier JS. TLR4 links innate immunity and fatty acid-induced insulin resistance. *J Clin Invest*. 2006;116(11):3015-25. Epub 2006/10/21. doi: 10.1172/JCI28898. PubMed PMID: 17053832; PubMed Central PMCID: PMC1616196.
50. Lee JY, Ye J, Gao Z, Youn HS, Lee WH, Zhao L, Sizemore N, Hwang DH. Reciprocal modulation of Toll-like receptor-4 signaling pathways involving MyD88 and phosphatidylinositol 3-kinase/AKT by saturated and polyunsaturated fatty acids. *J Biol*

- Chem. 2003;278(39):37041-51. Epub 2003/07/17. doi: 10.1074/jbc.M305213200. PubMed PMID: 12865424.
51. Lee JY, Sohn KH, Rhee SH, Hwang D. Saturated fatty acids, but not unsaturated fatty acids, induce the expression of cyclooxygenase-2 mediated through Toll-like receptor 4. *J Biol Chem.* 2001;276(20):16683-9. Epub 2001/03/30. doi: 10.1074/jbc.M011695200. PubMed PMID: 11278967.
 52. Wei Y, Wang D, Topczewski F, Pagliassotti MJ. Saturated fatty acids induce endoplasmic reticulum stress and apoptosis independently of ceramide in liver cells. *Am J Physiol Endocrinol Metab.* 2006;291(2):E275-81. Epub 2006/02/24. doi: 10.1152/ajpendo.00644.2005. PubMed PMID: 16492686.
 53. Holland WL, Bikman BT, Wang LP, Yuguang G, Sargent KM, Bulchand S, Knotts TA, Shui G, Clegg DJ, Wenk MR, Pagliassotti MJ, Scherer PE, Summers SA. Lipid-induced insulin resistance mediated by the proinflammatory receptor TLR4 requires saturated fatty acid-induced ceramide biosynthesis in mice. *The Journal of clinical investigation.* 2011;121(5):1858-70. doi: 10.1172/JCI43378. PubMed PMID: 21490391; PubMed Central PMCID: PMC3083776.
 54. Ichi I, Nakahara K, Fujii K, Iida C, Miyashita Y, Kojo S. Increase of ceramide in the liver and plasma after carbon tetrachloride intoxication in the rat. *Journal of nutritional science and vitaminology.* 2007;53(1):53-6. PubMed PMID: 17484380.
 55. Yetukuri L, Katajamaa M, Medina-Gomez G, Seppanen-Laakso T, Vidal-Puig A, Oresic M. Bioinformatics strategies for lipidomics analysis: characterization of obesity related hepatic steatosis. *BMC systems biology.* 2007;1:12. doi: 10.1186/1752-0509-1-12. PubMed PMID: 17408502; PubMed Central PMCID: PMC1839890.
 56. Malhi H, Gores GJ. Molecular mechanisms of lipotoxicity in nonalcoholic fatty liver disease. *Seminars in liver disease.* 2008;28(4):360-9. Epub 2008/10/29. doi: 10.1055/s-0028-1091980. PubMed PMID: 18956292; PubMed Central PMCID: PMC2908270.
 57. Choi SS, Diehl AM. Hepatic triglyceride synthesis and nonalcoholic fatty liver disease. *Curr Opin Lipidol.* 2008;19(3):295-300. Epub 2008/05/08. doi: 10.1097/MOL.0b013e3282ff5e55. PubMed PMID: 18460922.
 58. Holland WL, Brozinick JT, Wang LP, Hawkins ED, Sargent KM, Liu Y, Narra K, Hoehn KL, Knotts TA, Siesky A, Nelson DH, Karathanasis SK, Fontenot GK, Birnbaum MJ, Summers SA. Inhibition of ceramide synthesis ameliorates glucocorticoid-, saturated-fat-, and obesity-induced insulin resistance. *Cell metabolism.* 2007;5(3):167-79. doi: 10.1016/j.cmet.2007.01.002. PubMed PMID: 17339025.
 59. Scherer PE, Williams S, Fogliano M, Baldini G, Lodish HF. A novel serum protein similar to C1q, produced exclusively in adipocytes. *J Biol Chem.* 1995;270(45):26746-9.
 60. Turer AT, Scherer PE. Adiponectin: mechanistic insights and clinical implications. *Diabetologia.* 2012;55(9):2319-26. Epub 2012/06/13. doi: 10.1007/s00125-012-2598-x. PubMed PMID: 22688349.
 61. Yamauchi T, Kamon J, Minokoshi Y, Ito Y, Waki H, Uchida S, Yamashita S, Noda M, Kita S, Ueki K, Eto K, Akanuma Y, Froguel P, Foufelle F, Ferre P, Carling D, Kimura S, Nagai R, Kahn BB, Kadowaki T. Adiponectin stimulates glucose utilization and fatty-acid oxidation by activating AMP-activated protein kinase. *Nat Med.* 2002;8(11):1288-95.
 62. Berg AH, Combs T, Du X, Brownlee M, Scherer PE. The Adipocyte-Secreted Protein Acrp30 Enhances Hepatic Insulin Action. *Nat Med.* 2001;7(8):947-53.
 63. Combs TP, Berg AH, Obici S, Scherer PE, Rossetti L. Endogenous Glucose Production is Inhibited by the Adipose-Derived Protein Acrp30. *J Clin Inv.* 2001;108:1875-81.
 64. Holland WL, Miller RA, Wang ZV, Sun K, Barth BM, Bui HH, Davis KE, Bikman BT, Halberg N, Rutkowski JM, Wade MR, Tenorio VM, Kuo MS, Brozinick JT, Zhang BB, Birnbaum MJ, Summers SA, Scherer PE. Receptor-mediated activation of ceramidase activity initiates the pleiotropic actions of adiponectin. *Nature medicine.* 2011;17(1):55-

63. doi: 10.1038/nm.2277. PubMed PMID: 21186369; PubMed Central PMCID: PMC3134999.
65. Ma H, Gomez V, Lu L, Yang X, Wu X, Xiao SY. Expression of adiponectin and its receptors in livers of morbidly obese patients with non-alcoholic fatty liver disease. *Journal of gastroenterology and hepatology*. 2009;24(2):233-7. Epub 2008/08/21. doi: 10.1111/j.1440-1746.2008.05548.x. PubMed PMID: 18713296.
66. Halberg N, Schraw TD, Wang ZV, Kim JY, Yi J, Hamilton MP, Luby-Phelps K, Scherer PE. Systemic Fate of the Adipocyte-Derived Factor Adiponectin. *Diabetes*. 2009. Epub 2009/07/08. doi: db08-1750 [pii]10.2337/db08-1750. PubMed PMID: 19581422.
67. Zhou H, Summers SA, Birnbaum MJ, Pittman RN. Inhibition of Akt kinase by cell-permeable ceramide and its implications for ceramide-induced apoptosis. *J Biol Chem*. 1998;273(26):16568-75. Epub 1998/06/20. PubMed PMID: 9632728.
68. Summers SA, Garza LA, Zhou H, Birnbaum MJ. Regulation of insulin-stimulated glucose transporter GLUT4 translocation and Akt kinase activity by ceramide. *Mol Cell Biol*. 1998;18(9):5457-64. Epub 1998/08/26. PubMed PMID: 9710629; PubMed Central PMCID: PMC109130.
69. Schwabe RF, Brenner DA. Mechanisms of Liver Injury. I. TNF-alpha-induced liver injury: role of IKK, JNK, and ROS pathways. *Am J Physiol Gastrointest Liver Physiol*. 2006;290(4):G583-9. Epub 2006/03/16. doi: 10.1152/ajpgi.00422.2005. PubMed PMID: 16537970.
70. Summers SA. Ceramides in insulin resistance and lipotoxicity. *Prog Lipid Res*. 2006;45(1):42-72. Epub 2006/02/01. doi: 10.1016/j.plipres.2005.11.002. PubMed PMID: 16445986.
71. Scherer PE. Adipose tissue: from lipid storage compartment to endocrine organ. *Diabetes*. 2006;55(6):1537-45. PubMed PMID: 16731815.
72. Laviola L, Perrini S, Cignarelli A, Giorgino F. Insulin signalling in human adipose tissue. *Archives of physiology and biochemistry*. 2006;112(2):82-8. Epub 2006/08/26. doi: 10.1080/13813450600736174. PubMed PMID: 16931450.
73. Spiegelman BM, Hotamisligil GS. Through thick and thin: wasting, obesity, and TNF α . *Cell*. 1993;73:625-7.
74. Hotamisligil GS, Spiegelman BM. Tumor necrosis factor alpha: a key component of the obesity-diabetes link. *Diabetes*. 1994;43(11):1271-8.
75. Long SD, Pekala PH. Lipid mediators of insulin resistance: ceramide signalling down-regulates GLUT4 gene transcription in 3T3-L1 adipocytes. *Biochem J*. 1996;319 (Pt 1):179-84. Epub 1996/10/01. PubMed PMID: 8870666; PubMed Central PMCID: PMC1217752.
76. Tagami S, Inokuchi Ji J, Kabayama K, Yoshimura H, Kitamura F, Uemura S, Ogawa C, Ishii A, Saito M, Ohtsuka Y, Sakaue S, Igarashi Y. Ganglioside GM3 participates in the pathological conditions of insulin resistance. *J Biol Chem*. 2002;277(5):3085-92. Epub 2001/11/15. doi: 10.1074/jbc.M103705200. PubMed PMID: 11707432.
77. Kolak M, Westerbacka J, Velagapudi VR, Wagsater D, Yetukuri L, Makkonen J, Rissanen A, Hakkinen AM, Lindell M, Bergholm R, Hamsten A, Eriksson P, Fisher RM, Oresic M, Yki-Jarvinen H. Adipose tissue inflammation and increased ceramide content characterize subjects with high liver fat content independent of obesity. *Diabetes*. 2007;56(8):1960-8. Epub 2007/07/11. doi: 10.2337/db07-0111. PubMed PMID: 17620421.
78. Shimabukuro M, Higa M, Zhou YT, Wang MY, Newgard CB, Unger RH. Lipoapoptosis in beta-cells of obese prediabetic fa/fa rats. Role of serine palmitoyltransferase overexpression. *J Biol Chem*. 1998;273(49):32487-90. Epub 1998/11/26. PubMed PMID: 9829981.

79. Boslem E, MacIntosh G, Preston AM, Bartley C, Busch AK, Fuller M, Laybutt DR, Meikle PJ, Biden TJ. A lipidomic screen of palmitate-treated MIN6 beta-cells links sphingolipid metabolites with endoplasmic reticulum (ER) stress and impaired protein trafficking. *Biochem J.* 2011;435(1):267-76. Epub 2011/01/27. doi: 10.1042/BJ20101867. PubMed PMID: 21265737.
80. Veluthakal R, Palanivel R, Zhao Y, McDonald P, Gruber S, Kowluru A. Ceramide induces mitochondrial abnormalities in insulin-secreting INS-1 cells: potential mechanisms underlying ceramide-mediated metabolic dysfunction of the beta cell. *Apoptosis.* 2005;10(4):841-50. Epub 2005/09/01. doi: 10.1007/s10495-005-0431-4. PubMed PMID: 16133874.
81. Maedler K, Spinass GA, Dytar D, Moritz W, Kaiser N, Donath MY. Distinct effects of saturated and monounsaturated fatty acids on beta-cell turnover and function. *Diabetes.* 2001;50(1):69-76. Epub 2001/01/09. PubMed PMID: 11147797.
82. McGavock JM, Lingvay I, Zib I, Tillery T, Salas N, Unger R, Levine BD, Raskin P, Victor RG, Szczepaniak LS. Cardiac steatosis in diabetes mellitus: a 1H-magnetic resonance spectroscopy study. *Circulation.* 2007;116(10):1170-5. Epub 2007/08/19. doi: 10.1161/CIRCULATIONAHA.106.645614. PubMed PMID: 17698735.
83. Christoffersen C, Bollano E, Lindegaard ML, Bartels ED, Goetze JP, Andersen CB, Nielsen LB. Cardiac lipid accumulation associated with diastolic dysfunction in obese mice. *Endocrinology.* 2003;144(8):3483-90. Epub 2003/07/17. PubMed PMID: 12865329.
84. Di Paola M, Cocco T, Lorusso M. Ceramide interaction with the respiratory chain of heart mitochondria. *Biochemistry.* 2000;39(22):6660-8. Epub 2000/06/01. PubMed PMID: 10828984.
85. Bielawska AE, Shapiro JP, Jiang L, Melkonyan HS, Piot C, Wolfe CL, Tomei LD, Hannun YA, Umansky SR. Ceramide is involved in triggering of cardiomyocyte apoptosis induced by ischemia and reperfusion. *Am J Pathol.* 1997;151(5):1257-63. Epub 1997/11/14. PubMed PMID: 9358751; PubMed Central PMCID: PMC1858093.
86. Park TS, Hu Y, Noh HL, Drosatos K, Okajima K, Buchanan J, Tuinei J, Homma S, Jiang XC, Abel ED, Goldberg IJ. Ceramide is a cardiotoxin in lipotoxic cardiomyopathy. *J Lipid Res.* 2008;49(10):2101-12. Epub 2008/06/03. doi: 10.1194/jlr.M800147-JLR200. PubMed PMID: 18515784; PubMed Central PMCID: PMC2533410.
87. Shibata R, Sato K, Pimentel DR, Takemura Y, Kihara S, Ohashi K, Funahashi T, Ouchi N, Walsh K. Adiponectin protects against myocardial ischemia-reperfusion injury through AMPK- and COX-2-dependent mechanisms. *Nat Med.* 2005;11(10):1096-103. Epub 2005/09/13. doi: 10.1038/nm1295. PubMed PMID: 16155579; PubMed Central PMCID: PMC2828682.
88. Zhang Y, Proenca R, Maffei M, Barone M, Leopold L, Friedman JM. Positional cloning of the mouse obese gene and its human homologue. *Nature.* 1994;372(6505):425-32. Epub 1994/12/01. doi: 10.1038/372425a0. PubMed PMID: 7984236.
89. Ahima RS, Prabakaran D, Mantzoros C, Qu D, Lowell B, Maratos-Flier E, Flier JS. Role of leptin in the neuroendocrine response to fasting. *Nature.* 1996;382(6588):250-2. PubMed PMID: 8717038.
90. Maffei M, Halaas J, Ravussin E, Pratley RE, Lee GH, Zhang Y, Fei H, Kim S, Lallone R, Ranganathan S, et al. Leptin levels in human and rodent: measurement of plasma leptin and ob. *Nat Med.* 1995;1(11):1155-61.
91. Halaas JL, Gajiwala KS, Maffei M, Cohen SL, Chait BT, Rabinowitz D, Lallone RL, Burley SK, Friedman JM. Weight-reducing effects of the plasma protein encoded by the obese gene. *Science.* 1995;269(5223):543-6. PubMed PMID: 7624777.

92. Minokoshi Y, Haque MS, Shimazu T. Microinjection of leptin into the ventromedial hypothalamus increases glucose uptake in peripheral tissues in rats. *Diabetes*. 1999;48(2):287-91. Epub 1999/05/20. PubMed PMID: 10334303.
93. Bonzon-Kulichenko E, Schwudke D, Gallardo N, Molto E, Fernandez-Agullo T, Shevchenko A, Andres A. Central leptin regulates total ceramide content and sterol regulatory element binding protein-1C proteolytic maturation in rat white adipose tissue. *Endocrinology*. 2009;150(1):169-78. Epub 2008/09/20. doi: 10.1210/en.2008-0505. PubMed PMID: 18801905.
94. Potthoff MJ, Kliewer SA, Mangelsdorf DJ. Endocrine fibroblast growth factors 15/19 and 21: from feast to famine. *Genes Dev*. 2012;26(4):312-24. Epub 2012/02/04. doi: 10.1101/gad.184788.111. PubMed PMID: 22302876; PubMed Central PMCID: PMC3289879.
95. Zhao Y, Dunbar JD, Kharitonov A. FGF21 as a therapeutic reagent. *Advances in experimental medicine and biology*. 2012;728:214-28. Epub 2012/03/08. doi: 10.1007/978-1-4614-0887-1_14. PubMed PMID: 22396172.
96. Holland WL, Adams AC, Brozinick JT, Bui HH, Miyauchi Y, Kusminski CM, Bauer SM, Wade M, Singhal E, Cheng CC, Volk K, Kuo MS, Gordillo R, Kharitonov A, Scherer PE. An FGF21-adiponectin-ceramide axis controls energy expenditure and insulin action in mice. *Cell Metab*. 2013;17(5):790-7. Epub 2013/05/15. doi: 10.1016/j.cmet.2013.03.019. PubMed PMID: 23663742; PubMed Central PMCID: PMC3667496.
97. Dutchak PA, Katafuchi T, Bookout AL, Choi JH, Yu RT, Mangelsdorf DJ, Kliewer SA. Fibroblast growth factor-21 regulates PPARgamma activity and the antidiabetic actions of thiazolidinediones. *Cell*. 2012;148(3):556-67. Epub 2012/02/07. doi: 10.1016/j.cell.2011.11.062. PubMed PMID: 22304921; PubMed Central PMCID: PMC3273727.
98. Sun K, Kusminski CM, Scherer PE. Adipose tissue remodeling and obesity. *J Clin Invest*. 2011;121(6):2094-101. Epub 2011/06/03. doi: 10.1172/JCI45887. PubMed PMID: 21633177; PubMed Central PMCID: PMC3104761.
99. Kim JY, van de Wall E, Laplante M, Azzara A, Trujillo ME, Hofmann SM, Schraw T, Durand JL, Li H, Li G, Jelicks LA, Mehler MF, Hui DY, Deshaies Y, Shulman GI, Schwartz GJ, Scherer PE. Obesity-associated improvements in metabolic profile through expansion of adipose tissue. *J Clin Invest*. 2007;117(9):2621-37. PubMed PMID: 17717599.
100. Kusminski CM, Holland WL, Sun K, Park J, Spurgin SB, Lin Y, Askew GR, Simcox JA, McClain DA, Li C, Scherer PE. MitoNEET-driven alterations in adipocyte mitochondrial activity reveal a crucial adaptive process that preserves insulin sensitivity in obesity. *Nature medicine*. 2012;18(10):1539-49. doi: 10.1038/nm.2899. PubMed PMID: 22961109; PubMed Central PMCID: PMC3745511.

Figure 1

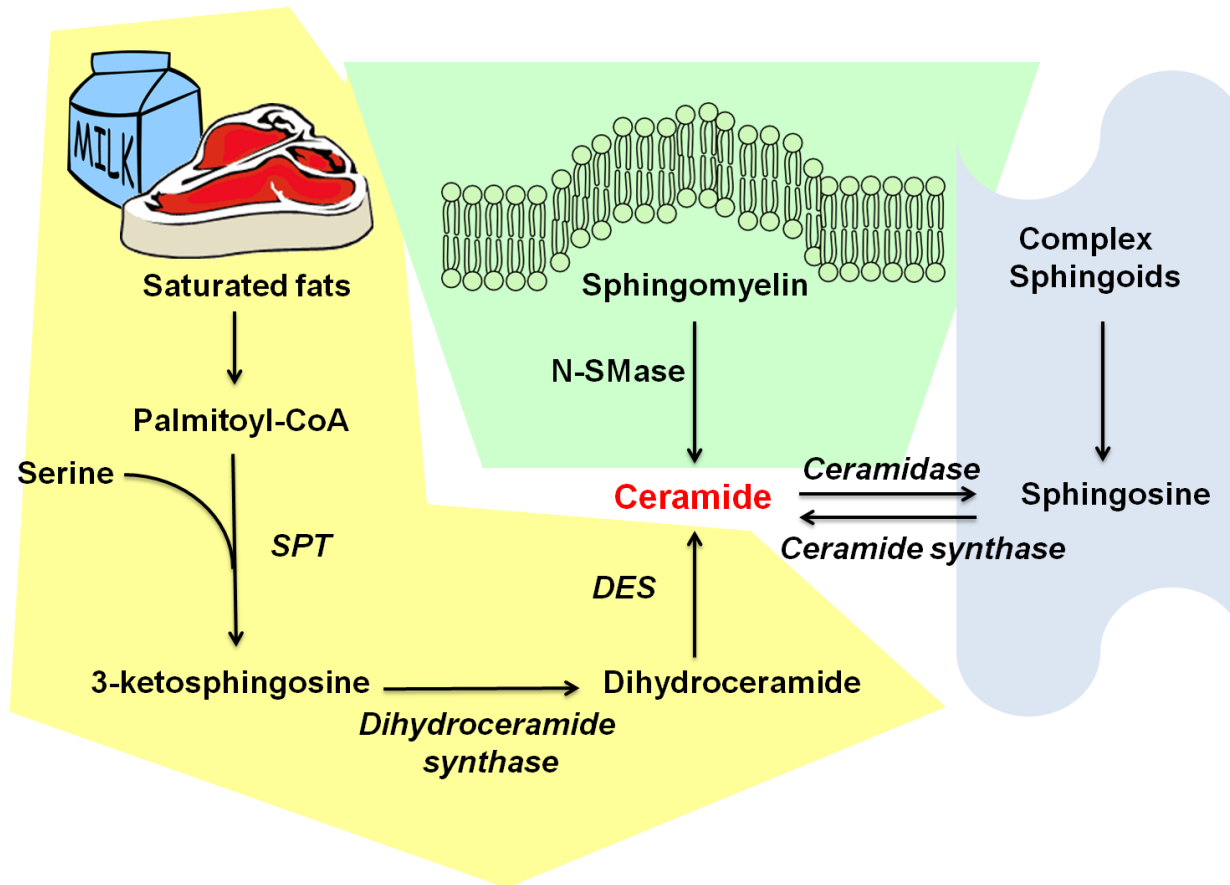


Fig. 1: Ceramides can be synthesized through three different pathways: *de novo* biosynthesis, sphingomyelinase pathway, and the salvage pathway. The *de novo* pathway of ceramide generation is regulated by its rate-limiting enzyme, serine palmitoyl-CoA transferase (SPT). Furthermore, SPT has high specificity for its substrate, palmitoyl-CoA, a saturated fatty acid that is required for the formation of the sphingoid backbone of ceramides. Distinct from the *de novo* pathway, ceramides can also be generated by neutral sphingomyelinase (N-SMase)-catalyzed hydrolysis of sphingomyelin in cell membranes. Finally, ceramides can also be synthesized through the “salvage pathway” by breakdown of complex sphingolipids mediated by ceramide synthase.

Figure 2

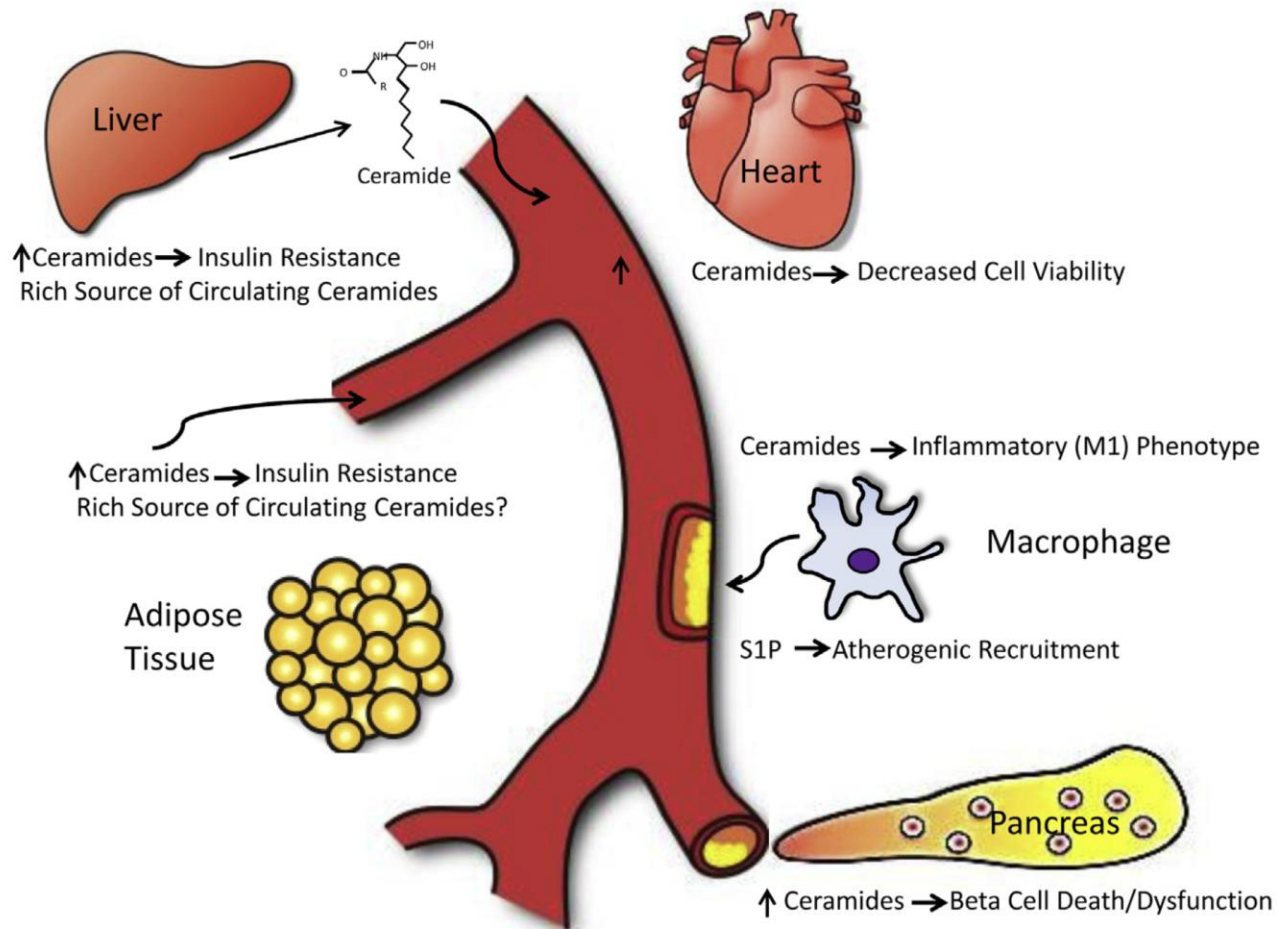


Fig. 2: Overview of the key target tissues and cell types discussed here in the context of metabolic effects of sphingolipids. One of the major unresolved questions remains what the major sources for circulating sphingolipids are and whether there are differences in the tissue origins of different ceramide subspecies circulating in plasma.

Chapter 2

Targeted Induction of Ceramide Degradation Leads to Improved Systemic Metabolism and Reduced Hepatic Steatosis

(The following section is part of a manuscript that is in press)

**Jonathan Y. Xia^{1*}, William L. Holland^{1*}, Christine M. Kusminski¹, Kai Sun¹, Ankit
X. Sharma¹, Mackenzie J. Pearson¹, Angelika J. Sifuentes¹, Jeffrey G. McDonald²,
Ruth Gordillo¹ and Philipp E. Scherer^{1,3†}**

¹Touchstone Diabetes Center, Department of Internal Medicine, The University of
Texas Southwestern Medical Center, Dallas, Texas 75390-8549.

²Department of Molecular Genetics and ³Department of Cell Biology, The
University of Texas Southwestern Medical Center, Dallas, Texas 75390-8549

*Contributed equally to this work

† Correspondence should be addressed to:
Philipp E. Scherer
Touchstone Diabetes Center
Department of Internal Medicine
University of Texas Southwestern Medical Center
5323 Harry Hines Blvd.
Dallas, TX, 75390-8549, USA
E-mail: Philipp.Scherer@utsouthwestern.edu
Tel: 214-648-8715
Fax: 214-648-8720

Abstract

Sphingolipids have garnered attention for their role in insulin resistance and lipotoxic cell death. Aberrant accumulation of ceramides correlates with hepatic insulin resistance and steatosis. To further investigate the tissue-specific effects of local changes in ceramidase activity, we have developed transgenic mice inducibly expressing acid ceramidase, to trigger the deacylation of ceramides. This represents the first inducible genetic model that acutely manipulates ceramides in adult mouse tissues. Hepatic overexpression of acid ceramidase prevents hepatic steatosis and prompts improvements in insulin action in liver and adipose tissue. Conversely, overexpression of acid ceramidase within adipose tissue prevents hepatic steatosis and insulin resistance. Induction of ceramidase activity in either tissue promotes a lowering of hepatic ceramides and reduced activation of the ceramide-activated protein kinase C isoform PKC-zeta. These observations suggest the existence of a rapidly acting "cross-talk" between liver and adipose tissue sphingolipids, critically regulating glucose metabolism and hepatic lipid uptake.

Introduction

The prevalence of non-alcoholic fatty liver disease (NAFLD), an emerging obesity-related disorder that ranges from simple steatosis to the more severe steatohepatitis and cirrhosis, has been steadily rising and becoming a worldwide health issue (1). NAFLD has been reported in 17-33% of the general population, making it one of the most common chronic diseases in the United States (2).

Numerous studies in humans and animals have shown that hepatic steatosis is strongly associated with insulin resistance. Mice challenged with a high-fat diet develop severe insulin resistance and hepatic steatosis (3-5). However, the causal relationship between hepatic steatosis and insulin resistance is unclear and controversial. Murine models with altered hepatic lipid storage (6, 7), mobilization (8-10) and oxidation (11) all exhibit greatly increased hepatic lipid accumulation without accompanying insulin resistance. Conversely, alterations in hepatic insulin signaling are sufficient to induce hepatic steatosis (12). From these studies, a possible explanation for the variable relationship between hepatic steatosis and insulin resistance maybe the existence of unidentified hepatic lipid species or inflammatory mediators that lead to a modulation of insulin sensitivity.

Ceramides are important members of the sphingolipid family and are essential precursors for complex sphingolipids. The potential association of sphingolipids and NAFLD was first revealed by non-biased bioinformatics screens from two independent groups. The Oresic group, using computational and lipidomic approaches applied to rodent models of obesity, identified parallel associations between hepatic triglycerides with ceramides and ceramide biosynthetic pathways (13). Similarly, Yki-Järvinen and

colleagues observed ceramide signaling and metabolism genes to be significantly altered in microarrays of human subjects with extreme steatosis, without histological signs of inflammation (14). These observations were further supported by lipidomic data from patients with steatotic livers revealing significant correlations between liver triglycerides and ceramides, while displaying an inverse relationship of these parameters with the insulin sensitizing adipokine adiponectin (15).

A series of studies have shown that increased ceramide levels in both liver and plasma coincide with the development of liver dysfunction, hepatic insulin resistance, and steatosis in rodents (13, 16, 17). Previous work has identified the liver as a target of ceramide-induced insulin resistance and inhibition of whole-body ceramide synthesis reduces obesity-induced insulin resistance in rodents (18). In particular, ceramides derived from C16 fatty acids appear to oppose insulin action most potently (19, 20). Breakdown of ceramides are initiated by enzymes called ceramidases, which are categorized by homology and pH optima at which they can hydrolyze ceramides into sphingosines and free fatty acids (17). The anti-diabetic and anti-steatotic adipokine, adiponectin rapidly lowers hepatic ceramide content, thereby improving glucose homeostasis through its receptor-associated ceramidase activity (21). Similarly, overexpression of acid ceramidase in cultured cells prevents saturated fatty acids from impairing insulin action in cultured C2C12 myotubes (22).

Previous studies on the role of sphingolipid biosynthetic enzymes in systemic metabolism have employed constitutive gain-of-function or loss-of-function models. However, the usefulness of these constitutive models has been limited by complex phenotypes due to compensatory mechanisms and developmental issues. This is in

part due to the fact that sphingolipids are involved in fundamental cellular signaling processes during development. Cell-specific ablation in some tissues has caused minimal impact on ceramide accumulation (23, 24), likely due to a high level of sphingolipid uptake from the serum. To overcome these issues and to further investigate the physiological effects of an acute increase in ceramidase activity in a tissue-specific manner, we have developed transgenic mice that express acid ceramidase under the control of a tetracycline response element. Using tissue-specific reverse tetracycline transactivators (“rtTA”), we target ceramide degradation specifically in the hepatocyte or adipocyte via taking advantage of albumin (hepatocyte-specific) and adiponectin (adipocyte-specific) promoters, respectively. This allows us to induce ceramide deacylation in response to doxycycline exposure, resulting in the degradation of ceramides made within the cell or following uptake from serum. Both mouse models reveal profound improvements in hepatic steatosis and glucose metabolism with strong evidence for interorgan cross-talk as sphingolipids are shunted back and forth between liver and adipose. Thus, this system enables us, for the first time, to probe the impact of a genetically-induced, acute change in ceramide levels on local and systemic insulin sensitivity.

Results

Overexpression of acid ceramidase in the liver reduces hepatic ceramide levels and improves hepatic and adipose insulin sensitivity.

We and others have previously noted that strategies aimed at whole-body reduction of ceramide biosynthesis improve insulin action. Myriocin, an inhibitor of *de novo* ceramide synthesis, also robustly protects against hepatic steatosis when wildtype

mice are maintained on a high fat diet (**Supplemental Fig. 1A**). To disrupt the over-accumulation of ceramides in the liver, we generated an inducible, liver-specific acid ceramidase transgenic (Alb-AC) mouse, which combines three transgenic lines: the albumin promoter-driven Cre line, a transgenic line carrying a Rosa26 promoter-driven loxP-stop-loxP-reverse tetracycline-controlled transactivator (rtTA) gene (Rosa26-loxP-stop-loxP-rtTA), and a Tet-responsive human acid ceramidase transgenic line (TRE-AC) (**Supplemental Fig. 1B**). In the absence of doxycycline, there is no AC transgene expression in the liver when using a primer set that recognizes both human and mouse acid ceramidase sequences equally well. Upon treatment with doxycycline, AC gene expression in the triple transgenics reaches approximately four times the levels seen in wild-type (WT) littermates. The overexpression is liver-specific, as it is not detected in any other tissues (**Supplemental Fig. 1C**). The increase in hepatic AC mRNA levels resulted in a three-fold increase in acid ceramidase enzyme activity in the liver (**Supplemental Fig. 1D**). Serum ceramidase activity was not changed between WT and Alb-AC mice after doxycycline induction (**Supplemental Fig. 1E**).

To test whether the increased ceramidase activity has a functional impact on ceramide levels in hepatocytes, we challenged the WT and Alb-AC mice with a high fat diet (60% calories from fat) containing 200mg/kg doxycycline (HFD-dox). After 8 weeks of HFD-dox exposure, wildtype mice showed a 2.4 fold increase in hepatic ceramides compared to chow-fed controls (**Supplemental Fig. 1F**). Alb-AC mice showed a significant reduction in C_{16:0} and C_{18:0} hepatic ceramide species (**Fig. 1A**). In parallel, a significant lowering of C_{16:0} and C_{18:0} ceramide species was also observed in the *serum* (**Fig. 1A**). Interestingly, although levels of *liver* sphingoid species did not change

significantly compared to WT except for the levels of sphingosine, *serum* sphingoid species exhibited a sharp decline compared to WT (**Supplemental Fig. 1G**). Since past evidence showing the negative correlation between the signaling lipid diacylglycerol (DAG) and hepatic steatosis and insulin resistance (25), we also measured hepatic levels of DAGs. Surprisingly, we found that levels of DAG in the liver were significantly higher in our Alb-AC mice compared to WT (**Fig. 1B**). Transcriptionally, we found mRNA levels of DGAT1 decreased to 30% of WT, while levels of DGAT2 increased to almost five-fold above WT levels (**Supplemental Fig. 1H**). Serum levels of DAGs were comparable between WT and Alb-AC mice (**Fig. 1B**).

To determine the role of hepatic ceramides in diet-induced obesity and associated metabolic disorders, we exposed Alb-AC and WT littermate control mice to HFD-dox for 8 weeks. Body weights of the mice were monitored on a weekly basis during the HFD feeding period. We observed similar weight gain curves for the Alb-AC and WT mice and comparable body weights at the end of the 8 weeks of HFD-dox exposure (**Supplemental Fig. 1I**). However, compared to WT controls, Alb-AC mice exhibited significantly reduced blood glucose levels during the oral glucose tolerance test (OGTT) (**Fig. 1C**), indicating an improvement in systemic glucose tolerance. Additionally, the plasma insulin levels during the OGTT were also markedly lower in the Alb-AC mice (**Fig. 1D**). Furthermore, HFD-dox-fed Alb-AC mice also had substantially decreased blood glucose levels after insulin injection during an insulin tolerance test (ITT) (**Fig. 1E**), suggesting enhanced insulin sensitivity.

In order to assess the specific tissues that are responsible for improved glucose homeostasis and insulin sensitivity, we performed hyperinsulinemic-euglycemic clamp

studies in a cohort Alb-AC and WT animals. The glucose infusion rate needed to maintain euglycemic conditions (~150 mg/dl) was increased in Alb-AC mice compared to their littermate controls (**Fig. 1F, left panel**), demonstrating that whole-body insulin sensitivity is improved. Whole body glucose disposal was not altered (**Supplemental Fig. 1J**), suggesting minimal effects on muscle insulin action. There were no significant changes in lipolysis between WT and Alb-AC mice under clamped or under insulinopenic conditions where insulin-induced suppression of lipolysis is more pronounced (**Table 1, Supplemental Fig. 1K**). Hepatic glucose production under hyperinsulinemic clamp conditions was suppressed more efficiently in Alb-AC mice (**Fig. 1F, right panel**). Specifically, hyperinsulinemic clamp conditions suppressed hepatic glucose production of Alb-AC mice by ~47% compared to ~15% of WT mice (**Supplemental Fig. 1L**). At the molecular level, insulin signaling in the liver and adipose tissue was assessed by insulin-stimulated phosphorylation of Akt. After an injection of insulin, p-Akt levels were greatly increased in the liver of transgenic animals, reflecting improved insulin sensitivity. Moreover, even though the increase in ceramidase activity is restricted to hepatocytes, insulin-stimulated p-Akt in gonadal adipose tissue was also elevated, indicating enhanced insulin sensitivity at the molecular level in the adipocyte as well (**Fig. 1G**). Consistent with these observations, 2-deoxyglucose uptake during clamped hyperinsulinemic conditions showed that the gonadal (gWAT), subcutaneous (sWAT) and mesenteric (mWAT) fat pads of Alb-AC mice had increased 2-deoxyglucose uptake compared to WT (**Fig. 1H**). Differences in glucose disposal and glucose production could not be explained by minimal differences in body weight or concentrations glucose and insulin during the clamped state (**Table**

1). These data suggest that hepatocyte-specific overexpression of AC attenuates diet-induced systemic insulin resistance by improving insulin sensitivity not only in the liver, but also in adipose tissue.

Overexpression of AC in the hepatocyte prevents HFD-mediated hepatic lipid accumulation and attenuates adipose tissue inflammation and fibrosis.

Prolonged HFD exposure often causes the accumulation of lipids in the liver. While the HFD causes a marked increase in the liver weights of both Alb-AC and WT mice, the livers from Alb-AC mice are qualitatively smaller and less lipid-laden compared to WT (**Fig. 2A, left**). Consistent with this observation, the weights of the Alb-AC mouse livers were lower than that of WT mice, even after normalizing to body weight (**Fig. 2A, right**). Histologically, the Alb-AC liver exhibited substantially less lipid accumulation compared to that of the WT control (**Fig. 2B, left**). Mirroring the histological findings, Alb-AC mice exhibited almost a three-fold decrease in hepatic triglyceride (TG) content compared to WT mice (**Fig. 2B, right**). These findings show that hepatic ceramide levels play an important role in the accumulation of ectopic lipids in the liver.

In order to assess the effects of liver overexpression of AC on *systemic* lipid homeostasis, we performed a triglyceride clearance test by gavaging a lipid emulsion (20% Intralipid) to both Alb-AC and WT mice. The WT mice had the expected hyperlipidemic excursion after the gavage. Surprisingly, the Alb-AC mice peaked at higher levels and had a lower rate of triglyceride clearance compared to WT mice as observed by consistently higher levels of serum triglycerides during the seven-hour

period after gavage (**Fig. 2C**). To determine whether AC overexpression affected hepatic VLDL production, mice were fasted for 3 hours followed by intravenous injection of tyloxapol, a potent inhibitor of capillary lipoprotein lipase. Alb-AC mice had higher plasma TG levels compared to WT mice two hours post-injection, indicating that the rate of VLDL production in Alb-AC mice is markedly higher compared to WT mice (**Fig. 2D**). To further investigate the role of hepatic AC expression in lipid metabolism, we intravenously injected a ^3H -triolein tracer into Alb-AC and WT mice which allows for assessments of lipid storage and β oxidation rates in different tissues. Alb-AC mice have a reduced lipid uptake in the liver compared to WT mice; concurrent increases were observed in the gonadal and brown fat pads (**Fig. 2E**). Lipid oxidation was not significantly altered (**Supplemental Fig. 2A**). These findings suggest that local changes in hepatic ceramide influence the development of NAFLD through decreased uptake of fatty acids and an increased release of VLDL.

In order to determine how overexpression of AC ameliorates hepatic steatosis, we performed microarray analyses on liver tissues specifically at 2 weeks post induction and then at 2 months post induction of the AC transgene in the *liver*. A *reduction* of genes in fatty acid (FA) synthesis and uptake pathways was evident. Quantitative PCR analyses confirmed the reduction in FA synthesis genes (ACC, FAS, Scd-1, Elovl5, and SREBP-1a) and FA uptake genes (CD36, FATP2, FATP5, L-FABP) by the end of week 8 (**Supplemental Fig. 2B & C**). Surprisingly, qPCR of the fatty acid synthesis genes and fatty acid uptake genes in *gWAT* showed a corresponding *increase* during this same period (**Supplemental Fig. 2B & C**).

Other than its striking effects on the liver, one noticeable observation was the differences in fat pad distribution in Alb-AC mice compared to WT mice when challenged with HFD-dox. Visually and quantitatively, Alb-AC gWAT was substantially larger than the corresponding pads in WT mice after HFD-dox challenge when normalized to body weight, while the mWAT of Alb-AC was relatively smaller than its counterpart in WT littermates (**Supplemental Fig. 2D & E**). Furthermore, whole body NMR data shows that the overall composition of fat and lean mass in Alb-AC and WT mice are comparable (**Supplemental Fig. 2F**), thus suggesting that changes in fat pad weights are the result of redistribution rather than an overall increase or decrease of overall adipose tissue mass. This leads to the rather surprising observation that the gonadal versus the mesenteric fat pads differentially respond to altered hepatic ceramidase activity.

Given the close association between obesity, insulin resistance, adipose tissue inflammation and fibrosis, we evaluated gonadal adipose tissue for histological differences (**Fig. 2F**). While WT mice on HFD-dox displayed crown-like structures characteristic of immune infiltration, Alb-AC fat pads showed far fewer signs of inflammation. Mac-2 immunohistochemistry staining confirmed that Alb-AC fat pads had greatly reduced levels of infiltrated macrophages compared to those of WT. In addition, we found markedly less fibrosis in the fat pads of Alb-AC compared to their WT counterparts, as determined by trichrome staining (**Fig. 2F**). Expression of several inflammatory or fibrosis markers in white adipose tissue (WAT) of HFD-fed Alb-AC and WT mice were also different. Expression of inflammatory cytokines such as TNF- α , IL-6, and IL-10 were substantially reduced in the gWAT of Alb-AC mice (**Supplemental**

Fig. 2G). Furthermore, fibrosis markers such as Col1 α , Col3 α , and Col6 α 1 were also lower in the gWAT of Alb-AC mice compared to WT (**Supplemental Fig. 2H**). Considering the link between ceramides and inflammation, we examined the levels of ceramides in the gWAT of HFD-dox-fed Alb-AC and WT mice. We found that dihydroceramides and hexosyl-ceramide species to be significantly lowered in Alb-AC mice after HFD-dox challenge compared to WT controls, while other ceramide species remained unaltered (**Fig. 2G**). Furthermore, there are no significant alterations in specific chain lengths of gWAT ceramides (**Supplemental Fig. 2I**). Moreover, gWAT sphingoid species levels, especially sphingosine and sphinganine, were also significantly lowered in Alb-AC mice compared to WT (**Fig. 2H**). Correspondingly, ceramide synthesis pathway genes (SPT2, SK1, CerS6) were found to be significantly *reduced* in the gWAT of Alb-AC mice compared to WT at the end of 8 weeks of HFD-dox feeding (**Supplemental Fig. 2J**). By contrast, examination by qPCR of the genes in the ceramide synthesis pathway in the Alb-AC *liver* showed a profound *increase* in several ceramide synthase (CerS) genes including CerS2, CerS5, and CerS6. In contrast, CerS1 expression was significantly reduced (**Supplemental Fig. 2J**).

Combined, these observations suggest that acid ceramidase-induced lowering of hepatic ceramides leads to a profound response directly in the liver, as well as in adipose tissues, ultimately resulting in much healthier fat pads.

Acid Ceramidase Overexpression in White Adipose Tissue Improves Glucose Metabolism.

By crossing the Tet-responsive acid ceramidase transgenic line (TRE-AC) with an adiponectin-rtTA transgenic allele (Art) we were able to achieve inducible overexpression of acid ceramidase (Art-AC) within multiple WAT depots (**Supplemental Fig. 3A**). Upon doxycycline induction, AC overexpression is achieved exclusively in the fat pads and remains unchanged in other tissues, such as the liver (**Supplemental Fig. 3B**). In the absence of doxycycline, overexpression was not detected, but acid ceramidase expression rose 3.5-fold following exposure to doxycycline in the diet (200 mg/kg, 10 days, **Supplemental Fig. 3C**). This corresponded to a 1.8, 1.3, and 3.7-fold increase in acid ceramidase activity in sWAT, gWAT, and mWAT respectively, without alterations in hepatic ceramidase activity (**Supplemental Fig. 3D**). Furthermore, serum ceramidase activity in WT and Art-AC were not significantly altered (**Supplemental Fig. 3E**). The lack of ceramide hydrolysis was further confirmed with C17 ceramide, showing no alterations in hepatic ceramidase activity (**Supplemental Fig. 3F**). On a doxycycline-enriched chow diet, several ceramide subspecies were significantly reduced in mWAT, while total ceramides were significantly decreased in the liver (**Supplemental Fig. 3G & H**). Concomitant decreases in fasting glucose and glucose excursion during oral glucose tolerance tests were evident (**Supplemental Fig. 3I**) without any changes in body weight (34.4±3.1 versus 32.7±3.3 for wildtype and Art-AC, respectively).

When challenged with a high fat diet, Art-AC transgenic mice have a marked ability to maintain normal glucose homeostasis. Total ceramides were reduced in

mesenteric (67%), gonadal (40%) and subcutaneous (30%) fat pads, with C16 and C18 ceramides showing the most consistent and robust changes (**Fig. 3A**). Serum sphingolipid species were also altered (**Fig. 3B**). Specifically, serum levels of C_{20:0} ceramides were reduced to 42% of WT levels (**Supplemental Fig. 3J**). Glucose levels were lower during the fasted state and following an oral glucose challenge (**Fig. 3C**), while insulin levels remained markedly lower during fasting and 15 minutes following glucose administration (**Fig. 3D**). Improvements in insulin sensitivity were confirmed by the enhanced lowering of glucose upon insulin administration (**Fig. 3E**) and occurred without changes in body weight (40.0±5.0 versus 38.4±6.1 for wildtype and Art-AC, respectively). The improvements in whole-body glucose homeostasis and insulin sensitivity could hardly be explained by the relatively minor contribution of adipose to glucose disposal. To address this more specifically, we performed hyperinsulinemic-euglycemic clamps to assess the tissue-specific contributions to improvements in glucose disposal. The glucose infusion rate required to maintain euglycemia was markedly higher in Art-AC transgenic mice, confirming improvements in whole body insulin sensitivity (**Fig. 3F**). The kinetics of ³H-glucose disposal were not altered, suggesting negligible changes in insulin stimulated glucose disposal by muscle (**Supplemental Fig. 3K**). Rather, Art-AC transgenic mice showed improvements in the ability of insulin to suppress endogenous glucose production (**Fig. 3G**). Specifically, endogenous glucose production was suppressed by ~60% in Art-AC compared to ~15% in WT (**Supplemental 3L**). These improvements in insulin sensitivity could not be explained by changes in body weight, circulating insulin during the clamped state, or variations in the achieved glucose concentrations during the clamped state (**Table 1**).

Furthermore, there were no significant changes in lipolysis between WT and Art-AC mice under clamped or insulinopenic conditions (**Table 1, Supplemental Fig. 3M**). Consistent with the improved capacity for insulin to suppress hepatic glucose efflux, enhanced insulin-stimulated phosphorylation of Akt was present in livers of these mice 30-minutes after insulin stimulation (**Fig. 3H**). Lowering ceramides in adipose also enhanced insulin-stimulated phosphorylation of Akt in gonadal fat pads, while changes in total Akt expression were not altered in either tissue (**Fig. 3H**). Consistent with increased Akt phosphorylation in adipose, the rate of 2-deoxyglucose uptake doubled in gonadal, mesenteric and subcutaneous fat of Art-AC transgenic mice (**Fig. 3I**). These robust changes in whole-body glucose homeostasis therefore include contributions from adipose tissue, but appear largely governed by improvements in hepatic insulin action.

Acid Ceramidase Overexpression in White Adipose Tissue Improves Hepatic Lipid Accumulation.

Since the accumulation of ceramide in adipose tissue is closely associated with inflammation and fibrosis, we evaluated gonadal adipose tissue for histological differences (**Fig. 4A**). While WT mice on HFD-dox displayed crown-like structures characteristic of immune infiltration, Art-AC fat pads showed far fewer signs of inflammation. Mac-2 immunohistochemistry staining confirmed that Art-AC fat pads had greatly reduced levels of infiltrated macrophages compared to those of WT. In addition, we found markedly less fibrosis in the fat pads of Art-AC compared to their WT counterparts, as determined by trichrome staining (**Fig. 4A**). Correspondingly, mRNA levels of TNF- α and pro-fibrotic genes (Col1 α 1, Col3 α 1, Col6 α 1) were found to be notably lowered in WAT compared to WT (**Supplemental Fig. 4A**)

Considering the fact that overexpression of AC in the *liver* resulted in improvements in *adipose* tissue metabolic health, we wanted to examine if the reverse is also true. Dissection of the livers of the Art-AC transgenic mice clearly revealed less steatotic livers, judged by both overall appearance and color (**Fig 4B, left**). Hepatomegaly caused by a high fat diet is diminished by transgene overexpression in adipose tissue (**Fig 4B, right**). Lowering of hepatic triglyceride content was also evident histologically (**Fig. 4C, left**). Transgene overexpression in adipose tissue decreased hepatic triglyceride accumulation on chow diet by 45% (**Supplemental Fig. 4B**) and caused a 57% decrease in hepatic triglyceride while on high-fat diet (**Fig. 4C, right**). To determine if the lowering of ceramides alters liver homeostasis by enhancing the storage capacity of the adipocyte to protect the liver from excess FFA exposure, we evaluated lipid metabolism in more detail. Neither fatty acids (**Table 1**) nor serum triglycerides (**Fig. 4D**) were different during the basal state. During hyperinsulinemic clamps, Art-AC mice showed a trend toward improved suppression of lipolysis ($p=0.06$), as serum fatty acids trended lower in Art-AC transgenic mice during the clamped state (**Table 1**). By contrast, no changes in glycerol were apparent in the clamped state. Following lipid gavage, the triglyceride clearance was not different between WT and Art-AC transgenic mice (**Fig. 4D**). Hepatic secretion of triglyceride was not affected by adipose-restricted expression of acid ceramidase (**Fig 4E**). In a complimentary approach, uptake of tritiated oleate was not significantly altered in any of the fat pads evaluated following an intravenous bolus of ^3H -Triolein (**Fig. 4F**). Lipid oxidation was not altered in any of the tissues evaluated (**Supplemental Fig. 4C**). Unlike adipose tissues, livers of transgenic mice displayed a 3.8-fold decrease in lipid uptake (**Fig. 4F**).

Furthermore, levels of C_{16:0} and C_{18:0} ceramide species were also markedly lower in Art-AC compared to WT (**Fig. 4G**). Hepatic diacylglycerols were not significantly altered (**Supplemental Fig. 4D**). Collectively, these experiments suggested that lowering of ceramides in adipose tissue affects hepatic lipid accumulation by altering hepatic lipid uptake, not by altering hepatic exposure to free fatty acids released from the adipocytes.

Adipose-specific ceramidase reverses insulin resistance and hepatic steatosis more rapidly than liver-specific ceramidase induction.

To determine whether the induction of AC in the liver or adipose is able to reverse impairments in total body glucose metabolism and *rescue* hepatic steatosis, Alb-AC, Art-AC, and WT mice were first fed a doxycycline-free HFD for 2 months to facilitate the development of hepatic steatosis prior to transgene induction. At the end of the 2 months, diets were switched to HFD-dox to induce AC overexpression. Approximately one month after transgene induction in the *liver*, we found C_{16:0} and C_{18:0} ceramide levels to be appreciably lowered along with concurrent improvements in insulin signaling, as indicated by increased phosphorylation of Akt (**Fig. 5A & B**). Furthermore, hepatic lipid accumulation was significantly lowered 4-weeks after inducing overexpression of the transgene in the liver (**Fig. 5C**). An insulin tolerance test does not reveal any changes 3 days post induction of AC in the liver (**Fig. 5D**). Our data not only showed that the effects of the transgene take about one month to result in significant physiological effects, but also that the local overexpression of AC in the liver can rescue livers with severe steatosis *after* the steatosis has fully developed.

Overexpression of AC within the adipocyte offers a much more rapid rescue of insulin resistance and hepatic steatosis. C16 and C18 hepatic ceramides are substantially decreased within 3 days of treatment (**Fig. 5E**). Western blotting for p-Akt in the liver of Art-AC mice shows improvements in p-Akt levels upon insulin administration within as short as three days post induction of AC (**Fig. 5F**). Within 3 days of transgene activation in the adipocyte, hepatic triglyceride content is lower and continues to improve substantially throughout the 4-week doxycycline treatment (**Fig. 5G**). Remarkably, insulin-stimulated lowering of blood glucose is improved compared to wildtype littermates during insulin tolerance tests after just 3 days (**Fig. 5H**). Collectively, these data show the ability of ceramidase to overcome previously established metabolic perturbations promoted by diet-induced obesity, with slightly different kinetics depending on whether we express AC in hepatocytes or in adipocytes.

Ceramides influence hepatic lipid uptake via PKC ζ -mediated influence on CD36, and AC downregulates lipid uptake and fatty acid synthesis genes in the liver.

Livers from Alb-AC and Art-AC mice showed comparable decreases in expression of CD36 as compared to WT littermates (**Fig. 6A**). The relative abundance of hepatic CD36 protein was also clearly reduced in both Art-AC and Alb-AC transgenic mice (**Fig. 6B**).

In addition to their roles as mediators of ceramide-induced insulin resistance, atypical PKCs have been noted to relay critical signals for lipogenesis and lipid uptake (26-29). As such, we hypothesized that an aPKC may play a critical role in governing the influence of ceramides on hepatic steatosis. Consistent with this, aPKC expression

(**Fig. 6C**) and activity (**Fig. 6D**) were decreased in the livers of Alb-AC and Art-AC transgenic mice. Furthermore, aPKC activity was significantly lowered in Art-AC mice after only three days of doxycycline treatment (**Supplemental Fig. 6A**).

Since aPKCs can play a permissive role in CD36 translocation, we evaluated the propensity for ceramide to facilitate lipid uptake. In cultured H4Ile hepatocyte cells, a 1 hour pre-incubation with the short chain ceramide analog C2-ceramide was sufficient to stimulate a 63% increase in palmitate uptake (**Fig. 6E**) and markedly enhanced aPKC activity (**Fig. 6F**). Incubation of cells with C2-ceramide yielded the same lipid uptake results as when cells were pretreated with palmitate, which promotes the formation of endogenous ceramides intracellularly (**Supplemental Fig. 6B**). To evaluate the requirement for aPKC in this effect, we blocked aPKC activation by including a myristoylated PKC ζ pseudosubstrate inhibitor which completely prevented ceramide-induced lipid uptake, as it prevented ceramide from activating PKC ζ (**Fig. 6E and F**). To confirm this genetically, we achieved overexpression of dominant negative (dn)PKC ζ or expression of constitutively active (ca)PKC ζ via transient transfection. Following overexpression with dnPKC ζ , C2-ceramide failed to stimulate PKC ζ activity in cells expressing dnPKC ζ , and it also failed to stimulate lipid uptake. By contrast, overexpression of (ca)PKC ζ stimulated PKC ζ activity to the same degree as C2-ceramide, and was sufficient to increase palmitate uptake, but could not be further enhanced by ceramide addition (**Fig. 6E and F**). Immunohistological staining of H4Ile cells grown in glass bottom culture dishes showed that treatment with C2-ceramide resulted in both an increase in CD36 translocation to the membrane as judged by an increase in plasma membrane localized intensity of CD36 signal compared to cells

treated with DMSO (**Fig. 6G**). Following overexpression with dnPKC ζ , C2-ceramide failed to stimulate CD36 translocation to the membrane, as there is no change between plasma membrane localized intensity of CD36 signal between C2-ceramide and DMSO treated cells (**Fig. 6G**). Conversely, overexpression of (ca)PKC ζ in H4Ile cells resulted in an increase in CD36 translocation to the membrane, treatment with C2-ceramide of the (ca)PKC ζ transfected cells did not increase the signal intensity of CD36 in the plasma membrane (**Fig. 6G**). As sphingosine, a byproduct of the ceramidase reaction is a known inhibitor of multiple PKCs we also evaluated the propensity for sphingosine to alter α PKC activation and lipid uptake. Incubation of H4Ile cells with sphingosine, rather than ceramide impaired α PKC activity (**Supplemental Fig. 6C**) and diminished palmitate uptake (**Supplemental Fig. 6D**).

To confirm our findings *in vivo*, we first induced hepatic steatosis in Alb-AC and Art-AC mice and their littermate controls with four weeks of HFD feeding. We subsequently injected both the transgenic and WT mice with either PBS or 2-acetyl-1,3-cyclopentanedione (ACPD), a known PKC ζ inhibitor demonstrated in previous studies to effectively reduce PKC ζ activity (30), and compared the results with WT and transgenic mice fed a doxycycline diet. For the Alb-AC cohort, we found that injection of ACPD for one month in WT and Alb-AC mice resulted in the same improvements in insulin sensitivity and reduction in hepatic lipid accumulation as Alb-AC mice fed a HFD-dox diet for the same time (**Fig. 6H and I**). Similarly, injection of ACPD in Art-AC and WT mice resulted in a more rapid improvement in insulin sensitivity and hepatic lipid accumulation after three days of injection, mimicking the effects of three days of HFD-dox diet in Art-AC mice (**Fig. 6H and I**). Overall, these data show that diminishing

excessive activation of aPKC is capable of reducing the effects of ceramide-induced insulin resistance and lipid accumulation both *in vitro* and *in vivo*.

Discussion

Here, we report the first mouse models demonstrating inducible decreases of ceramide within the liver and adipose. The use of an adiponectin promoter-driven rtTA (Art) has allowed us to evaluate the adipocyte-specific contributions of sphingolipids to whole-body metabolic dysfunction for the first time. Our inducible acid ceramidase model bypasses the compensatory mechanisms and developmental issues present in constitutive models, and gives us the opportunity to study acute modifications of ceramide-induced metabolic dysfunction in adult mice. With this system, we demonstrate that the acute depletion of ceramide in hepatocytes or adipocytes of adult mice can prevent and reverse the development of hepatic steatosis while simultaneously improving systemic glucose tolerance and insulin sensitivity in adult mice with diet-induced obesity. These studies highlight the prominent cross-talk between the liver and adipose tissue that allows for equilibration of sphingolipids between the two tissues. Furthermore, these studies are the first to define a causal role for ceramide in the pathogenesis of diet-induced NAFLD.

We found that that C_{16:0} and C_{18:0} ceramide levels to be 50% of WT in Alb-AC mice livers, indicating that the hepatic accumulation of particular ceramide subspecies more prominently contributes to the development of NAFLD and systemic insulin resistance. Consistent with our findings, recent work has shown that mice with ceramide synthase 6 deficiency (*cerS6^{Δ/Δ}*) exhibit reduced C_{16:0} ceramide levels and are protected from high fat diet-induced obesity and glucose intolerance (20). By contrast, heterozygous deletion of ceramide synthase 2 promotes a paradoxical increase in C_{16:0} ceramides to confer greater susceptibility to diet induced insulin resistance (19).

Importantly, we also observed that concurrent with the lowering of hepatic ceramides, hepatic DAG levels were *increased* in our Alb-AC mice to almost double of those measured in WT mice. In line with several studies, these findings further question the role of liver DAGs as a causative agent of hepatic steatosis and insulin resistance (6, 8, 9, 31, 32). Nonetheless, this does not rule out the possibility that a particular DAG subspecies (i.e. sn-1,2-diacylglycerols) is able to induce hepatic steatosis and insulin resistance under certain conditions (33). Thus, these studies directly link excess accumulation of hepatic ceramide to the development of non-alcoholic fatty liver disease and systemic insulin resistance in rodents.

Elevated circulating ceramides are observed in patients with type 2 diabetes and these levels correlate with the severity of insulin resistance (34-36). Whether plasma ceramides are a contributor or merely a marker of systemic insulin resistance has been unresolved. We show that when ceramide species are acutely broken down in liver and adipose of obese mice, there is also a corresponding significant lowering of plasma ceramides. Past studies have suggested the liver as the major source of plasma ceramides due to the fact that they are contained in various lipoprotein particles (35, 37). Thus, our current findings not only suggest that the liver can be a major contributor of circulating ceramide species, but also reveal that the adipocyte may also contribute substantially to changes in serum ceramides. While it appears likely that these two tissues shuttle a common pool of sphingolipids back and forth through the circulation, it remains uncertain if the adipose supplies the liver with ceramides- where they can be repackaged into lipoprotein particles. Alternatively, each of these tissues may function as a sink whereby excess circulating ceramides may be taken up from the circulation for

storage or metabolism. Furthermore, these findings point to the notion that plasma ceramide levels reflect changes in hepatic ceramide levels and are valuable markers of hepatic metabolic health.

Many past studies have focused on the crosstalk between liver and adipose tissue in the development of obesity and metabolic syndrome. Past work has shown that impaired liver interleukin-6 signaling leads to not only hepatic insulin resistance but also defects in insulin action in adipose tissue (38). Similarly, in liver specific toll-like receptor 4 (TLR4) knockout mice, we have shown that changes in hepatic TLR4 prompt profound reduction in adipose tissue inflammation (39). Our model also induced changes on this hepato-adipo axis. Overexpression of hepatic AC in our model results in alterations of adipose tissue ceramide levels which in turn resulted in redistribution of lipids to different fat pads and reduction of inflammation and fibrosis in WAT both transcriptionally and histologically. Considering that TLR4 is an upstream signaling component required for saturated fatty acid-induced ceramide biosynthesis in liver (40) and both models presented here result in profound reduction in WAT inflammation, perhaps the mechanism of action for this hepato-adipo crosstalk might be similar between these two models. Whether these changes are due to specific circulating sphingolipid populations or a unknown powerful hepatokine is not known. However, the fact that changes in hepatic ceramide levels result in changes in adipose tissue ceramide levels could be a reflection of the altered contributions of the hepatocyte or respectively the adipocyte to circulating ceramide pools, which in turn are subject to cellular uptake.

The roles of atypical PKCs as mediators of ceramide-induced insulin resistance have been previously reported. In particular, C16 ceramides are potent activators of PKC ζ activity *in vitro* (41). Specifically, in cultured muscle cell lines PKC ζ can phosphorylate the pleckstrin homology domain of Akt on threonine residue 34 (42). This phosphorylation site alters the affinity for Akt to 3,4,5-trisphosphate, thus interfering with Akt translocation to plasma membrane microdomains where it is activated (43). A recent report by the Farese group suggests that aberrant activation of atypical PKC, is evident in livers of Lep^{ob/ob} mice and is essential for impairments in Akt mediated signaling to FoxO1; this is rescued *in vivo* by pharmacological inhibition of atypical PKCs (30). PKC ζ has also attracted attention for its role in lipid homeostasis, particularly as a mediator of SREBP-1c driven lipogenesis (26-28). Moreover, PKC ζ has also been previously noted to play a facilitative role in CD36 activation to promote lipid uptake into cardiomyocytes (29). We show here, for the first time, that targeted manipulation of ceramide alters atypical PKC activation in the liver, which can critically influence lipid uptake and lipogenic programs. As such, our data support the notion that ceramides may be a causal effector of selective insulin resistance by driving atypical PKC activation and associated lipogenic and lipid uptake processes, while simultaneously impairing Akt-mediated regulation of hepatic glucose output. The contribution of sphingoid bases to this process is intriguing, as sphingosine can stimulate or suppress PKC ζ activation, depending on the dosage (41). Here, we note the potential of sphingosine to impair the activation of aPKC and prevent lipid uptake. The rapid release of sphingosine from the adipocyte into the portal circulation for delivery to the liver may explain how adipose-specific ceramidase activation exerts

more rapid beneficial effects on the liver. In this context, sphingosine may act as a “lipokine” capable of signaling to diminish lipid uptake. Of note, mice globally lacking sphingosine phosphate lyase, which irreversibly degrades the sphingolipid backbone, develop fatty livers in concert with ceramide over-accumulation without changes in sphingosine (44).

Collectively, our data suggest that the accumulation of ceramides is critical in the development of non-alcoholic fatty liver disease and hepatic insulin resistance in mice with diet-induced obesity. Our data also demonstrate that the induction of AC activity rescues existing hepatic steatosis and metabolic syndrome in mice with diet induced obesity, suggesting that it is a potential therapeutic target. Strategies for AC enzyme replacement have been under development for the treatment of Farber Disease (AC deficiency) (45), and this may provide additional benefits in the form of systemic metabolic improvements. Past clinical data has shown that serum adiponectin levels inversely correlate with hepatic triglyceride content (46). Considering that adiponectin’s main target tissue is the liver and it is known to confer ceramidase activity through its receptors AdipoR1 and R2, we expect adiponectin to exert similar effects as seen for our acid ceramidase transgene, such as reducing hepatic triglyceride accumulation and improving hepatic insulin sensitivity (21). Thus, orally active small-molecule adiponectin receptor agonists, such as AdipoRon, could potentially be an important therapeutic agent for patients with non-alcoholic fatty liver disease and its related metabolic syndrome (47).

Author contributions

JYX and WLH are co-first authors. JYX designed the studies, carried out the research, interpreted the results, and wrote the manuscript related to AC expression in the liver. WLH designed the studies, carried out the research, interpreted the results, and wrote the manuscript related to AC expression in the adipocyte. CMK, KS, AXS, MJP, AJS, JGM and RG assisted in study design, performed research, and reviewed the manuscript. PES designed the study, analysed the data, reviewed and revised the manuscript, and is responsible for the integrity of this work. All authors approved the final version of the manuscript

Acknowledgements

We thank Dr. Bob Hammer and the Transgenic Core Facility at UTSW for the generation of the transgenic lines, John Shelton and the Histology Core for assistance with histology and the UTSW Metabolic Core Unit for help in phenotyping. We would also like to thank Shimadzu Scientific Instruments for the collaborative effort and the expert advice on the mass spec instrumentation side. Supported by the National Institutes of Health (grants R01-DK55758, R01-DK099110 and P01DK088761-01 to PES). JYX is supported by a NIH fellowship 1F30-DK100095. WLH is supported by a K99-DK094973, JDRF Award 5-CDA-2014-185-A-N, and an AHA Beginning Grant in Aid 12BGI-A8910006. CMK was supported by a fellowship from the Juvenile Diabetes Foundation (JDRF 3-2008-130). The authors declare no conflicts of interest.

References

1. Browning JD, Horton JD. Molecular mediators of hepatic steatosis and liver injury. *The Journal of clinical investigation*. 2004;114(2):147-52. doi: 10.1172/JCI22422. PubMed PMID: 15254578; PubMed Central PMCID: PMC449757.
2. Pagadala M, Kasumov T, McCullough AJ, Zein NN, Kirwan JP. Role of ceramides in nonalcoholic fatty liver disease. *Trends in endocrinology and metabolism: TEM*. 2012;23(8):365-71. doi: 10.1016/j.tem.2012.04.005. PubMed PMID: 22609053; PubMed Central PMCID: PMC3408814.
3. Shimomura I, Bashmakov Y, Ikemoto S, Horton JD, Brown MS, Goldstein JL. Insulin selectively increases SREBP-1c mRNA in the livers of rats with streptozotocin-induced diabetes. *Proceedings of the National Academy of Sciences of the United States of America*. 1999;96(24):13656-61. PubMed PMID: 10570128; PubMed Central PMCID: PMC24120.
4. Shimomura I, Bashmakov Y, Horton JD. Increased levels of nuclear SREBP-1c associated with fatty livers in two mouse models of diabetes mellitus. *The Journal of biological chemistry*. 1999;274(42):30028-32. PubMed PMID: 10514488.
5. Birkenfeld AL, Shulman GI. Nonalcoholic fatty liver disease, hepatic insulin resistance, and type 2 diabetes. *Hepatology*. 2014;59(2):713-23. doi: 10.1002/hep.26672. PubMed PMID: 23929732; PubMed Central PMCID: PMC3946772.
6. Monetti M, Levin MC, Watt MJ, Sajan MP, Marmor S, Hubbard BK, Stevens RD, Bain JR, Newgard CB, Farese RV, Sr., Hevener AL, Farese RV, Jr. Dissociation of hepatic steatosis and insulin resistance in mice overexpressing DGAT in the liver. *Cell metabolism*. 2007;6(1):69-78. doi: 10.1016/j.cmet.2007.05.005. PubMed PMID: 17618857.
7. Yu XX, Murray SF, Pandey SK, Booten SL, Bao D, Song XZ, Kelly S, Chen S, McKay R, Monia BP, Bhanot S. Antisense oligonucleotide reduction of DGAT2 expression improves hepatic steatosis and hyperlipidemia in obese mice. *Hepatology*. 2005;42(2):362-71. doi: 10.1002/hep.20783. PubMed PMID: 16001399.
8. Minehira K, Young SG, Villanueva CJ, Yetukuri L, Oresic M, Hellerstein MK, Farese RV, Jr., Horton JD, Preitner F, Thorens B, Tappy L. Blocking VLDL secretion causes hepatic steatosis but does not affect peripheral lipid stores or insulin sensitivity in mice. *Journal of lipid research*. 2008;49(9):2038-44. doi: 10.1194/jlr.M800248-JLR200. PubMed PMID: 18515909; PubMed Central PMCID: PMC3837456.
9. Brown JM, Betters JL, Lord C, Ma Y, Han X, Yang K, Alger HM, Melchior J, Sawyer J, Shah R, Wilson MD, Liu X, Graham MJ, Lee R, Crooke R, Shulman GI, Xue B, Shi H, Yu L. CGI-58 knockdown in mice causes hepatic steatosis but prevents diet-induced obesity and glucose intolerance. *Journal of lipid research*. 2010;51(11):3306-15. doi: 10.1194/jlr.M010256. PubMed PMID: 20802159; PubMed Central PMCID: PMC2952571.
10. Hoy AJ, Bruce CR, Turpin SM, Morris AJ, Febbraio MA, Watt MJ. Adipose triglyceride lipase-null mice are resistant to high-fat diet-induced insulin resistance despite reduced energy expenditure and ectopic lipid accumulation. *Endocrinology*. 2011;152(1):48-58. doi: 10.1210/en.2010-0661. PubMed PMID: 21106876.
11. Monsenego J, Mansouri A, Akkaoui M, Lenoir V, Esnous C, Fauveau V, Tavernier V, Girard J, Prip-Buus C. Enhancing liver mitochondrial fatty acid oxidation capacity in obese mice improves insulin sensitivity independently of hepatic steatosis. *Journal of hepatology*. 2012;56(3):632-9. doi: 10.1016/j.jhep.2011.10.008. PubMed PMID: 22037024.
12. Taniguchi CM, Ueki K, Kahn R. Complementary roles of IRS-1 and IRS-2 in the hepatic regulation of metabolism. *The Journal of clinical investigation*. 2005;115(3):718-27. doi: 10.1172/JCI23187. PubMed PMID: 15711641; PubMed Central PMCID: PMC548317.

13. Yetukuri L, Katajamaa M, Medina-Gomez G, Seppanen-Laakso T, Vidal-Puig A, Oresic M. Bioinformatics strategies for lipidomics analysis: characterization of obesity related hepatic steatosis. *BMC systems biology*. 2007;1:12. doi: 10.1186/1752-0509-1-12. PubMed PMID: 17408502; PubMed Central PMCID: PMC1839890.
14. Greco D, Kotronen A, Westerbacka J, Puig O, Arkkila P, Kiviluoto T, Laitinen S, Kolak M, Fisher RM, Hamsten A, Auvinen P, Yki-Jarvinen H. Gene expression in human NAFLD. *American journal of physiology Gastrointestinal and liver physiology*. 2008;294(5):G1281-7. doi: 10.1152/ajpgi.00074.2008. PubMed PMID: 18388185.
15. Kolak M, Westerbacka J, Velagapudi VR, Wagsater D, Yetukuri L, Makkonen J, Rissanen A, Hakkinen AM, Lindell M, Bergholm R, Hamsten A, Eriksson P, Fisher RM, Oresic M, Yki-Jarvinen H. Adipose tissue inflammation and increased ceramide content characterize subjects with high liver fat content independent of obesity. *Diabetes*. 2007;56(8):1960-8. Epub 2007/07/11. doi: 10.2337/db07-0111. PubMed PMID: 17620421.
16. Ichi I, Nakahara K, Fujii K, Iida C, Miyashita Y, Kojo S. Increase of ceramide in the liver and plasma after carbon tetrachloride intoxication in the rat. *Journal of nutritional science and vitaminology*. 2007;53(1):53-6. PubMed PMID: 17484380.
17. Xia JY, Morley TS, Scherer PE. The adipokine/ceramide axis: key aspects of insulin sensitization. *Biochimie*. 2014;96:130-9. doi: 10.1016/j.biochi.2013.08.013. PubMed PMID: 23969158; PubMed Central PMCID: PMC3859861.
18. Holland WL, Brozinick JT, Wang LP, Hawkins ED, Sargent KM, Liu Y, Narra K, Hoehn KL, Knotts TA, Siesky A, Nelson DH, Karathanasis SK, Fontenot GK, Birnbaum MJ, Summers SA. Inhibition of ceramide synthesis ameliorates glucocorticoid-, saturated-fat-, and obesity-induced insulin resistance. *Cell metabolism*. 2007;5(3):167-79. doi: 10.1016/j.cmet.2007.01.002. PubMed PMID: 17339025.
19. Raichur S, Wang ST, Chan PW, Li Y, Ching J, Chaurasia B, Dogra S, Ohman MK, Takeda K, Sugii S, Pewzner-Jung Y, Futerman AH, Summers SA. CerS2 Haploinsufficiency Inhibits beta-Oxidation and Confers Susceptibility to Diet-Induced Steatohepatitis and Insulin Resistance. *Cell metabolism*. 2014;20(4):687-95. doi: 10.1016/j.cmet.2014.09.015. PubMed PMID: 25295789.
20. Turpin SM, Nicholls HT, Willmes DM, Mourier A, Brodessaer S, Wunderlich CM, Mauer J, Xu E, Hammerschmidt P, Bronneke HS, Trifunovic A, LoSasso G, Wunderlich FT, Kornfeld JW, Bluher M, Kronke M, Bruning JC. Obesity-Induced CerS6-Dependent C16:0 Ceramide Production Promotes Weight Gain and Glucose Intolerance. *Cell metabolism*. 2014;20(4):678-86. doi: 10.1016/j.cmet.2014.08.002. PubMed PMID: 25295788.
21. Holland WL, Miller RA, Wang ZV, Sun K, Barth BM, Bui HH, Davis KE, Bikman BT, Halberg N, Rutkowski JM, Wade MR, Tenorio VM, Kuo MS, Brozinick JT, Zhang BB, Birnbaum MJ, Summers SA, Scherer PE. Receptor-mediated activation of ceramidase activity initiates the pleiotropic actions of adiponectin. *Nature medicine*. 2011;17(1):55-63. doi: 10.1038/nm.2277. PubMed PMID: 21186369; PubMed Central PMCID: PMC3134999.
22. Chavez JA, Knotts TA, Wang LP, Li G, Dobrowsky RT, Florant GL, Summers SA. A role for ceramide, but not diacylglycerol, in the antagonism of insulin signal transduction by saturated fatty acids. *The Journal of biological chemistry*. 2003;278(12):10297-303. doi: 10.1074/jbc.M212307200. PubMed PMID: 12525490.
23. Li Z, Li Y, Chakraborty M, Fan Y, Bui HH, Peake DA, Kuo MS, Xiao X, Cao G, Jiang XC. Liver-specific deficiency of serine palmitoyltransferase subunit 2 decreases plasma sphingomyelin and increases apolipoprotein E levels. *The Journal of biological chemistry*. 2009;284(39):27010-9. doi: 10.1074/jbc.M109.042028. PubMed PMID: 19648608; PubMed Central PMCID: PMC2785386.

24. Lee SY, Kim JR, Hu Y, Khan R, Kim SJ, Bharadwaj KG, Davidson MM, Choi CS, Shin KO, Lee YM, Park WJ, Park IS, Jiang XC, Goldberg IJ, Park TS. Cardiomyocyte specific deficiency of serine palmitoyltransferase subunit 2 reduces ceramide but leads to cardiac dysfunction. *The Journal of biological chemistry*. 2012;287(22):18429-39. doi: 10.1074/jbc.M111.296947. PubMed PMID: 22493506; PubMed Central PMCID: PMC3365730.
25. Shulman GI. Ectopic fat in insulin resistance, dyslipidemia, and cardiometabolic disease. *The New England journal of medicine*. 2014;371(12):1131-41. doi: 10.1056/NEJMra1011035. PubMed PMID: 25229917.
26. Taniguchi CM, Kondo T, Sajan M, Luo J, Bronson R, Asano T, Farese R, Cantley LC, Kahn CR. Divergent regulation of hepatic glucose and lipid metabolism by phosphoinositide 3-kinase via Akt and PKC λ /zeta. *Cell metabolism*. 2006;3(5):343-53. doi: 10.1016/j.cmet.2006.04.005. PubMed PMID: 16679292.
27. Sajan MP, Standaert ML, Rivas J, Miura A, Kanoh Y, Soto J, Taniguchi CM, Kahn CR, Farese RV. Role of atypical protein kinase C in activation of sterol regulatory element binding protein-1c and nuclear factor kappa B (NF κ B) in liver of rodents used as a model of diabetes, and relationships to hyperlipidaemia and insulin resistance. *Diabetologia*. 2009;52(6):1197-207. doi: 10.1007/s00125-009-1336-5. PubMed PMID: 19357831.
28. Sajan MP, Standaert ML, Miura A, Kahn CR, Farese RV. Tissue-specific differences in activation of atypical protein kinase C and protein kinase B in muscle, liver, and adipocytes of insulin receptor substrate-1 knockout mice. *Molecular endocrinology*. 2004;18(10):2513-21. doi: 10.1210/me.2004-0045. PubMed PMID: 15256535.
29. Luiken JJ, Ouwens DM, Habets DD, van der Zon GC, Coumans WA, Schwenk RW, Bonen A, Glatz JF. Permissive action of protein kinase C-zeta in insulin-induced CD36- and GLUT4 translocation in cardiac myocytes. *The Journal of endocrinology*. 2009;201(2):199-209. doi: 10.1677/JOE-09-0046. PubMed PMID: 19273501.
30. Sajan MP, Ivey RA, Lee MC, Farese RV. Hepatic insulin resistance in ob/ob mice involves increases in ceramide, atypical PKC activity and selective impairment of Akt-dependent FoxO1 phosphorylation. *Journal of lipid research*. 2014. doi: 10.1194/jlr.M052977. PubMed PMID: 25395359.
31. Voshol PJ, Haemmerle G, Ouwens DM, Zimmermann R, Zechner R, Teusink B, Maassen JA, Havekes LM, Romijn JA. Increased hepatic insulin sensitivity together with decreased hepatic triglyceride stores in hormone-sensitive lipase-deficient mice. *Endocrinology*. 2003;144(8):3456-62. doi: 10.1210/en.2002-0036. PubMed PMID: 12865325.
32. Farese RV, Jr., Zechner R, Newgard CB, Walther TC. The problem of establishing relationships between hepatic steatosis and hepatic insulin resistance. *Cell metabolism*. 2012;15(5):570-3. doi: 10.1016/j.cmet.2012.03.004. PubMed PMID: 22560209; PubMed Central PMCID: PMC3767424.
33. Boni LT, Rando RR. The nature of protein kinase C activation by physically defined phospholipid vesicles and diacylglycerols. *The Journal of biological chemistry*. 1985;260(19):10819-25. PubMed PMID: 3161882.
34. Haus JM, Kashyap SR, Kasumov T, Zhang R, Kelly KR, Defronzo RA, Kirwan JP. Plasma ceramides are elevated in obese subjects with type 2 diabetes and correlate with the severity of insulin resistance. *Diabetes*. 2009;58(2):337-43. doi: 10.2337/db08-1228. PubMed PMID: 19008343; PubMed Central PMCID: PMC2628606.
35. Boon J, Hoy AJ, Stark R, Brown RD, Meex RC, Henstridge DC, Schenk S, Meikle PJ, Horowitz JF, Kingwell BA, Bruce CR, Watt MJ. Ceramides contained in LDL are elevated in type 2 diabetes and promote inflammation and skeletal muscle insulin resistance. *Diabetes*. 2013;62(2):401-10. Epub

- 2012/11/10. doi: 10.2337/db12-0686. PubMed PMID: 23139352; PubMed Central PMCID: PMC3554351.
36. Lopez X, Goldfine AB, Holland WL, Gordillo R, Scherer PE. Plasma ceramides are elevated in female children and adolescents with type 2 diabetes. *Journal of pediatric endocrinology & metabolism* : JPEM. 2013;26(9-10):995-8. doi: 10.1515/jpem-2012-0407. PubMed PMID: 23612696.
 37. Wiesner P, Leidl K, Boettcher A, Schmitz G, Liebisch G. Lipid profiling of FPLC-separated lipoprotein fractions by electrospray ionization tandem mass spectrometry. *Journal of lipid research*. 2009;50(3):574-85. doi: 10.1194/jlr.D800028-JLR200. PubMed PMID: 18832345.
 38. Wunderlich FT, Strohle P, Konner AC, Gruber S, Tovar S, Bronneke HS, Juntti-Berggren L, Li LS, van Rooijen N, Libert C, Berggren PO, Bruning JC. Interleukin-6 signaling in liver-parenchymal cells suppresses hepatic inflammation and improves systemic insulin action. *Cell metabolism*. 2010;12(3):237-49. doi: 10.1016/j.cmet.2010.06.011. PubMed PMID: 20816090.
 39. Jia L, Vianna CR, Fukuda M, Berglund ED, Liu C, Tao C, Sun K, Liu T, Harper MJ, Lee CE, Lee S, Scherer PE, Elmquist JK. Hepatocyte Toll-like receptor 4 regulates obesity-induced inflammation and insulin resistance. *Nature communications*. 2014;5:3878. doi: 10.1038/ncomms4878. PubMed PMID: 24815961; PubMed Central PMCID: PMC4080408.
 40. Holland WL, Bikman BT, Wang LP, Yuguang G, Sargent KM, Bulchand S, Knotts TA, Shui G, Clegg DJ, Wenk MR, Pagliassotti MJ, Scherer PE, Summers SA. Lipid-induced insulin resistance mediated by the proinflammatory receptor TLR4 requires saturated fatty acid-induced ceramide biosynthesis in mice. *The Journal of clinical investigation*. 2011;121(5):1858-70. doi: 10.1172/JCI43378. PubMed PMID: 21490391; PubMed Central PMCID: PMC3083776.
 41. Muller G, Ayoub M, Storz P, Rennecke J, Fabbro D, Pfizenmaier K. PKC zeta is a molecular switch in signal transduction of TNF-alpha, bifunctionally regulated by ceramide and arachidonic acid. *The EMBO journal*. 1995;14(9):1961-9. PubMed PMID: 7744003; PubMed Central PMCID: PMC398295.
 42. Powell DJ, Hajduch E, Kular G, Hundal HS. Ceramide disables 3-phosphoinositide binding to the pleckstrin homology domain of protein kinase B (PKB)/Akt by a PKCzeta-dependent mechanism. *Molecular and cellular biology*. 2003;23(21):7794-808. PubMed PMID: 14560023; PubMed Central PMCID: PMC207567.
 43. Fox TE, Houck KL, O'Neill SM, Nagarajan M, Stover TC, Pomianowski PT, Unal O, Yun JK, Naides SJ, Kester M. Ceramide recruits and activates protein kinase C zeta (PKC zeta) within structured membrane microdomains. *The Journal of biological chemistry*. 2007;282(17):12450-7. doi: 10.1074/jbc.M700082200. PubMed PMID: 17308302.
 44. Bektas M, Allende ML, Lee BG, Chen W, Amar MJ, Remaley AT, Saba JD, Proia RL. Sphingosine 1-phosphate lyase deficiency disrupts lipid homeostasis in liver. *The Journal of biological chemistry*. 2010;285(14):10880-9. doi: 10.1074/jbc.M109.081489. PubMed PMID: 20097939; PubMed Central PMCID: PMC2856294.
 45. Schuchman EH, Galanin I. Development of enzyme replacement therapy for Farber disease and other disorders with ceramide storage. *Mol Genet Metab*. 2014;111(2):S94-S. doi: DOI 10.1016/j.ymgme.2013.12.229. PubMed PMID: WOS:000330746000218.
 46. Turer AT, Browning JD, Ayers CR, Das SR, Khera A, Vega GL, Grundy SM, Scherer PE. Adiponectin as an independent predictor of the presence and degree of hepatic steatosis in the Dallas Heart Study. *The Journal of clinical endocrinology and metabolism*. 2012;97(6):E982-6. doi: 10.1210/jc.2011-3305. PubMed PMID: 22438228.
 47. Okada-Iwabuchi M, Yamauchi T, Iwabuchi M, Honma T, Hamagami K, Matsuda K, Yamaguchi M, Tanabe H, Kimura-Someya T, Shirouzu M, Ogata H, Tokuyama K, Ueki K, Nagano T, Tanaka A,

- Yokoyama S, Kadowaki T. A small-molecule AdipoR agonist for type 2 diabetes and short life in obesity. *Nature*. 2013;503(7477):493-9. doi: 10.1038/nature12656. PubMed PMID: 24172895.
48. Bedia C, Camacho L, Abad JL, Fabrias G, Levade T. A simple fluorogenic method for determination of acid ceramidase activity and diagnosis of Farber disease. *Journal of lipid research*. 2010;51(12):3542-7. doi: 10.1194/jlr.D010033. PubMed PMID: 20871013; PubMed Central PMCID: PMC2975727.
 49. Kusminski CM, Holland WL, Sun K, Park J, Spurgin SB, Lin Y, Askew GR, Simcox JA, McClain DA, Li C, Scherer PE. MitoNEET-driven alterations in adipocyte mitochondrial activity reveal a crucial adaptive process that preserves insulin sensitivity in obesity. *Nature medicine*. 2012;18(10):1539-49. doi: 10.1038/nm.2899. PubMed PMID: 22961109; PubMed Central PMCID: PMC3745511.
 50. Livak KJ, Schmittgen TD. Analysis of relative gene expression data using real-time quantitative PCR and the 2(-Delta Delta C(T)) Method. *Methods*. 2001;25(4):402-8. Epub 2002/02/16. doi: 10.1006/meth.2001.1262. PubMed PMID: 11846609.
 51. Ye R, Holland WL, Gordillo R, Wang M, Wang QA, Shao M, Morley TS, Gupta RK, Stahl A, Scherer PE. Adiponectin is essential for lipid homeostasis and survival under insulin deficiency and promotes beta-cell regeneration. *eLife*. 2014;3. doi: 10.7554/eLife.03851. PubMed PMID: 25339419; PubMed Central PMCID: PMC4228265.
 52. Sajan MP, Acevedo-Duncan ME, Standaert ML, Ivey RA, Lee M, Farese RV. Akt-dependent phosphorylation of hepatic FoxO1 is compartmentalized on a WD40/ProF scaffold and is selectively inhibited by aPKC in early phases of diet-induced obesity. *Diabetes*. 2014;63(8):2690-701. doi: 10.2337/db13-1863. PubMed PMID: 24705403; PubMed Central PMCID: PMC4113067.
 53. Soh JW, Weinstein IB. Roles of specific isoforms of protein kinase C in the transcriptional control of cyclin D1 and related genes. *The Journal of biological chemistry*. 2003;278(36):34709-16. doi: 10.1074/jbc.M302016200. PubMed PMID: 12794082.
 54. Chou MM, Hou W, Johnson J, Graham LK, Lee MH, Chen CS, Newton AC, Schaffhausen BS, Toker A. Regulation of protein kinase C zeta by PI 3-kinase and PDK-1. *Current biology : CB*. 1998;8(19):1069-77. PubMed PMID: 9768361.

Methods and Materials

Animals

All animal experimental protocols were approved by the Institutional Animal Care and Use Committee of University of Texas Southwestern Medical Center at Dallas. TRE-AC mice were generated by subcloning the mouse AC gene into a plasmid containing the TetO element. Following linearization, the construct was injected into C57/Bl6-derived blastocysts. Transgene-positive offspring were genotyped using PCR with the following primer sets: TRE-AC, 5'-GACTGTATTCAACCTTGATG and 5'-CATCTTCCCATTCTAAACAAC.

The *Rosa26-loxP-stop-loxP-rtTA* and *Albumin-Cre* mice were lines were obtained from Jackson Laboratories. *Albumin-Cre* mice were bred with the *Rosa26-loxP-stop-loxP-rtTA* mice to achieve liver-specific expression of rtTA. This mouse was subsequently crossed to the TRE-AC transgenic mice. The resulting triple transgenic mice expressed AC in liver only after exposure to doxycycline (Dox). All overexpression experiments were performed in a pure C57/Bl6 background. All experiments were conducted using littermate-controlled male mice. All Dox-chow diet (200 mg/kg Dox) or HFD-Dox (200 mg/kg Dox) experiments were initiated at approximately 6-16 weeks of age.

Acid ceramidase activity assay

Acid ceramidase activity was determined by a fluorimetric assay using the substrate Rbm 14-12, a synthetic ceramide analog that possess a 12-carbon fatty acid chain length, at 20 uM after incubation for 3 hours with tissue lysates (20 ug protein) of both wild-type mice (WT) and Alb-AC mice after 8 weeks of HFD-dox (48).

Systemic tests

For OGTTs, mice were fasted for 3 hours prior to administration of glucose (2.5 g/kg body-weight by gastric gavage). At the indicated time-points, venous blood samples were collected in heparin-coated capillary tubes from the tail-vein. Glucose levels were measured using an oxidase-peroxidase assay (Sigma-Aldrich). Mice did not have access to food throughout the experiment. Glucose levels were determined using an oxidase-peroxidase assay (Sigma-Aldrich). Insulin levels were measured using commercial ELISA kits (Millipore Linco Research). For triglyceride clearance, mice were fasted overnight (~15 h), then gavaged with 15 ul/g body weight of 20% intralipid (Fresenius Kabi Clyton, L.P.). Blood was collected hourly and then assayed for triglyceride (Infinity, Thermo Fisher Scientific). In the hepatic VLDL-TG production assay, mice were fasted for 5 hours, followed by intravenous injection of 10% tyloxapol (Sigma-Aldrich) at 500 mg/kg body weight. Blood was collected hourly and then assayed for plasma triglyceride. The lipolysis suppression assay was initiated by i.p. injection of bovine insulin (0.1 mU/g) and serum was collected at 0, 15, 30, 60, and 120 mins for glycerol assays.

Hyperinsulinemic-euglycemic clamps

Hyperinsulinemic-euglycemic clamps were performed on conscious, unrestrained male C57 black WT and Alb-AC mice, as previously described (21, 49).

³H-triolein uptake and β -oxidation

For measurements of endogenous triolein clearance rates, tissue-specific lipid uptake and β -oxidation rates in transgenic tissues, methodologies were adapted from previously detailed studies. Briefly, ³H-triolein was tail-vein injected (2 uCi per mouse in

100 ul of 5% intralipid) into mice after a 5-hour fast. Briefly, blood samples (10 ul) were then collected at 1, 2, 5, 10 and 15 min after injection. At 20 minutes following injection, mice were euthanized, blood samples were taken and tissues were quickly excised, weighed and frozen at -80°C until processing. Lipids were then extracted using a chloroform-to-methanol based extraction method. The radioactivity content of tissues, including blood samples, was quantified as described previously (49).

Quantitative real-time PCR

Tissues were excised from mice and snap-frozen in liquid nitrogen. Total RNA was isolated following tissue homogenization in Trizol (Invitrogen, Carlsbad, CA) using a TissueLyser (MagNA Lyser, Roche), then isolated using an RNeasy RNA extraction kit (Qiagen). The quality and quantity of the RNA was determined by absorbance at 260/280 nm. cDNA was prepared by reverse transcribing 1 ug of RNA with an iScript cDNA Synthesis Kit (BioRad). **Supplementary Table 1** details the primer sequences that were utilized for quantitative RT-PCR. Results were calculated using the threshold cycle method (50), with β -actin used for normalization.

Histology, immunohistochemistry (IHC) and immunofluorescence (IF)

The relevant adipose and liver tissues were excised and fixed in 10% PBS-buffered formalin for 24 h. Following paraffin embedding and sectioning (5 μm), tissues were stained with H&E or a Masson's trichrome stain. For IHC, paraffin-embedded sections were stained using monoclonal antibodies to Mac2 (1:500, CL8942AP, CEDARLANE Laboratories USA Inc.). For IF, cells were grown on glass bottom culture dishes (MatTek Corporation) and were stained with polyclonal antibodies to CD36 (1:200, Novus Biologicals, USA).

Immunoblotting

Frozen tissue was homogenized in TNET buffer (50 mM Tris-HCl, pH 7.6, 150 mM NaCl, 5 mM EDTA, phosphatase inhibitors (Sigma-Aldrich) and protease inhibitors (Roche) and then centrifuged to remove any adipose layer present. After the addition of Triton X-100 (final concentration of 1%), protein concentrations were determined using a bicinchoninic acid assay (BCA) kit (Pierce). Proteins were resolved on 4–20% TGX gel (Bio-Rad) then transferred to nitrocellulose membranes (Protran). pAkt (Ser473, 4060) and total Akt (2920) (Cell Signaling Technology, Inc.) were used (1:1,000) for insulin signaling studies. Anti-CD36 (Novus Biologicals, USA) and anti-PKC ζ (Santa Cruz, USA) polyclonal antibodies were used (1:1000) for Westerns and immunoprecipitations. Primary antibodies were detected using secondary IgG labeled with infrared dyes emitting at 700 nm (926-32220) or 800 nm (926-32211) (both at 1:5,000 dilutions) (Li-Cor Bioscience) and then visualized on a Li-Cor Odyssey infrared scanner (Li-Cor Bioscience). The scanned data were analyzed and quantitated using Odyssey Version 2.1 software (Li-Cor Bioscience).

Lipid quantifications

Sphingolipids were quantified as described previously by LC/ESI/MS/MS using a Shimadzu Nexera X2 UHPLC system coupled to a Shimadzu LCMS-8050 triple quadrupole mass spectrometer (21). Diacylglycerol and C17 FFA were quantified using an ABI 5600+ (AB Sciex) following direct infusion of extracted lipids containing 18 mM ammonium fluoride to aid in ionization of neutrals and to reduce salt adducts. Data from the AB Sciex 5600+ was collected and calibrated with Analyst and PeakView Software

(AB Sciex, Framingham, MA). Lipid species were identified based on exact mass and fragmentation patterns, and verified by lipid standards.

Streptozotocin (STZ) administration

Mice were fasted for 6 hrs and subjected to a single i.p. injection of streptozotocin (STZ, Sigma #S1030, St. Louis, MO) at the dose of 135 ug/g BW. STZ was stored at -20 °C as powder, and freshly diluted in ice-cold sodium citrate buffer (0.1M, pH 4.5) before injection as previously described (51).

aPKC inhibitor

Inhibitor of aPKCs, PKC- η and PKC- ζ , 2-acetyl-1,3-cyclopentanedione (ACPD), was purchased from Sigma (St. Louis, MO). Its specificity was reported previously (52). In addition, we presently found that ACPD did not inhibit kinases, Akt2, FGFR1/2/3/4, mTOR, GSK3 β , IRAK1/4, JAK1/2, MEK1, ERK1/2, JNK1/2, PKA, Src, ROCK2, ROS1, or PI3K α/β , as tested by Life Technologies (Madison WI). Alb-AC and WT controls were injected subcutaneously daily with ACPD (10 mg/kg) in PBS or PBS only for one month. Art-AC and WT controls were injected subcutaneously daily with ACPD (10 mg/kg) in PBS or PBS only for 3 days.

Cell culture

H4IIE rat hepatoma cells were cultured in low glucose DMEM supplemented with 10% fetal bovine serum. Dominant negative PKC ζ (53) and caPKC ζ (54) were purchased from Addgene (Cambridge MA) and transfections were performed with lipofectamine 3000 (Invitrogen, Grand Island NY) according to the manufacturer's instructions. For experiments, cells were grown to 90-100% confluence in 6 well culture dishes. Cells were removed into serum-free media supplemented with 0.2% fatty acid-

free BSA for 90 minutes in the presence or absence of PKC ζ pseudosubstrate inhibitor. Following 90-minute stepdown from serum cells were stimulated with C2-ceramide (100 μ M) or sphingosine (50 μ M) for 60 minutes. For lipid uptake, palmitate 50 μ M 3 μ Ci was included for 5 minutes. Cells were washed 3x in ice cold PBS and harvested in triton-free TNET. Then, 10 μ L of homogeneous lysate was counted. To evaluate background, a set of cells was harvested immediately after addition of palmitate for each experiment. Remaining TNET was processed for western blot confirmation of PKC ζ overexpression, and for PKC ζ activity assays.

In vitro PKC ζ activity assay

Reactions for atypical PKC activity were performed as reported previously (28, 29, 41). PKC ζ peptide substrate was purchased from ENZO life sciences (Farmingdale, NY).

Statistics

All results are provided as means \pm s.e.m. All statistical analyses were performed using GraphPad Prism. Differences between the two groups over time (indicated in the relevant figure legends) were determined by a two-way analysis of variance for repeated measures. For comparisons between two independent groups, a Student's *t* test was used. Significance was accepted at $P < 0.05$.

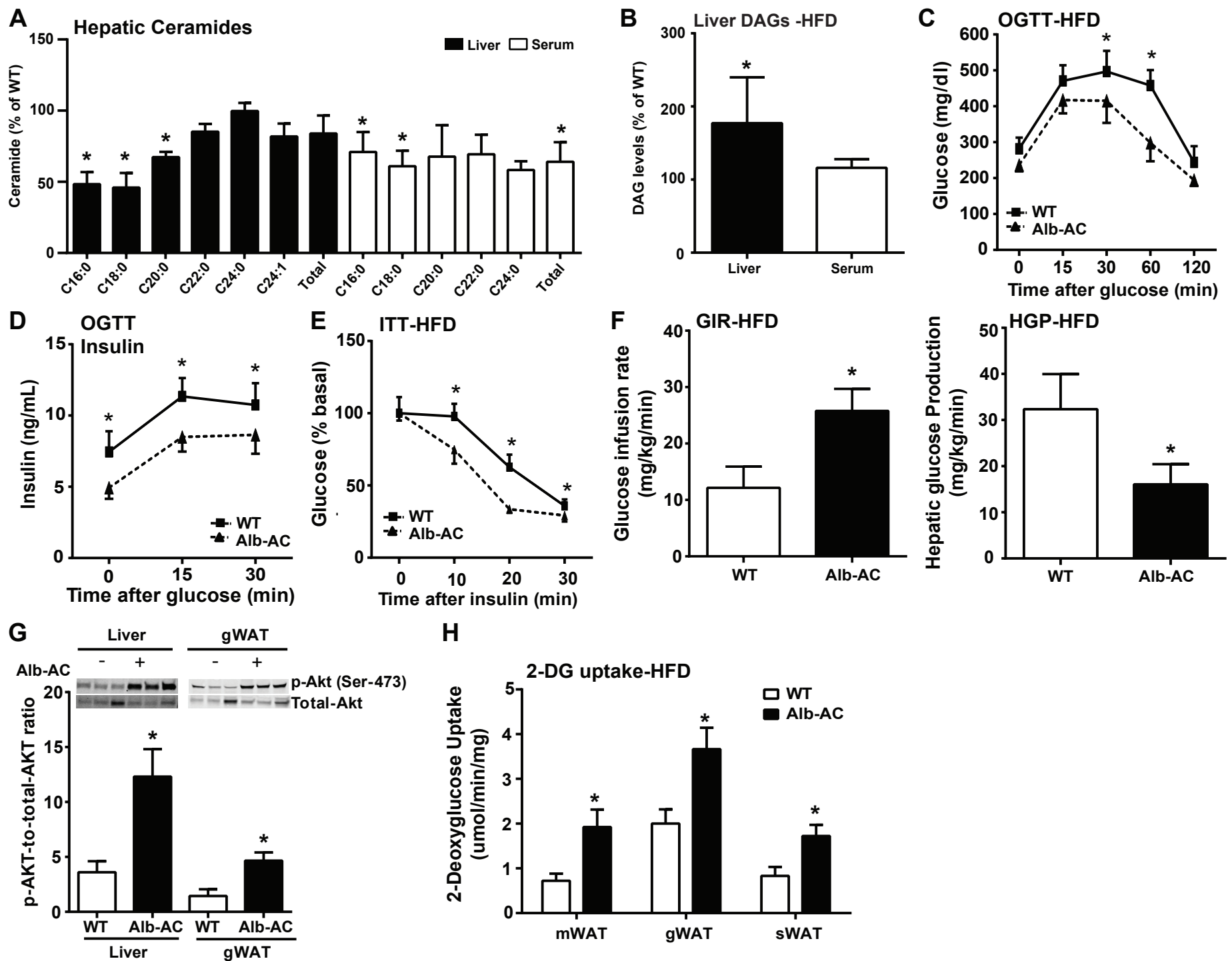
Figure 1

Fig. 1. Inducible liver-specific overexpression of acid ceramidase results in significantly reduced C_{16:0} ceramide species in the liver and improved total body glucose homeostasis and insulin sensitivity under HFD feeding. **A)** Analysis of liver and serum ceramide species from Alb-AC mice and WT littermates after 8 weeks of HFD-dox. **B)** Analysis of liver and serum diacylglycerol (DAG) levels in Alb-AC mice and control littermates after 8 weeks of HFD-dox. **C)** Circulating glucose levels were measured during an oral glucose tolerance test (OGTT) (2.5g/kg glucose per oral gavage). **D)** Serum insulin levels during the OGTT were quantified via ELISA. **E)** Circulating glucose levels measured during an insulin tolerance test (ITT) (0.75 U/kg). **F)** Glucose infusion rates (left) and hepatic glucose output (right) during hyperinsulinemic-euglycemic clamp experiments performed on conscious unrestrained 10-week-old WT and Alb-AC males. **G)** Representative immunoblots of phosphorylated and total Akt of insulin stimulated WT and Alb-AC mice, shown in triplicate. **H)** 2-deoxyglucose uptake quantification on conscious unrestrained 10-week-old WT mice and Alb-AC males. All samples are from Alb-AC mice and WT littermates after 8 weeks of HFD-dox challenge (n = 6), unless specified otherwise. *P<0.05 by Student's *t* test.

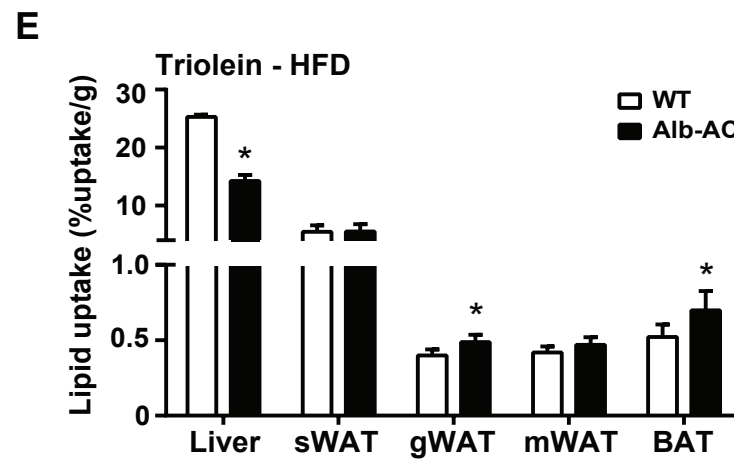
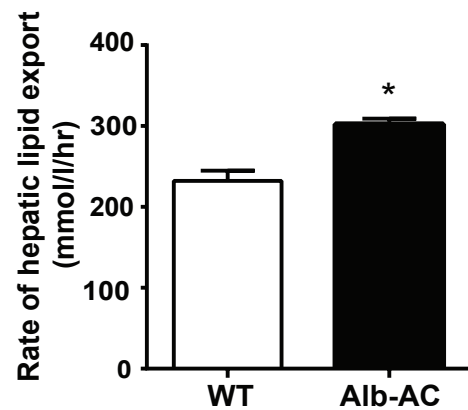
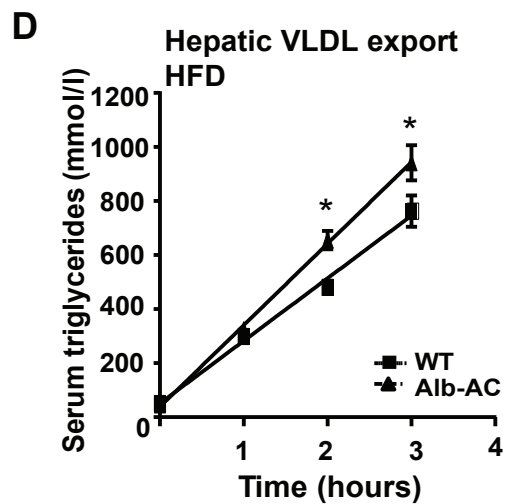
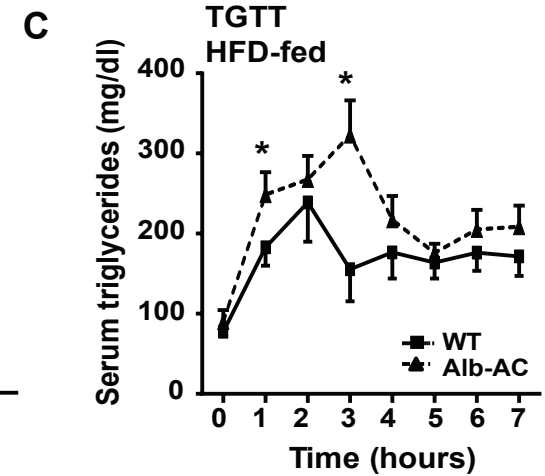
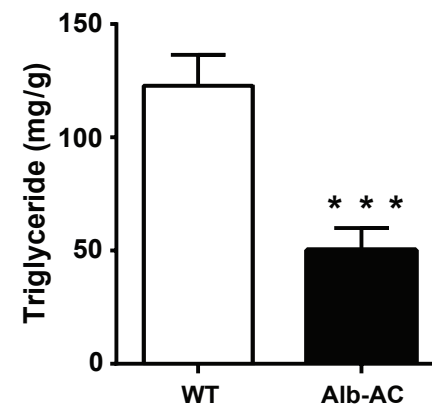
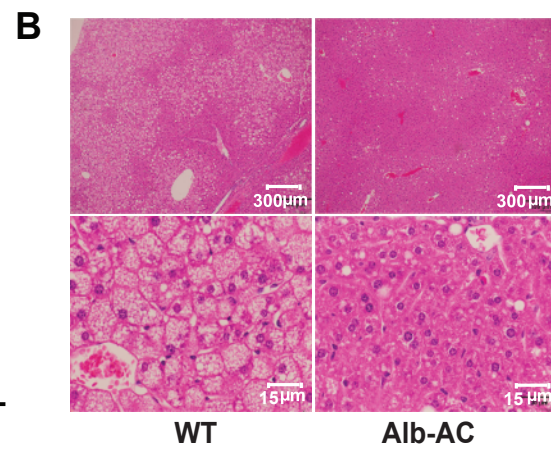
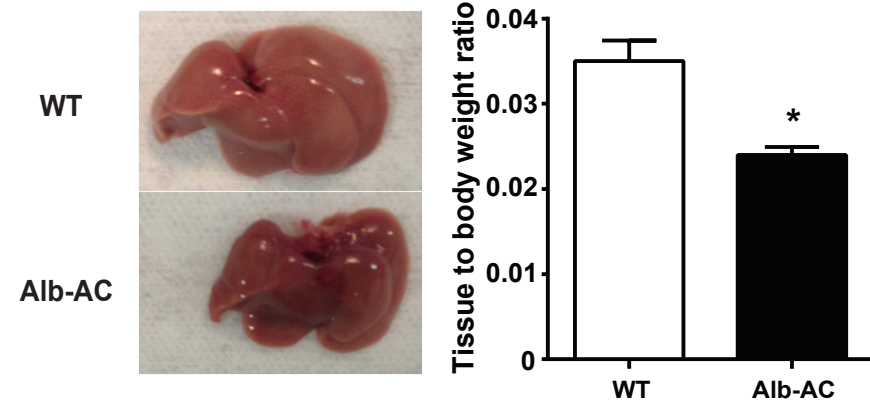
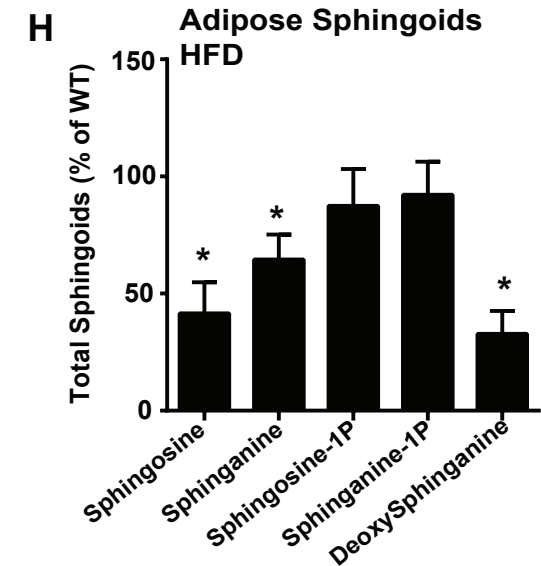
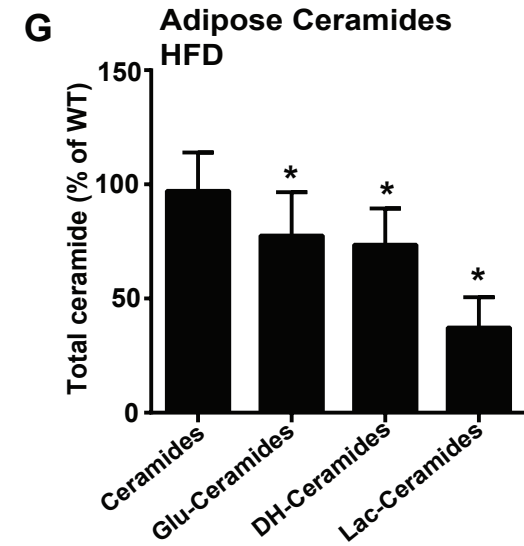
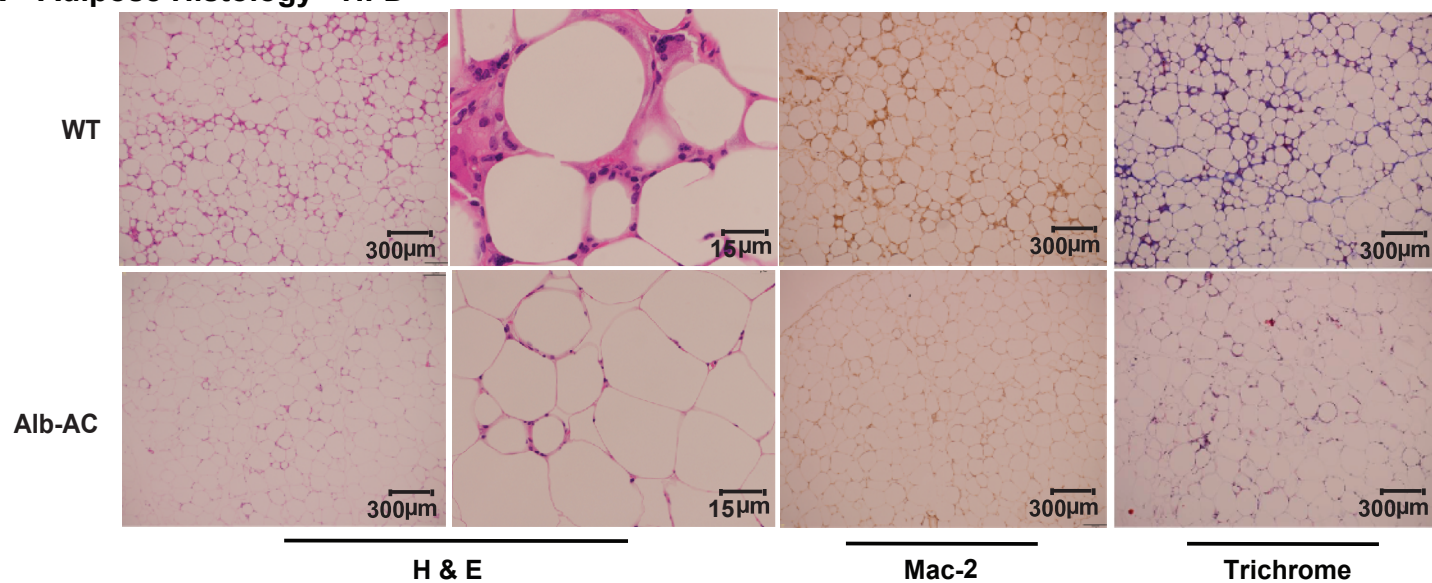
Figure 2**A** Livers - chronic HFD fed**F** Adipose Histology - HFD

Fig. 2. Liver specific overexpression of acid ceramidase significantly reduces hepatic lipid accumulation and improves adipose tissue metabolic health when challenged with HFD. **A)** A representative gross image of WT and Alb-AC livers. Bar graphs on the right represent the mass of the liver normalized to the total body weight of the mice. **B)** Representative H&E stained images of WT and Alb-AC livers. Bar graphs on the right represent quantification of liver triglyceride levels. **C)** Circulating triglyceride (TG) levels were measured during an oral TG clearance test (20% intralipid, 15 uL/g body weight; single gavage) in Alb-AC mice and WT littermate controls. **D)** Circulating triglyceride levels and the rate of hepatic VLDL export were measured following intravenous injection of tyloxapol (500 mg/kg) to inhibit plasma VLDL clearance in Alb-AC mice and WT littermate controls. **E)** Total ³H-triolein lipid-uptake per tissue in WT and Alb-AC males at 15 min after injection (2 µCi per mouse in 100 µl of 5% intralipid, single tail-vein injection). **F)** Representative images of H&E, Mac-2, and trichrome staining of WT and Alb-AC gonadal fat pads. **G)** Total WAT ceramide species levels were quantified by tandem MS/MS. **H)** Total WAT sphingoid species levels were quantified by tandem MS/MS. All samples are from Alb-AC mice and WT littermates after 8 weeks of HFD-dox challenge (n = 6), unless specified otherwise. **P*<0.05, ****P*<0.001 by Student's *t* test.

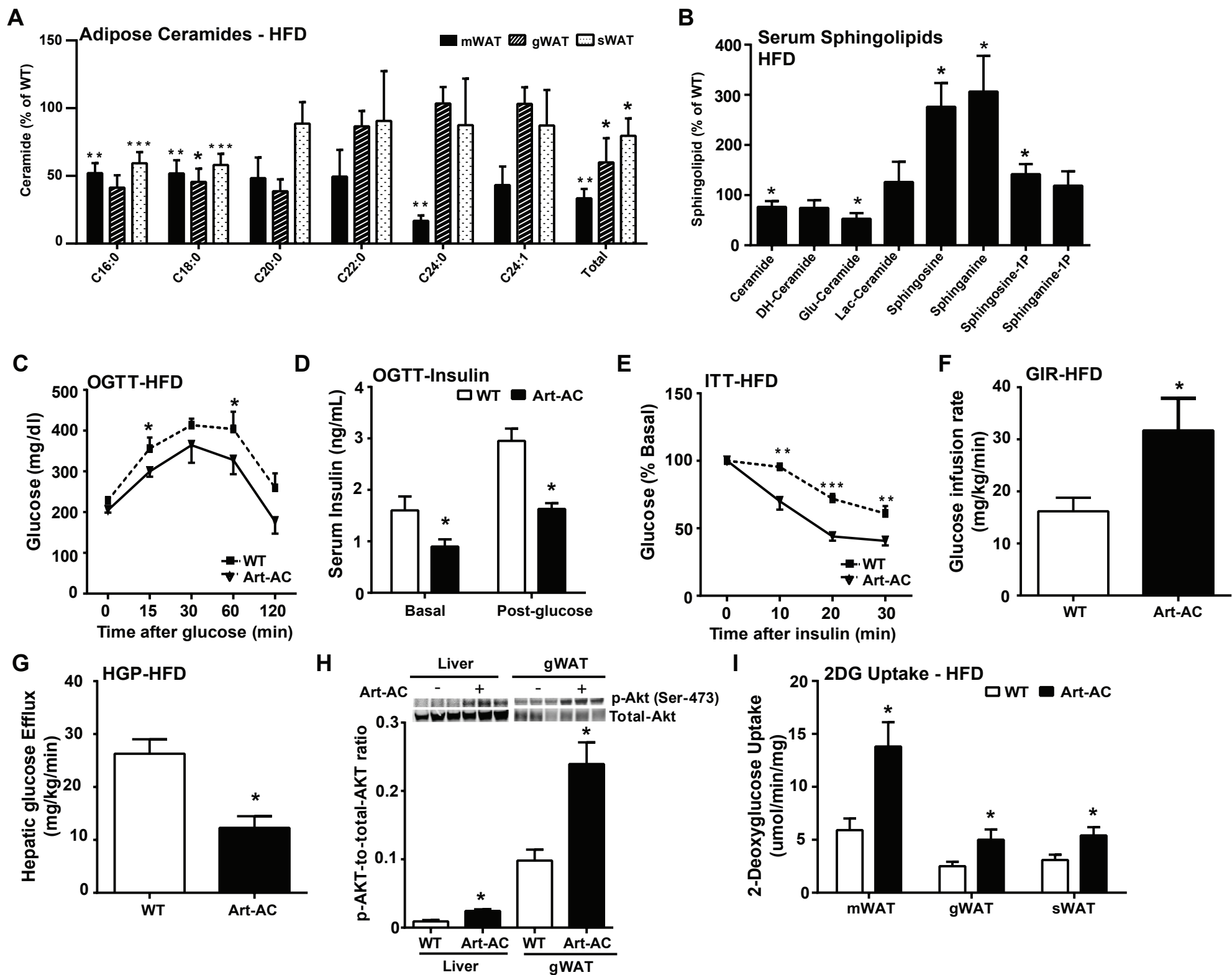
Figure 3

Fig. 3. Inducible adipose-specific overexpression of acid ceramidase results in ceramide species in the adipose and improved total body glucose homeostasis and insulin sensitivity under HFD feeding. **A)** Analysis of ceramide species of the indicated chain lengths from mesenteric (m), gonadal (g) and subcutaneous (s) fat pads from Art-AC mice and WT littermates after 8 weeks of HFD-dox. **B)** Analysis of total ceramide and sphingoid species from serum of Art-AC and WT littermates after 8 weeks of HFD-dox challenge. **C)** Circulating glucose levels were measured during an oral glucose tolerance test (OGTT) (2.5 g/kg glucose per oral gavage). **D)** Serum insulin levels before and 15 minutes after oral glucose. **E)** Circulating glucose levels measured during an insulin tolerance test (ITT) (0.75 U/kg). **F)** Glucose infusion rates during hyperinsulinemic-euglycemic clamp experiments performed on conscious unrestrained 14-week-old WT and Alb-AC males ($n = 6$ mice). **G)** Hepatic glucose efflux during hyperinsulinemic-euglycemic clamp experiments performed on conscious unrestrained 14-week-old WT and Alb-AC males ($n = 6$ mice). **H)** Representative immunoblots of phosphorylated and total Akt of insulin-stimulated livers and gWAT of WT and Art-AC mice, shown in triplicate. **I)** 2-deoxyglucose uptake into fat pads of WT mice and Art-AC mice was assessed during the hyperinsulinemic-euglycemic state ($n=6$ per group). All samples are from Alb-AC mice and WT littermates after 8 weeks of HFD –dox challenge ($n = 6-8$ per group). * $P < 0.05$, ** $P < 0.01$, *** $P < 0.001$ by Student's *t* test.

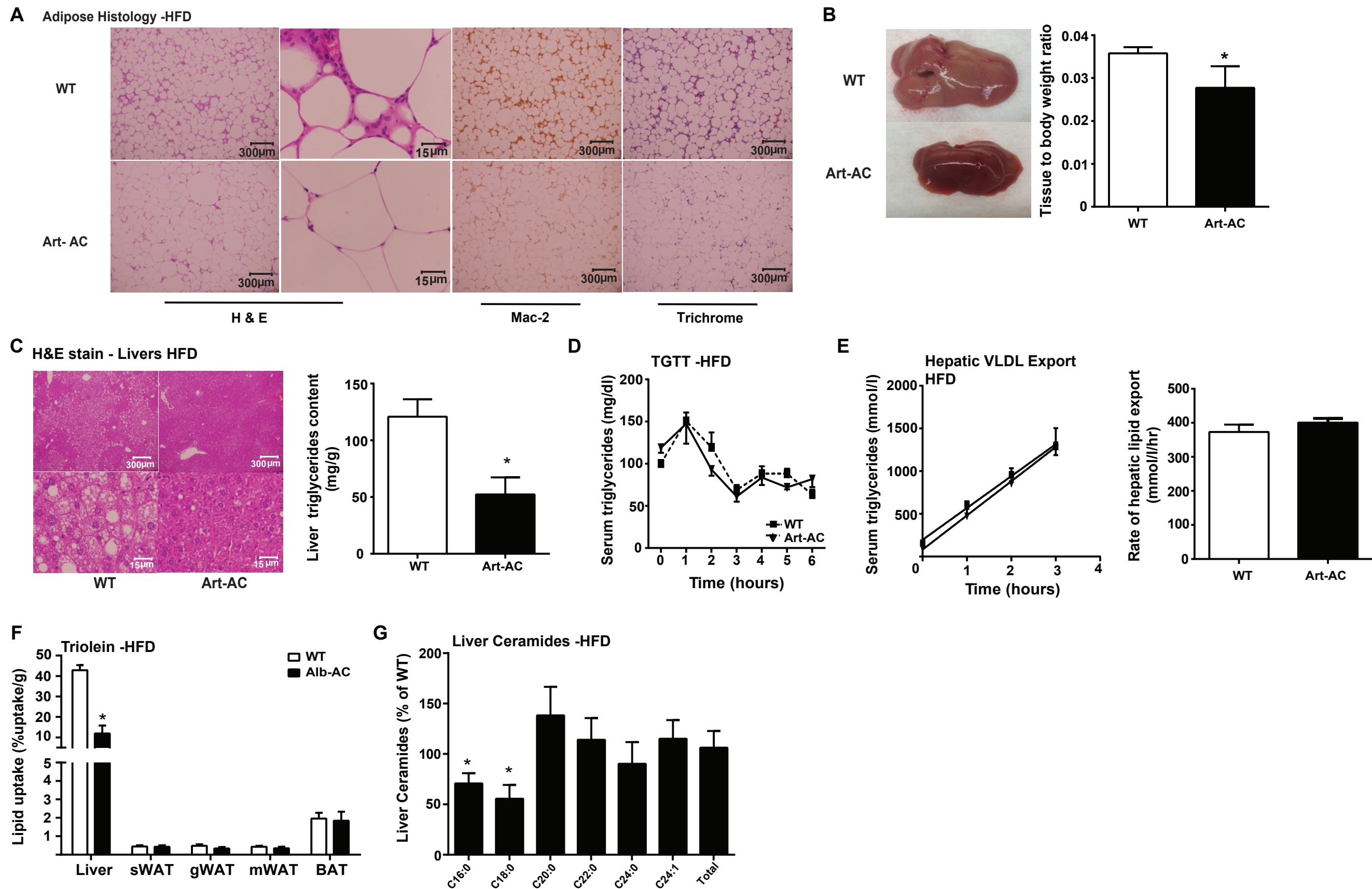
Figure 4

Fig. 4. Adipose-specific overexpression of acid ceramidase significantly reduces hepatic lipid accumulation and improves adipose tissue metabolic health when challenged with HFD. A) Representative images of H&E, Mac-2, and trichrome staining of WT and Art-AC gonadal fat pads. **B)** A representative gross image of WT and Art-AC livers. Bar graphs on the right represent the mass of the liver normalized to the total body weight of the mice. **C)** Representative H&E stained images of WT and Art-AC livers. Bar graphs on the right represent biochemical quantification of liver triglyceride levels. **D)** Circulating triglyceride (TG) levels were measured during an oral TG clearance test (20% intralipid, 15 uL/g body weight; single gavage) in Art-AC mice and WT littermate controls. **E)** Circulating triglyceride levels and the rate of hepatic VLDL export were measured following intravenous injection of tyloxapol (500 mg/kg) to inhibit plasma VLDL clearance in Alb-AC mice and WT littermate controls. **F)** Total ³H-triolein lipid-uptake per tissue in WT and Alb-AC males 15-minutes after injection. **G)** Liver ceramide species and total ceramides were quantified and presented relative to wt levels of the same lipid species. All samples are from Art-AC mice and WT littermates after 8 weeks of HFD–dox challenge (n = 6-10 per group). **P*<0.05 by Student's *t* test.

Figure 5

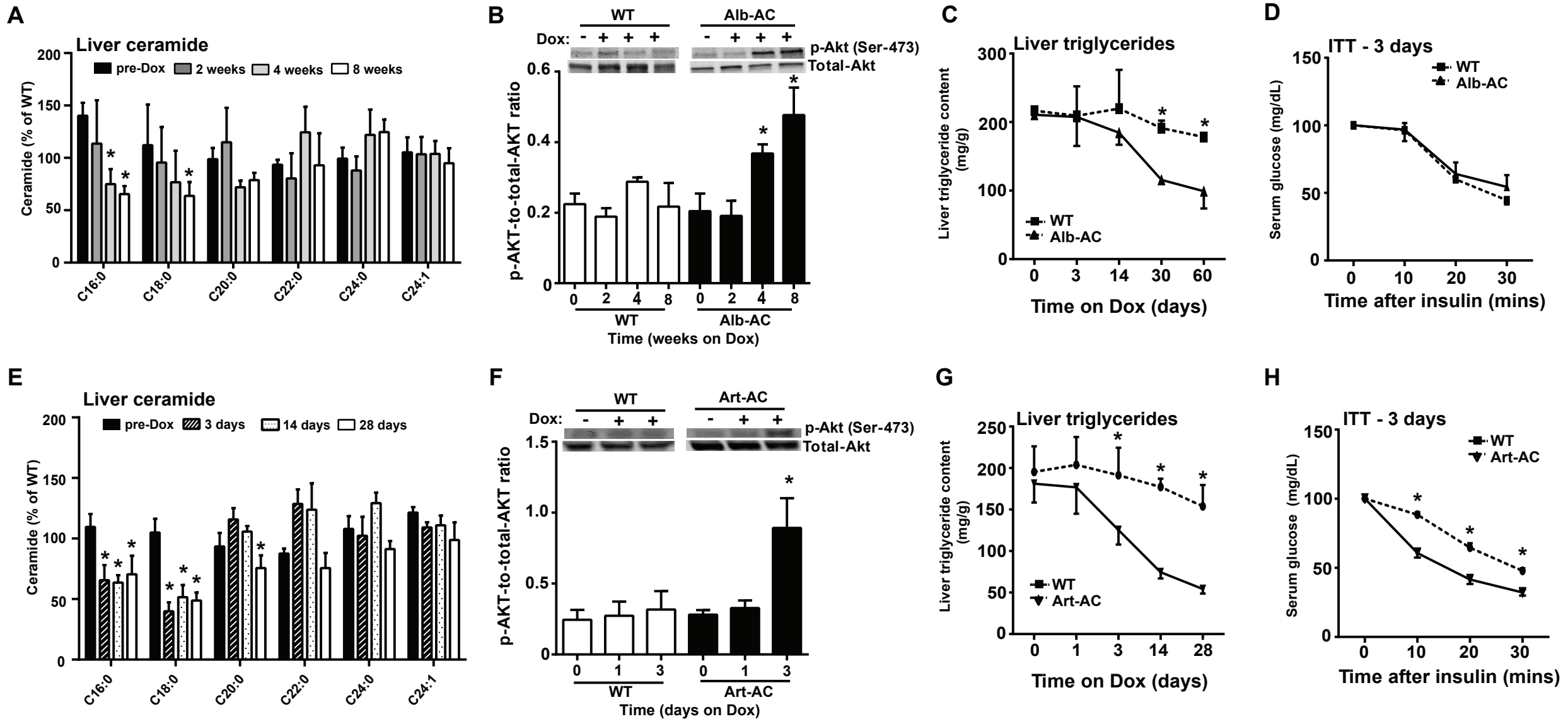
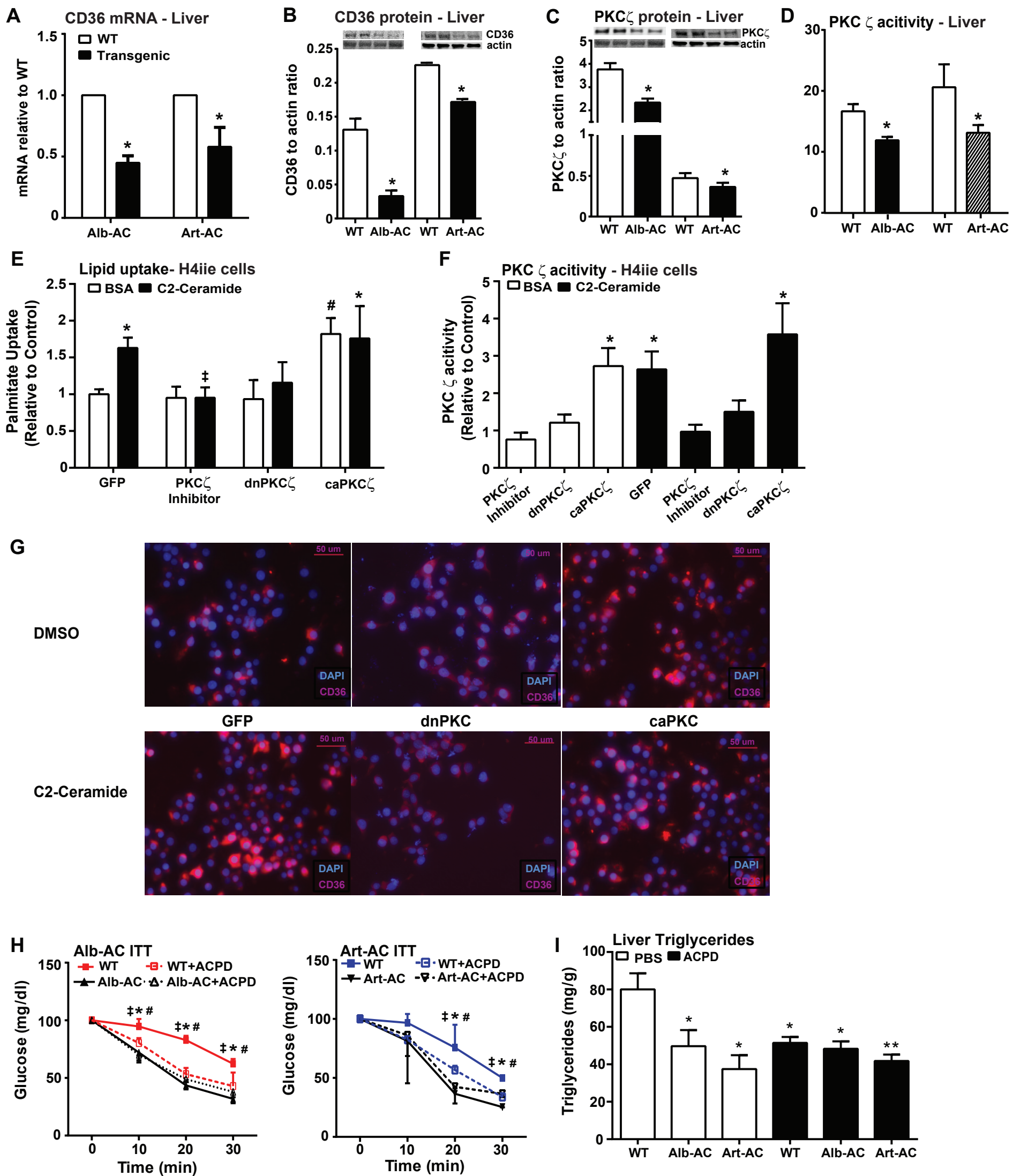


Fig. 5. Induction of acid ceramidase significantly improves insulin signaling and rescues hepatic steatosis in mice with diet induced obesity. All mice were maintained on high fat diets for 8 weeks prior to treatment with doxycycline. **A)** Liver ceramide species levels were quantified by tandem MS/MS for mice at pre-Dox treatment, 2 weeks, 4 weeks, and 8 weeks post-Dox treatment (n=4 at each time). **B)** Representative immunoblots of phosphorylated and total Akt from liver of insulin-stimulated WT and Alb-AC mice at pre-Dox treatment, at 2 weeks, 4 weeks, and 8 weeks post-Dox treatment (n=4 at each time). **C)** Liver triglycerides were quantified at different time points before or after Dox treatment (n=4 at each time). **D)** Circulating glucose levels measured during an insulin tolerance test (ITT) (0.75 U/kg) 3 days after HFD-dox treatment (n=4). **E)** Ceramides were quantified from liver of WT and Art-AC mice at pre-Dox treatment, 3 days, 14 days, and 28 days of doxycycline treatment (n=5 at each time). **F)** Representative immunoblots of phosphorylated and total Akt from liver of insulin-stimulated WT and Art-AC mice at pre-Dox treatment, at 24 hours, and 72 hours post-Dox treatment (n=4 at each time). **G)** Liver triglycerides were biochemically measured before and at the indicated time points after doxycycline addition to the diet in WT and Art-AC mice (n=6-10 at each time). **H)** Insulin tolerance tests were performed 3 days after doxycycline treatments in WT and AC-Art littermates (n=5). **P*<0.05 by Student's *t* test.

Figure 6**Fig. 6. Ceramides facilitate lipid uptake by mechanisms involving activation of PKC ζ and CD36.**

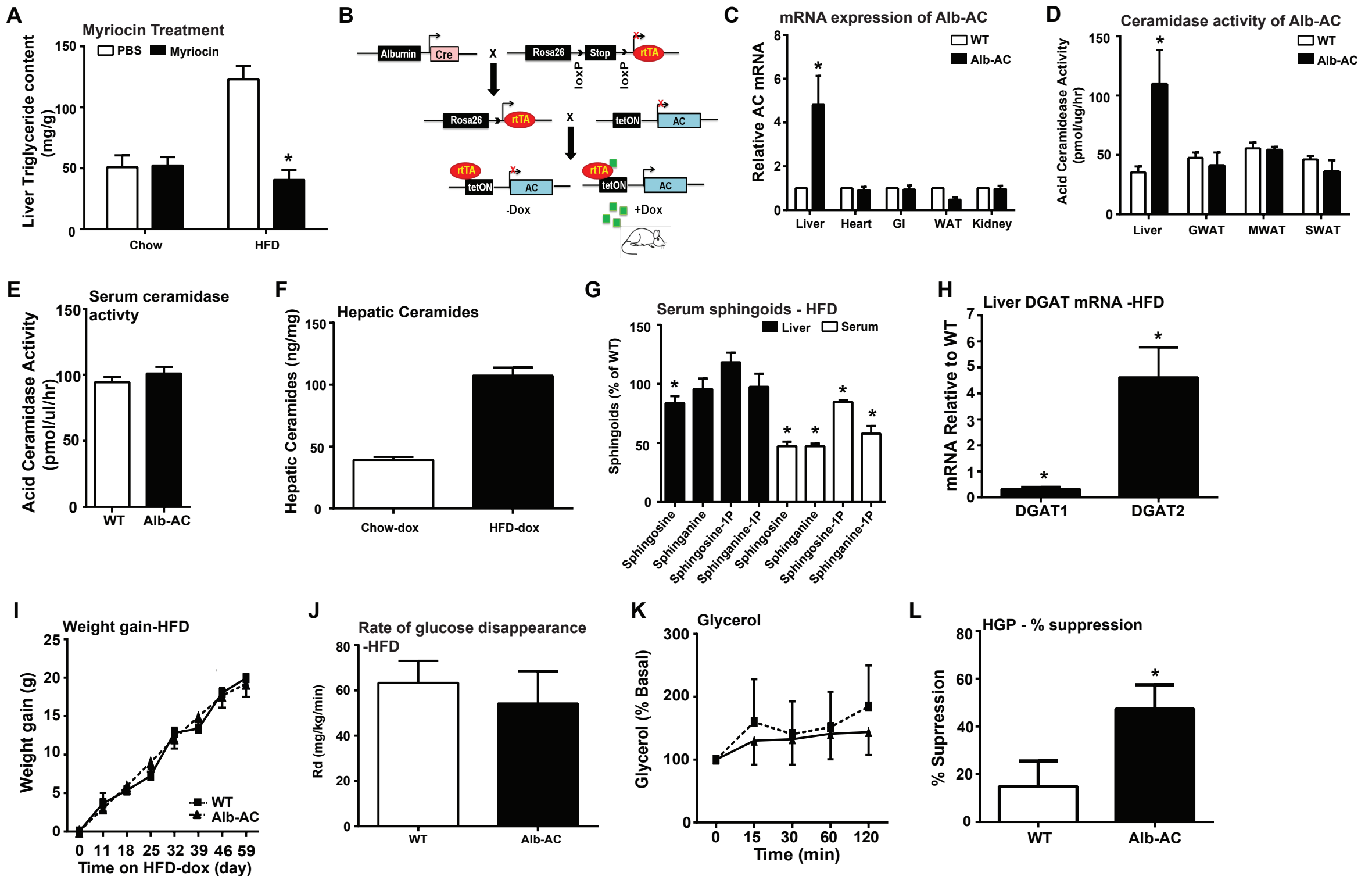
A) Relative abundance of CD36 mRNA was assessed by qPCR from livers of WT, Alb-AC, and Art-AC mice following 8 weeks of HFD-dox. **B)** Hepatic expression of CD36 was assessed by Western blotting, and representative results are shown in duplicate. **C)** Hepatic expression of PKC ζ were assessed by western blotting and representative results are shown in duplicate. **D)** PKC ζ activity was assessed from livers of WT, Alb-AC, and Art-AC mice following 8 weeks of HFD-dox. **E-F)** Following transfection with GFP, dnPKC ζ , or caPKC ζ H4IIE hepatocytes were treated with C2-ceramide (100 μ M, in 0.2% BSA) or BSA for 1 hour prior to assessment of 3 H-palmitate uptake. Myristoylated PKC ζ pseudosubstrate inhibitor was included for 90 minutes prior to ceramide treatments in non-transfected cells (n=4-8 from separate experiments). No difference was observed between GFP and non-transfected control cells. **F)** PKC ζ activity was assessed from cell lysates harvested from cells represented in panel D. ‡ corresponds to comparison of C2-Ceramide treated cells with or without the PKC ζ inhibitor. # corresponds to comparison of BSA treated cells that was transfected with either GFP or caPKC ζ . **G)** Representative immunofluorescence of CD36 in H4IIE cells transfected with GFP, dnPKC ζ , or caPKC ζ . Each group is treated with either DMSO or C2-Ceramide. **H)** Circulating glucose levels measured during an insulin tolerance test (ITT) (0.75 U/kg) of Alb-AC or Art-AC mice and littermate controls after daily injections of ACPD. * corresponds to comparison of WT to Alb or Art-AC. ‡ corresponds to comparison of WT and WT + ACPD. # corresponds to comparison of WT and Alb or Art-AC + ACPD. **I)** Biochemical quantification of hepatic lipid accumulation in Alb-AC or Art-AC mice and littermate controls after daily injections of ACPD. *, ‡, #: $P < 0.05$, ** $P < 0.01$ by Student's t test.

Table1

Metabolic parameters before and during hyperinsulinemic-euglycemic clamp study in WT and AC transgenics.

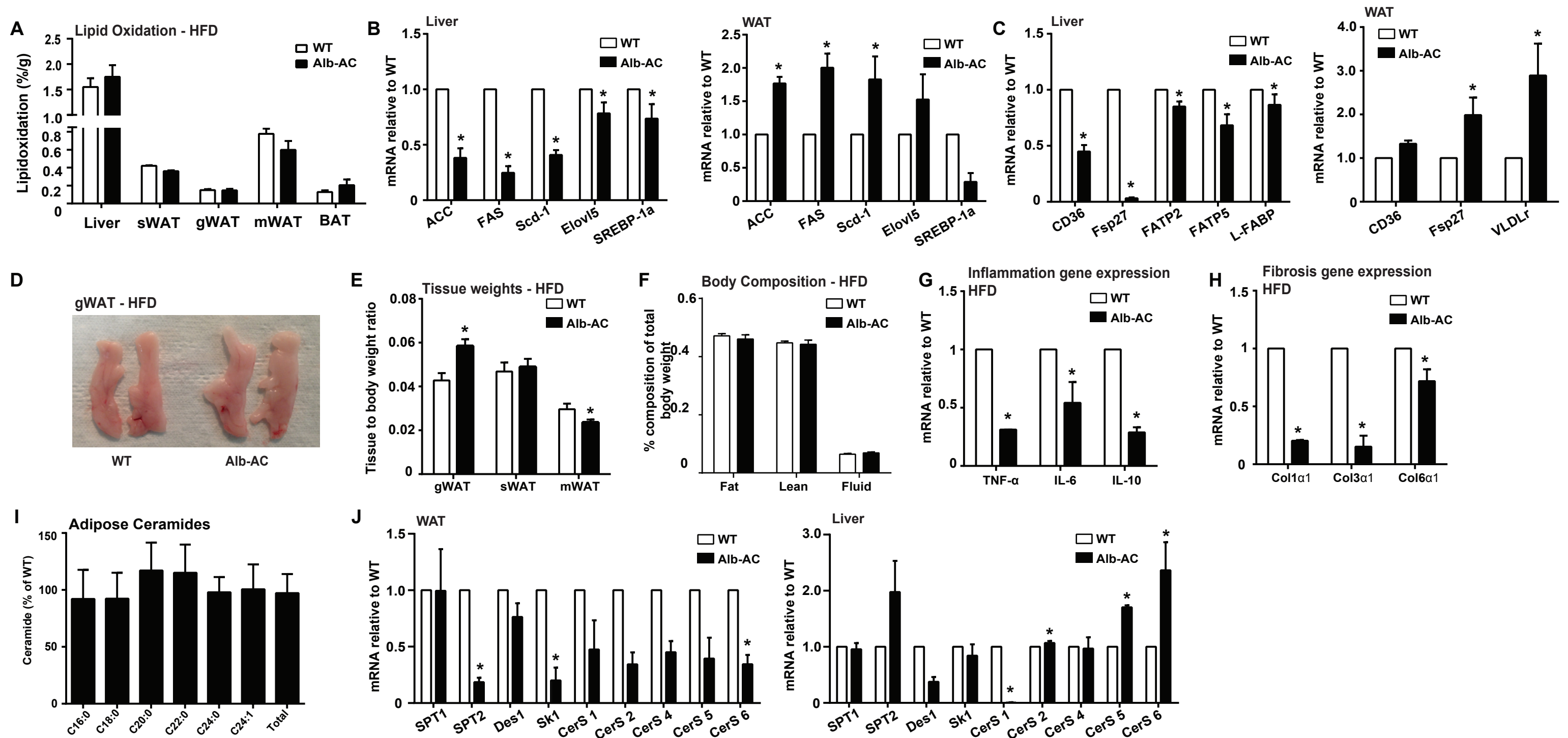
	Body weight (g)	Basal				Clamped			
		Plasma glucose (mg/dL)	Plasma insulin (ng/mL)	Plasma NEFA (mmol/L)	Plasma Glycerol (mg/mL)	Plasma glucose (mg/dL)	Plasma insulin (ng/mL)	Plasma NEFA (mmol/L)	Plasma Glycerol (mg/mL)
WT	49.4±1.8	208.2±7.8	0.87±0.13	0.47±0.06	0.41±0.04	177.4±5.1	3.58±0.47	0.33±0.06	0.47±0.11
Alb-AC	48.8±2.0	191±3.9	0.83±0.13	0.42±0.03	0.32±0.02	168±6.5	4.2±0.72	0.27±0.07	0.38±0.13
WT	30.8±1.6	207±2.4	0.98±0.1	0.51±0.08	0.59±0.15	153.9±4.6	3.4±0.61	0.51±0.06	0.41±0.1
Art-AC	30.9±1.06	174.2±23.3	0.66±0.16	0.42±0.04	0.38±0.09	142.7±3.5	3.4±0.5	0.34±0.08	0.36±0.09

Supplemental Figure 1



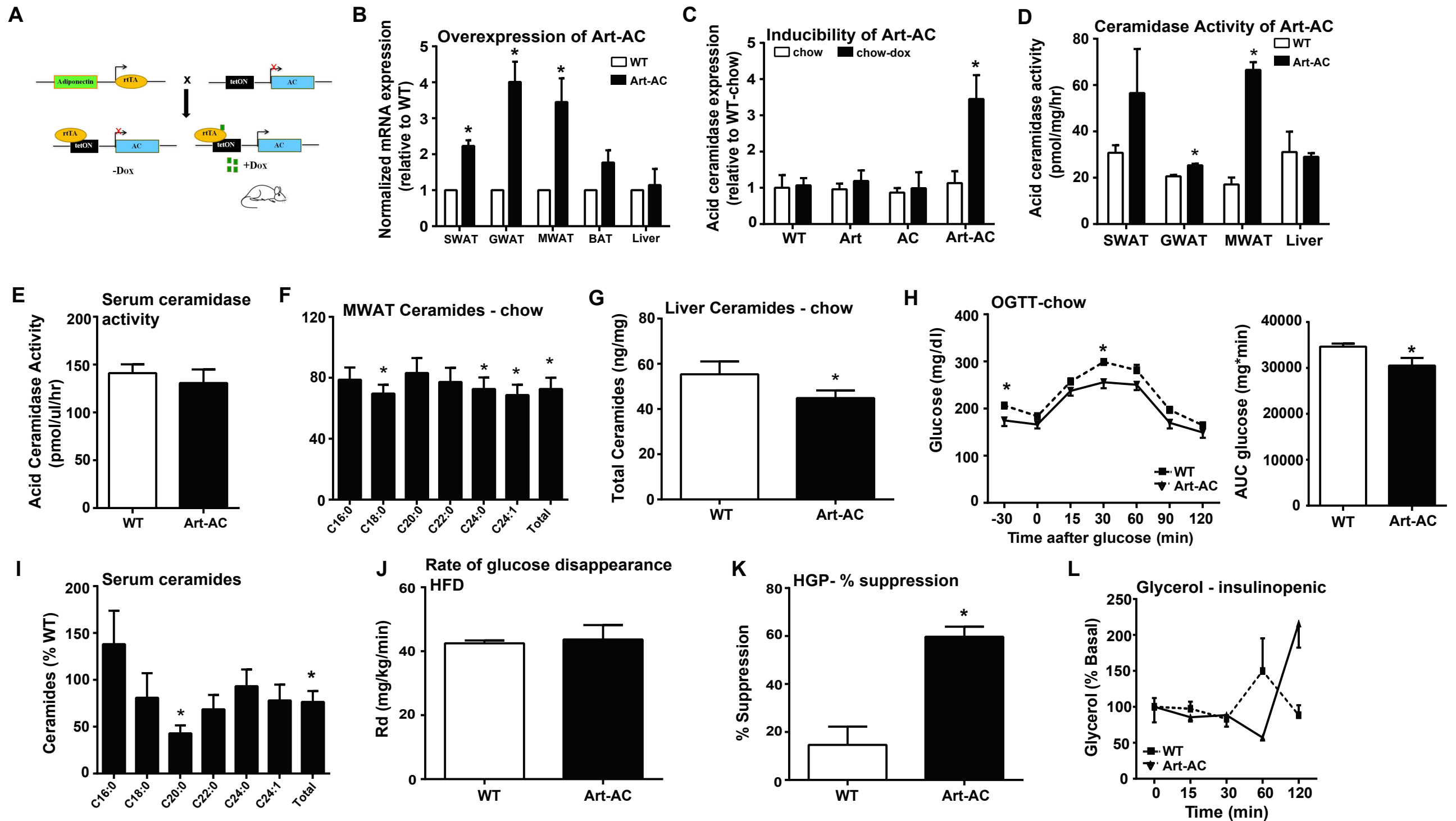
Supplemental Fig. 1 related to Fig. 1: Inducible liver-specific overexpression of acid ceramidase results in significantly reduced $C_{16:0}$ ceramide species in the liver and improves total body glucose homeostasis and insulin sensitivity under HFD feeding. **A)** WT mice fed either a chow or HFD for 8 weeks were sacrificed and liver triglycerides were quantified ($n=3$, * denotes $p<0.05$). **B)** Strategy of generating mice with liver-specific inducible expression of AC (Acid Ceramidase). **C)** Mice were fed with doxycycline chow diet for 7 days before sacrifice. mRNA levels for AC in liver, heart, small intestine (SI), white adipose tissue (WAT), and kidneys by qPCR were measured with relative to β -actin. Primers recognize both endogenous and transgenic AC ($n = 3$, * denotes $p<0.05$). **D)** Acid ceramidase activity was determined using Rbm 14-12 at 20 μ M after incubation for 3 hours with tissue lysates (20 μ g protein) of both WT and Alb-AC mice after 8 weeks of HFD-dox. ($n = 4$, * denotes $P<0.05$). **E)** Serum acid ceramidase activity was analyzed from Alb-AC mice and WT littermates after 8 weeks of HFD-dox diet. **F)** Analysis of hepatic ceramide accumulation after 8 weeks of either chow-dox or HFD-dox diet in mice ($n = 6$). **G)** Analysis of liver and serum sphingoid species of Alb-AC mice and control littermates after 8 weeks of HFD-dox ($n=6$, * denotes $P<0.05$). **H)** mRNA levels of diacylglycerol synthesis genes quantified by qPCR in whole liver tissue, normalized to actin ($n=4$, *denotes $p<0.05$). **I)** Weight gain in Alb-AC transgenic mice and WT littermates during 8 weeks of HFD-dox. **J)** Whole body glucose turnover was calculated from 3H glucose infusion administered prior to the clamp and throughout its duration. **K)** Low dose insulin was administered to STZ-treated mice (0.1 mU/g body weight) and circulating glycerol levels were measured under these conditions. **L)** Hepatic glucose output, represented as % suppression of basal levels, during hyperinsulinemic-euglycemic clamp experiments performed on conscious unrestrained 10-week-old WT and Alb-AC males.

Supplemental Figure 2



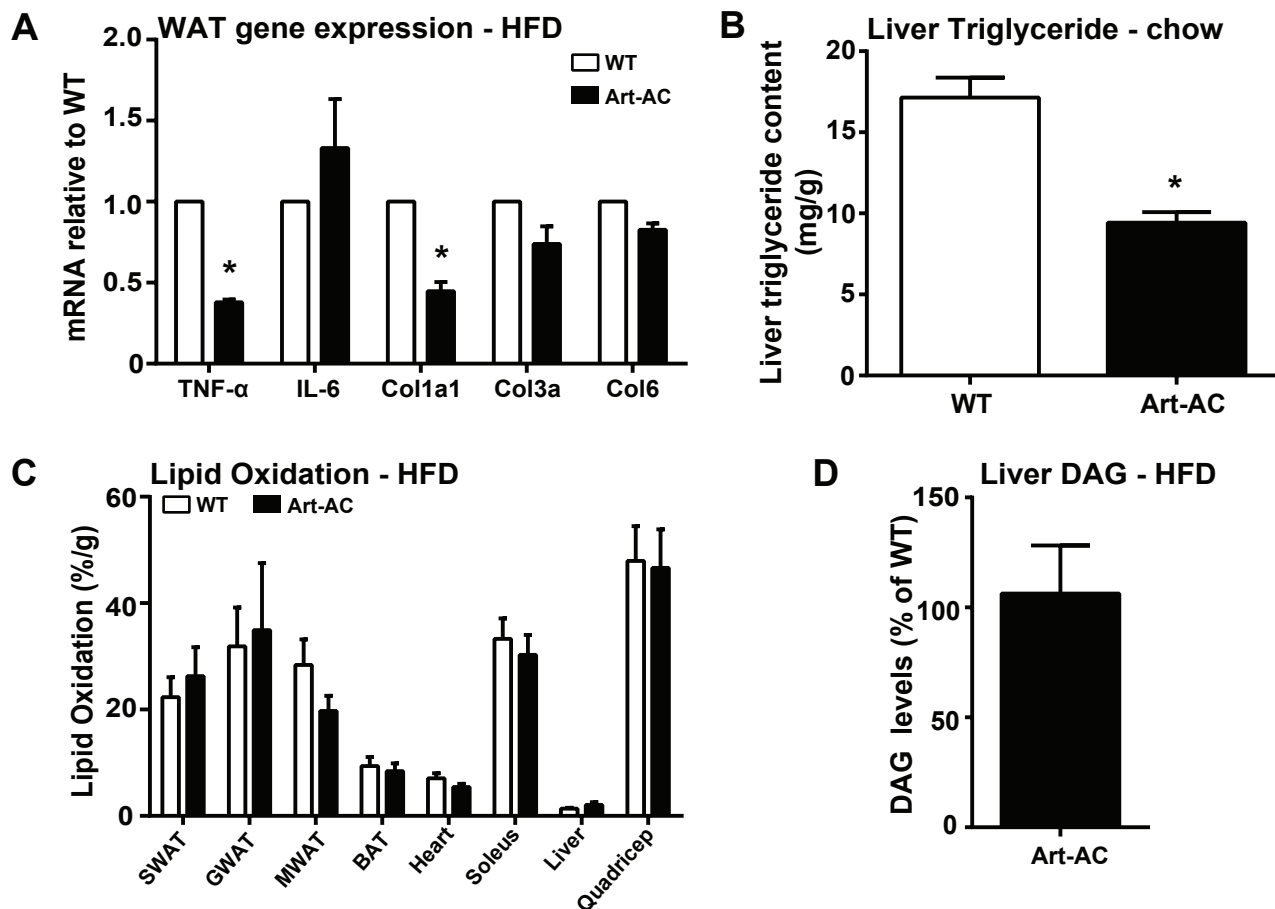
Supplemental Fig. 2 related to Fig. 2: Liver specific overexpression of acid ceramidase significantly reduces hepatic lipid accumulation and improves adipose tissue metabolic health when challenged with HFD. **A)** Total ^3H -triolein lipid-oxidation per tissue in WT and Alb-AC males at 15 min after injection (2 μCi per mouse in 100 μl of 5% intralipid, single tail-vein injection) ($n = 6$ mice per group). **B)** mRNA levels of fatty acid synthesis genes quantified using qPCR in whole liver and gWAT tissue, normalized to actin ($n=4$, *denotes $p<0.05$). **C)** mRNA levels of fatty acid uptake genes quantified using qPCR in whole liver and gWAT tissue, normalized to actin ($n=4$, *denotes $p<0.05$). **D)** Representative gross image of gonadal fat pads. **E)** The masses of the gonadal (gWAT), subcutaneous (sWAT), and mesenteric (mWAT) white adipose tissues of Alb-A mice and WT littermate controls were weighed and normalized to the total body weight of the mice (* denotes $p<0.05$). **F)** Body composition of fat and lean masses was quantified via NMR. **G)** mRNA levels of inflammatory genes (TNF α , IL-6, IL-10) quantified using qPCR in whole gWAT tissue, normalized to β -actin ($n=4$, *denotes $p<0.05$). **H)** mRNA levels of fibrosis genes (Col1 α 1, Col3 α 1, Col6 α 1) were quantified using qPCR in whole gWAT tissue, normalized to β -actin ($n=4$, *denotes $p<0.05$). **I)** Analysis of gWAT ceramide species from Alb-AC mice and WT littermates after 8 weeks of HFD-dox. **J)** mRNA levels of sphingolipid synthesis genes quantified using qPCR in whole liver and gWAT tissue, normalized to actin ($n=4$, *denotes $p<0.05$). All samples are from Alb-AC mice and WT littermates after 8 weeks of HFD –dox challenge ($n = 6$), unless specified otherwise.

Supplemental Fig. 3



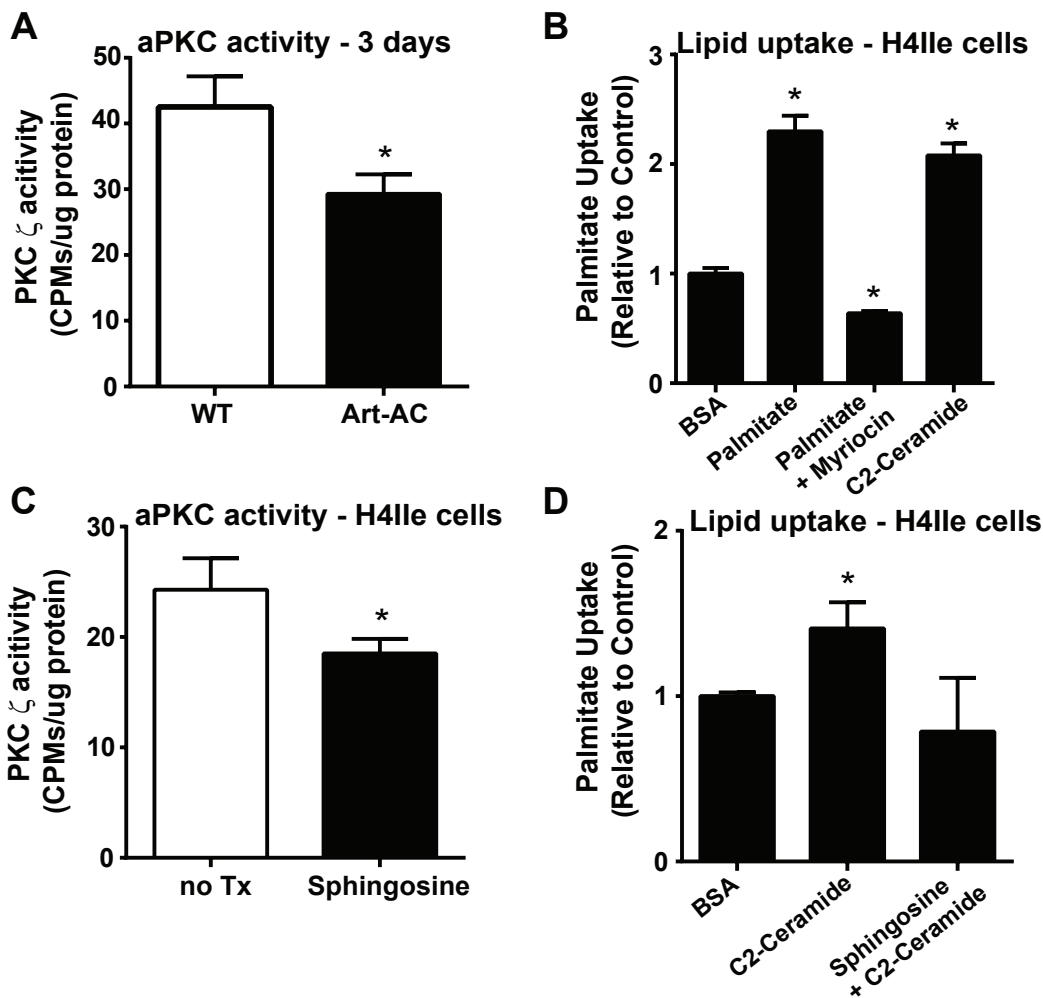
Supplemental Fig. 3 related to Fig. 3: Adipose-specific acid ceramidase overexpression improves glucose homeostasis. **A)** To allow for adipose-restricted expression of acid ceramidase in a doxycycline inducible manner, adiponectin rtTA (Art) mice were crossed with TRE-AC transgenic mice to generate Art-AC double transgenic mice. **B)** Following HFD-Dox treatment, major fat pads and liver were analyzed for expression of acid ceramidase message by qPCR and normalized to GAPDH message (n=6/group, * denotes p<0.05). **C)** To verify the doxycycline-restricted expression of the transgene, mesenteric adipose was analyzed by qPCR for acid ceramidase message from Art transgenic, TRE-AC transgenic, Art-AC double transgenic and wildtype mice following 10 days of treatment with dox chow or normal chow (n=4/group, * denotes p<0.05). **D)** Following 10 days of treatment with dox chow, acid ceramidase activity was analyzed from lysates of subcutaneous, gonadal, and mesenteric WAT and liver of WT and Art-AC transgenic mice (n=4/group, * denotes p<0.05). **E)** Analysis of liver C17 fatty acid levels in Art-AC mice and control littermates after 3 days of HFD-dox. **F)** Serum acid ceramidase activity was analyzed from Art-AC mice and WT littermates after 8 weeks of HFD and 3 days of HFD-dox diet. **G)** Following 3 weeks of dox chow, ceramides were quantified from mesenteric WAT of Art-AC transgenic mice and presented as normalized to wildtype littermates (n=6-8/group, * denotes p<0.05). **H)** Following 3 weeks of dox chow, ceramides were quantified from liver of Art-AC transgenic mice and WT mice and presented as sum of all chain lengths (n=6-8/group, * denotes p<0.05). **I)** Glucose tolerance tests were performed after 3 weeks of dox chow on WT and Art-AC transgenic mice (n=8-10 per group, p<0.05). The area under the curve during the GTT was calculated (p<0.05). **J)** Analysis of serum ceramide species from Art-AC mice and WT littermates after 8 weeks of HFD-dox (n=6/group, * denotes p<0.05). **K)** Whole body glucose turnover was calculated from the ³H glucose infusion administered prior to the clamp and throughout its duration. **L)** Hepatic glucose output, represented as % suppression of basal levels, during hyperinsulinemic-euglycemic clamp experiments performed on conscious unrestrained 8-week-old WT and Art-AC males (n=6-8/group, * denotes p<0.05). **M)** Low dose of insulin was administered to STZ-treated mice (0.1 mU/g body weight) and circulating glycerol levels were measured under these conditions.

Supplemental Figure 4



Supplemental Fig. 4 related to Fig. 4. Adipose-specific overexpression of acid ceramidase reduces hepatic lipid accumulation and improves adipose tissue metabolic health. **A)** Following 10 weeks of HFD dox administration, expression of inflammatory genes and fibrosis genes was assessed by qPCR from gonadal WAT, normalized to GAPDH (n=6/group, p<0.05). **B)** Liver triglycerides were biochemically measured following 3-week administration of dox chow diets (n=6-9/group, p<0.05). **C)** Lipid oxidation was determined for the indicated tissues following bolus injection of ^3H -Triolein into WT or Art-AC transgenic mice maintained on HFD-dox. **D)** Analysis of liver and serum diacylglycerol (DAG) levels in Art-AC mice and control littermates after 8 weeks of HFD-dox.

Supplemental Figure 5



Supplemental Fig. 5 related to Fig. 6: Ceramides facilitate lipid uptake by mechanisms involving activation of PKC ζ and CD36. **A)** PKC ζ activity was assessed from livers of WT and Art-AC mice following 3 days of HFD-dox. **B)** H4Ile hepatocytes were treated with either palmitate, C2-ceramide (100 μ M, in 0.2% BSA) or BSA for 1 hour prior to assessment of 3 H-palmitate uptake (n=4, * denotes p<0.05). **C)** PKC ζ activity was assessed from H4Ile cells with or without 1 hour pre-treatment of sphingosine (* denotes p<0.05). **D)** H4Ile hepatocytes were treated with either C2-ceramide (100 μ M, in 0.2% BSA), sphingosine and C2-ceramide or BSA for 1 hour prior to assessment of 3 H-palmitate uptake (*denotes p<0.05).

Supplementary Table 1 related to Supplemental Methods

List of qPCR primers used

β -actin	5'-TGGCATTGTTACCAACTGGG	5'-GGGTCATCTTTTCACGGTTG
SPT1	5'-TACTCAGAGACCTCCAGCTG	5'-CACCAGGGATATGCTGTCATC
SPT2	5'-GGAGATGCTGAAGCGGAAC	5'-GTATGAGCTGCTGACAGGCA
CerS1	5'-CTGTTCTACTTGGCCTGTTG	5'-TCATGCAGGAAGAACACGAG
CerS2	5'-TCTTCTCAAAAAGTTCCGAG	5'-AGTGATGATGAAAACGAATGG
CerS4	5'-TGTCGTTTACGCTTGAGTGAG	5'-AGCAGGCTTCACAGAATTC
CerS5	5'-CTCCAACGCTCACGAAATTC	5'-ATGCAGACAGAAGATGAGTG
Cers6	5'-GTTTCGGAGCATTCAACGCTG	5'-CTGAGTCGTGAAGACAGAGG
Des1	5'-CACCGGTACCTCGGAGCGGA	5'-GTTTGGGATTGATGAACAGGGGT
Sk1	5'-TCCTGGCACTGCTGCACTC	5'-TAACCATCAATTCCCATCCAC
AC	5'-CAGGACTGTTTACAGTCTTTCAC	5'-GAGTGATAAACCCCTACCCACT
ACC	5'-GGCAGCTCTGGAGGTGTATG	5'-TCCTTAAGCTGGCGGTGTT
FAS	5'-CCTGGATAGCATTCCGAACCT	5'-AGCACATCTCGAAGGCTACACA
Scd-1	5'-TCGCCCCTACGACAAGAACA	5'-CCGGTCGTAAGCCAGGCCCA
Elovl5	5'-TCAATGCTTTCTTGGACACATG	5'-GGTAAGAGTCCAGCAGGAACCA
SREBP-1a	5'-GGAGCCATGGATTGCACATT	5'-GGCCCGGGAAGTCACTGT
CD36	5'-TGAGACTGGGACCATTGGTGAT	5'-CCCAAGTAAGGCCATCTCTACCAT
Fsp27	5'-CAAGGCCAAGCGCATCGT	5'-TGCCAAGCAGCATGTGACCG
FATP2	5'-CAACACACCGCAGAAACA	5'-ATTTCCAGGGCTTTTTTCA
FATP5	5'-GACCACTGGACTCCCAAAGC	5'-GACAGCACGTTGCTCACTTGT
L-FABP	5'-GGTGACAACCTTCAAAGGCATAAA	5'-TGTCGCCCAATGTCATGGTA
VLDLr	5'-GAGCCCCTGAAGGAATGCC	5'-CCTATAACTAGGTCTTTGCAGATATGG
TNF- α	5'-TCTGTCTACTGAACTTCGGG	5'-ATCTGAGTGTGAGGGTCTG
IL-6	5'-TCCAGTTGCCTTCTTGGGAC	5'-GTACTIONCAGAAGACCAGAGG
IL-10	5'-TGGCCCAGAAATCAAGGAGC	5'-CAGCAGACTCAATACACACT

Col1 α 1	5'-GATGAGGGTGAAGTGGGAGA	5'-CAGCACGAAGAGGATGTCAA
Col3 α 1	5'-GGGTTTCCCTGGTCCTAAAG	5'-CCTGGTTTCCCATTTTCTCC
Col6 α 1	5'-GATGAGGGTGAAGTGGGAGA	5'-CAGCACGAAGAGGATGTCAA

Chapter 3

(The following section is manuscript prepared for submission)

Inducible Overexpression of Adiponectin Receptors Highlight the Roles of Adiponectin-Induced Ceramidase Signaling in Lipid and Glucose Homeostasis

**William L. Holland^{1*†}, Jonathan Y. Xia^{1*}, Joshua A. Johnson¹, Kai Sun¹,
Mackenzie J. Pearson¹, Ruth Gordillo¹ and Philipp E. Scherer^{1,2}**

¹Touchstone Diabetes Center, Department of Internal Medicine, The University of Texas Southwestern Medical Center, Dallas, Texas 75390-8549.

²Department of Cell Biology, The University of Texas Southwestern Medical Center, Dallas, Texas 75390-8549

*Contributed equally to this work

† Correspondence should be addressed to:
William L. Holland
Touchstone Diabetes Center
Department of Internal Medicine
University of Texas Southwestern Medical Center
5323 Harry Hines Blvd.
Dallas, TX, 75390-8549, USA
E-mail: William.Holland@utsouthwestern.edu
Tel: 214-648-2566
Fax: 214-648-8720

Running title: Tissue-Specific Effects of Adiponectin Receptors

Abstract

Adiponectin and the signaling induced by its cognate receptors, AdipoR1 and AdipoR2, have garnered attention for their ability to promote insulin sensitivity and oppose lipotoxicity. The lipid metabolites ceramide and glucosylceramide are lipids that play causal roles in impairing insulin signaling and are lowered by adiponectin action in several cell types. Having recently demonstrated that the induction of acid ceramidase activity in either the adipocyte or hepatocyte is sufficient to improve hepatic steatosis and whole body glucose homeostasis, we developed strategies for tissue-specific overexpression of AdipoR1 or AdipoR2 selectively within the adipocyte or hepatocyte. Here, we have developed transgenic mice inducibly-expressing AdipoR1 or AdipoR2 under the control of a tetracycline response element. This represents the first inducible genetic model that acutely manipulates adiponectin receptor signaling in adult mouse tissues, allowing us to directly assess the impact of AdipoR signaling on glucose and lipid metabolism. Overexpression of either AdipoR1 or AdipoR2 in the adipose is sufficient to enhance ceramidase activity, whole body glucose metabolism, and hepatic insulin sensitivity, while opposing hepatic steatosis. Unlike acid ceramidase, adiponectin receptors within the adipocyte facilitate lipid uptake and whole-body lipid clearance. Hepatic overexpression of either adiponectin receptor evokes ceramidase activity, opposes hepatic steatosis and prompts improvements in insulin action in liver and adipose tissue. Importantly, these metabolic improvements fail to occur in an adiponectin knockout background. Lastly, when challenged by a genetic model of type 2 diabetes, AdipoR2 expression in adipose or liver is sufficient to reverse hyperglycemia and glucose intolerance on a $Lep^{ob/ob}$ background. As with AdipoR overexpression, the

AdipoR agonist AdipoRon effectively lowers ceramides in each of these tissues. These observations reveal that adiponectin is critical for AdipoR-induced ceramidase activation which promotes effects via rapidly acting “cross-talk” between liver and adipose tissue sphingolipids, critically regulating glucose metabolism and hepatic lipid uptake.

Introduction

The discovery of adipocyte-specific secreted molecules, termed adipokines, have dispelled the notion of adipose tissue as an inert storage depot for lipids, and highlighted its role as an active endocrine organ that monitors and alters whole-body metabolism and maintains energy homeostasis. Since its identification in the mid-90's (1), the adipokine adiponectin (also known as Acrp30, AdipoQ and GBP28) has become best known as a regulator of insulin sensitivity. The two adiponectin receptor isoforms, AdipoR1 and AdipoR2, have been previously shown to be associated increases in activities of AMP-activated protein kinase (AMPK) and peroxisome-proliferator activated receptor (PPAR γ). Recently, our group has shown that adiponectin is capable of inducing of ceramidase activity through its receptors, which results in the hydrolysis of ceramide to form sphingosine and free fatty acid. Sphingosine produced in this reaction can go on to be phosphorylated by sphingosine kinase, and functions as an important signaling molecule in a number of different cellular processes. The ceramide lowering effect of the adiponectin receptors only marginally depends on the activity of AMP kinase (AMPK), but AMPK can be activated through increasing the local sphingosine-1-phosphate pool. Thus, this process appears to be a proximal event in adiponectin signaling since it is a necessary step in adiponectin's induction of AMPK activation. These data supported a previous model based on data from a heterologous system that connected the family of Progesterone and AdipoQ receptors (PAQRs), which includes AdipoR1 and AdipoR2, with ceramidase activity (2, 3) and suggested a revised view of adiponectin signaling with sphingolipid metabolism at its core.

Sphingolipids, such as ceramides and glucosylceramides, are an important class of bioactive lipids. The levels of these lipids change as a function of adipose tissue mass and functionality, and are partially driven by cellular availability of palmitoyl-CoA. Aberrant accumulation of ceramide, glucosylceramide, and GM3 ganglioside has been implicated in a multitude of metabolic processes, including atherosclerosis, insulin resistance, lipotoxic heart failure, β -cell apoptosis and β -cell dysfunction (reviewed in(4)). In stark opposition, the phosphorylated sphingoid base Sphingosine 1-phosphate (S1P) is a potent inducer of proliferation and inhibitor of apoptosis (5). The conversion of ceramide to S1P consists of deacylation of ceramide by ceramidase enzymes, and a subsequent phosphorylation of sphingosine by one of two sphingosine kinase isoforms (6). The opposing nature and simple 2-step conversion-process separating these lipids has led to speculation that the dynamic ratio of ceramide:S1P may constitute a physiological rheostat regulating in numerous cellular processes (5).

To gain further insights into the local physiological consequences of adiponectin and AdipoR-induced ceramidase activation we have embarked on two parallel approaches. Using a novel doxycycline-inducible model to allow for tissue-specific overexpression of acid ceramidase, we have determined that ceramidase activation in adipose or liver is sufficient to prevent or reverse diet-induced steatosis, insulin resistance, and glucose intolerance. Here we have generated similar models allowing for AdipoR1 or AdipoR2 to be expressed under the control of a tetracycline response element (TRE-AdipoR1 or TRE-AdipoR2). We use these in order to determine which adiponectin receptor may have the most beneficial effects on glucose tolerance and whole body insulin sensitivity. Furthermore we will determine whether targeting of adiponectin receptors within

hepatocytes or adipocytes provide the greatest metabolic improvements, and evaluate the effects of adiponectin receptor agonists for their ability to faithfully recapitulate these effects and further enhance them in transgenic mice.

Results

We recently reported that FGF21 rapidly promotes adiponectin secretion and lowers hepatic ceramides. Curiously, FGF21 promoted an increase in accumulation of ceramides (**Supplemental Fig 1A**) and glucosylceramides (**Supplemental Fig 1B**) within the adipose. As opposed to an increase in ceramidase activity in the liver (**Supplemental Fig 1C, top**), ceramidase activity in the adipose was decreased by FGF21 (**Supplemental Fig 1C, bottom**). These data (and others) prompted us to consider if adiponectin receptors promote ceramidase activity within adipocytes to convey adiponectin actions within adipose tissue.

Overexpression of adiponectin receptor 2 in the adipose reduces both adipose and hepatic ceramide levels and improves whole-body glucose and lipid homeostasis.

Following a cross to our established Adiponectin-rtTA (ART) tetracycline transactivator mouse (**Supplemental Fig 1D**), founder lines (R1-Art or R2-Art) for TRE-AdipoR1 and TRE-AdipoR2 were screened for inducible-expression in response to a doxycycline-supplemented diet (200 mg/kg). For TRE-AdipoR2, founder lines were identified which allowed for an 8.6 fold increase in AdipoR2 mRNA levels, which required the presence of doxycycline and an ART allele (**Supplemental Fig 1E**). Following 10 days of doxycycline chow, ceramidase activity was increased in mesenteric and gonadal fat pads, without altering ceramidase activity liver (**Figure 1A**). Under these conditions, the concentration of each major chain length of ceramide was diminished in mesenteric fat by AdipoR2 overexpression (**Supplemental Fig 1F**).

To evaluate the potential for AdipoR2 to maintain glucose homeostasis via local signaling within the adipose, we challenged mice with 8 weeks of high fat diet and 10 additional days of High fat diet supplemented with doxycycline (200 mg/kg). Prior to doxycycline, R2-Art mice and wildtype mice displayed identical degrees of diet-induced glucose intolerance, however, after 10 days of doxycycline, glucose tolerance improved. More importantly, R2-Art mice had markedly better glucose tolerance compared to wildtype littermates following doxycycline (**Fig.1B**). Lower serum insulin during fasting and during glucose tolerance tests suggests improved insulin sensitivity (**Fig.1C**), which was confirmed by superior glucose clearance during insulin tolerance tests (**Fig.1D**).

Adiponectin knockout mice appear to have impaired suppression of lipolysis, which is particularly evident in the relative absence of insulin. When orally challenged with triglyceride, R2-Art mice show improved clearance of lipid from the bloodstream; however, baseline circulating triglycerides are not different from wildtype mice (**Fig.1E**). Moreover, hepatic triglyceride accumulation is also diminished in R2-Art mice (**Fig.1F**). Since ceramidase overexpression in adipose prompts decreased circulating and hepatic ceramides, we addressed whether AdipoR2 related ceramidase activation could also diminish ceramides in serum and liver. Indeed, R2-Art mice have lower circulating ceramides for the majority of all major ceramide species (**Fig.1G**). The transgenic mice also, displayed significantly ($p < 0.05$) lower C16 and C18 ceramides in the liver. Neither glucosylceramides nor sphingoid bases were significantly altered in liver or serum (data not shown).

Overexpression of adiponectin receptor 1 and 2 in the liver reduces hepatic ceramide levels and improves total body glucose and lipid homeostasis.

We and others have previously shown that the adiponectin receptors, AdipoR1 and AdipoR2, mediate the anti-diabetic metabolic actions of adiponectin. To investigate the liver specific actions of adiponectin we generated an inducible, liver-specific AdipoR1 (Alb-R1) and AdipoR2 (Alb-R2) mouse, which combines three transgenic lines: the albumin promoter-driven Cre line, a transgenic line carrying a Rosa26 promoter-driven loxP-stop-loxP-reverse tetracycline-controlled transactivator (rtTA) gene (Rosa26-loxP-stop-loxP-rtTA), and a Tet-responsive AdipoR1 (TRE-R1) or AdipoR2 (TRE-R2) (**Supplemental Fig. 2A**). Upon doxycycline induction, we found that ceramidase activity in liver lysates of Alb-R2 mice to be ~2 times that of WT (**Supplemental Fig. 2B**).

To test whether the increased adiponectin receptor activity has a functional impact on ceramide levels in hepatocytes, we challenged the WT and Alb-R1 and R2 mice with a high fat diet (60% calories from fat) containing 200mg/kg doxycycline (HFD-dox). Past studies have shown that after 8 weeks of HFD-dox exposure, wildtype mice showed a 2.4 fold increase in hepatic ceramides compared to chow-fed controls (**Supplemental Fig. 2C**). Both Alb-R1 and R2 mice showed a significant reduction in C_{16:0} hepatic ceramide species (**Fig. 2A**). In parallel, a significant lowering of C_{16:0} and C_{18:0} ceramide species was also observed in the *serum* (data not shown). Interestingly, AdipoR2 overexpression, but not AdipoR1, also resulted in an increase in hepatic sphingosine-1-phosphate (**Fig. 2A**). Recent work has shown that alterations in hepatic ceramides levels can result in changes in adipose tissue ceramide levels. Hepatic overexpression of AdipoR2 resulted in a corresponding lowering of adipose levels of lactosyl, glucosyl, and total ceramide species (**Fig. 2B**). Liver overexpression of

AdipoR1 resulted in a corresponding lowering of adipose lactosyl and glucosyl ceramide species (**Fig.2B**).

To determine the role of hepatic overexpression of AdipoR1 and R2 in diet-induced obesity and associated metabolic disorders, we exposed Alb-R1, Alb-R2, and WT littermate control mice to HFD-dox for 10 weeks. Body weights of the mice were monitored on a weekly basis during the HFD feeding period. We observed similar weight gain curves for the Alb-R1, Alb-R2, and WT mice and comparable body weights at the end of the 10 weeks of HFD-dox exposure (**Supplemental Fig. 2D**). However, compared to WT controls, Alb-R1 mice exhibited reduced blood glucose levels during the oral glucose tolerance test (OGTT) (**Fig. 2C**), indicating an improvement in systemic glucose tolerance. Additionally, the plasma insulin levels during the OGTT were also lower in the Alb-R1 mice (**Fig. 2D**). Similarly, Alb-R2 mice also exhibited marked lowering of serum glucose levels during the OGTT, while also exhibiting lowered plasma insulin levels compared to WT controls (**Fig. 2E** and **Fig. 2F**). Furthermore, Alb-R2 transgenics required a higher glucose infusion rate to achieve a euglycemia of 120 mg/dL during the hyperinsulinemic-euglycemic clamp compared to their WT littermates, thus, confirming their overall improvement in total body insulin sensitivity (**Supplemental Figure 2E**). Overall, the improvements in systemic glucose homeostasis are much more pronounced in the Alb-R2 mice compared to Alb-R1 mice. Furthermore, insulin signaling in the liver of Alb-R1 and Alb-R2 mice was assessed by insulin-stimulated phosphorylation of Akt. After an injection of insulin, p-Akt levels were greatly increased in the liver of transgenic animals, reflecting improved insulin sensitivity (**Fig. 2G**).

In order to assess the effects of liver overexpression of AdipoR1 and R2 on *systemic* lipid homeostasis, we performed a triglyceride clearance test by gavaging a lipid emulsion (20% Intralipid) to both Alb-R1, Alb-R2 and WT mice. Both Alb-R1 and Alb-R2 had significantly lowered basal serum triglyceride levels compared to WT and at the same time exhibited higher rate of triglyceride clearance compared to their WT littermate controls (**Fig. 2H**). Furthermore, the increased rate of triglyceride clearance is more pronounced in Alb-R2 mice compared to Alb-R1 mice. Prolonged HFD exposure often causes the accumulation of lipids in the liver. Considering that serum adiponectin levels are inversely correlated with hepatic triglyceride content (7), we expect the both the Alb-R1 and Alb-R2 mice livers to have less lipid accumulation compared to WT controls. Livers were harvested from Alb-R1 and Alb-R2 mice after 10 weeks of HFD-dox diet. Histologically, both Alb-R1 and R2 livers exhibited substantially less lipid accumulation compared to WT controls (**Fig. 2I**). Biochemical analysis of hepatic triglyceride content of Alb-R1 and Alb-R2 livers showed that both Alb-R1 and Alb-R2 exhibited almost a 50% decrease in hepatic triglyceride accumulation compared to WT mice (**Fig. 2I**).

The metabolic improvements of adiponectin receptor overexpression in the liver are adiponectin dependent.

The liver is the main target tissue of adiponectin and AdipoR2 is the dominant adiponectin receptor isoform in the liver. To determine whether the beneficial effects of adiponectin receptor overexpression is ligand dependent, we crossed the Alb-R2 mice with the adiponectin knockout mice (APN KO) previously generated in our lab (8) to

generate a mouse devoid of endogenous adiponectin but still overexpressing AdipoR2 in the liver (R2-KO).

To test whether increasing adiponectin receptor activity alone has a functional impact on hepatic ceramide levels in the absence of adiponectin, we challenged R2-KO mice and APN KO mice with 10 weeks of HFD-dox and quantified hepatic and serum ceramides in both groups. We found that there were no significant differences in hepatic and serum ceramide species between R2-KO and APN KO mice (**Fig. 3A**). Metabolically, both groups developed insulin resistance and hyperglycemia as a result of the HFD-dox feeding. Surprisingly, R2-KO mice did not exhibit any improvements in glucose homeostasis during the OGTT at the end of the HFD-dox challenge compared to the APN KO mice (**Fig. 3B**). We observed there were no significant differences in weight gain between the APN KO and R2-KO during the 10 week period of HFD-dox feeding and both groups had comparable body weights at the end of the 10 weeks of HFD-dox feeding (**Fig. 3C**). Additionally, R2-KO mice had higher, but insignificant, levels of plasma insulin during the OGTT compared to its APN KO counterpart (**Fig. 3D**). Insulin signaling in the liver of R2-KO and APN KO mice was assessed by insulin-stimulated phosphorylation of Akt. After 15 minutes of insulin stimulation, p-Akt levels in R2-KO mice livers are similar to the levels in APN KO, thus indicating that insulin signaling was not improved (**Fig. 3E**). Overall, in the absence of adiponectin, liver specific overexpression of AdipoR2 loses its beneficial effects on body glucose homeostasis and insulin sensitivity that was previously observed.

In order to assess whether there were improvements in systemic lipid homeostasis in the R2-KO mice, we performed a triglyceride clearance test by orally

gavaging a lipid emulsion (20% Intraplipid) to both R2-KO and APN KO mice. Although R2-KO peaked at lower levels than APN KO the overall rate of triglyceride clearance between R2-KO and APN KO was not increased (**Fig. 3F**). Livers harvested from the R2-KO and APN KO mice after 10 weeks of HFD-dox were not different histologically. Livers from both groups had hepatic steatosis as a result of the HFD challenge, and biochemical analysis of hepatic triglyceride content of R2-KO and APN-KO livers showed that both groups had similar levels of hepatic triglyceride accumulation (**3G**). Therefore, in the absence of its ligand, adiponectin, liver overexpression of AdipoR2 also fails to improve total body lipid homeostasis and reduce hepatic triglyceride content.

Past work done by Okada-Iwabu et al has shown that an orally active small molecules that bind to and activate adiponectin receptors (AdipoRon) could ameliorate insulin resistance and glucose intolerance in mice fed a high fat diet (9) by similar cellular mechanisms as adiponectin. Thus we test whether providing AdipoRon to APN KO or R2-KO mice would elicit a similar effect on their glucose homeostasis. We fed APN KO and R2-KO mice a HFD-dox for 10 weeks and at the end of the 10 weeks we injected 5mg/kg of AdipoRon in both R2-KO and APN KO mice littermate controls. Two hours after AdipoRon injection, we observed that R2-KO mice had a more robust lowering of serum glucose (73% of basal) compared to APN KO controls (92% of basal) (**Fig. 3H**). Thus, the metabolically beneficial effect of liver AdipoR2 overexpression on systemic glucose homeostasis is restored upon stimulation by a ligand.

AdipoR2 overexpression in adipose or liver is capable of rescuing diabetic phenotype in ob/ob mice.

Past studies have shown that in insulin-resistant ob/ob mice the expression levels of both AdipoR1 and AdipoR2 are significantly decreased in tissues (10). In order to determine whether overexpression of adiponectin receptors in adipose or liver is capable of ameliorating the insulin resistance and glucose intolerance exhibited in ob/ob mice, we crossed the Art-R2 and Alb-R2 transgenic models into the ob/ob genetic background. In addition, we also bred adipose and liver specific overexpression of acid ceramidase (Art-AC and Alb-AC respectively) into ob/ob genetic background to study whether direct lowering of ceramides in those metabolic tissues can rescue the ob/ob phenotype. Adipose specific overexpression of R2 and AC, ob/ob^{Art-R2} and ob/ob^{Art-AC} respectively, showed marked reductions in WAT ceramide levels after 10 days of dox chow induction. This was especially evident in mWAT where transgene expression was the highest (**Fig. 4A**). In addition, ob/ob^{Art-R2} had significant lowering of mWAT C_{16:0} ceramide species whereas ob/ob^{Art-AC} did not exhibit this phenomenon (**Fig. 4A**). The lowering of WAT C_{16:0} ceramide in ob/ob^{Art-R2} corresponded with improvements in glucose homeostasis during an OGTT compared to ob/ob mice. ob/ob^{Art-AC} mice, however, did not exhibit any improvements in glucose homeostasis compared to ob/ob littermate controls (**Fig. 4B**).

To test whether *liver* overexpression of AdipoR2 (ob/ob^{Alb-R2}) or acid ceramidase (ob/ob^{Alb-AC}) is capable of rescuing the ob/ob phenotype, we put ob/ob, ob/ob^{Alb-R2}, and ob/ob^{Alb-AC} mice on chow-dox diet for 10 days and then assessed glucose homeostasis with an OGTT. We found that ob/ob^{Alb-R2} mice have markedly lowered serum glucose levels during the OGTT compared to ob/ob control, indicating vast improvements in glucose clearance (**Fig. 4C**). Although ob/ob^{Alb-AC} exhibited significantly lowered basal

serum glucose levels compared to ob/ob controls, the overall rate of glucose clearance in ob/ob^{Alb-AC} was not changed compared to ob/ob mice (**Fig. 4C**). In addition, ob/ob^{Alb-R2} had greatly lowered levels of serum insulin during the OGTT compared to ob/ob mice while ob/ob^{Alb-AC} had visibly lowered, but insignificant, levels of serum insulin compared to ob/ob during OGTT (**Fig. 4D**).

Discussion

Here, we report the first mouse models demonstrating inducible overexpression of adiponectin receptors. Our inducible AdipoR models bypasses the compensatory mechanisms and developmental issues present in constitutive models, and gives us the opportunity to study acute modifications of ceramide-induced metabolic dysfunction in adult mice. With this novel system, we demonstrate that the acute depletion of ceramide via adiponectin receptor expression and activation in hepatocytes or adipocytes of adult mice can prevent the development of hepatic steatosis while simultaneously improving systemic glucose tolerance and insulin sensitivity in adult mice with diet-induced obesity. These studies highlight the prominent cross-talk between the liver and adipose tissue that allows for equilibration of sphingolipids between the two tissues. Furthermore, these studies are the first to define a causal role for ceramide in the pathogenesis of diet-induced NAFLD.

Similar to our recent report of acid ceramidase overexpression we find that adiponectin receptors functionally prevent accumulation of C16 and C18 ceramides in DIO mice. We found that that C_{16:0} and C_{18:0} ceramide levels to be 50% of WT in Alb-AC mice livers, indicating that the hepatic accumulation of particular ceramide subspecies more prominently contributes to the development of NAFLD and systemic insulin resistance. Consistent with our findings, recent work has shown that mice with ceramide synthase 6 deficiency (*cerS6^{Δ/Δ}*) exhibit reduced C_{16:0} ceramide levels and are protected from high fat diet-induced obesity and glucose intolerance (11). By contrast, heterozygous deletion of ceramide synthase 2 promotes a paradoxical increase in C_{16:0} ceramides to confer greater susceptibility to diet induced insulin resistance (12). Thus,

these studies directly link excess accumulation of hepatic ceramide to the development of non-alcoholic fatty liver disease and systemic insulin resistance in rodents.

Preclinical models indicate roles for adiponectin in the maintenance of hepatic lipid metabolism. Adiponectin null mice develop fibrotic steatohepatitis and adenomas when maintained on high fat diets for 48 weeks (13) but not in response to shorter-term diet administration (14, 15). Genetic ablation of adiponectin in leptin-deficient (*ob/ob*) mice further exacerbates hepatic triglyceride accumulation (16). Conversely, adiponectin overexpression prevents accumulation of triglycerides or the deleterious lipid metabolites diacylglycerols or ceramides (17, 18). Similar effects are seen in other transgenic mice which develop hyperadiponectinemia secondary to changes in adipose mitochondrial function, as they are also refractory to TG, diacylglycerol, or ceramide overaccumulation (19). Administration of recombinant adiponectin in rodents results in beneficial effects on lipid metabolism, such as enhancing lipid clearance and increasing fatty acid oxidation in muscle and liver (20, 21). Several groups have also demonstrated that circulating adiponectin concentrations decrease during chronic ethanol experiments in rodents (22-24). Chronic consumption of high-fat ethanol-containing food has been shown in the past to lower plasma adiponectin in rodents within three weeks of treatment as steatosis progresses. Delivery of adenoviral adiponectin can attenuate hepatomegaly, steatosis and liver injury in these mice (23).

Adiponectin is anti-steatotic by decreasing free FFA influx into the liver and increased FFA oxidation and mitochondrial biogenesis (25). Studies with genetic manipulation of adiponectin receptors show similar trends as adiponectin itself, and human single nucleotide polymorphisms in either adiponectin receptor are significantly

associated with liver triglyceride accumulation (26, 27) and even risk for cirrhosis (28). Though not consistently seen in either human or animal studies (29), some reports indicate down regulation of adiponectin receptor transcription may be seen in livers of NAFLD and NASH patients (30, 31). Decreased expression of AdipoR2 has also been observed in murine models of hepatic steatosis (32). Conversely direct manipulation of adiponectin receptor expression demonstrates a potential causal relationship between adiponectin signaling and steatosis (33). Adenoviral-mediated overexpression of either adiponectin receptor is sufficient to stimulate lipid oxidation and diminish hepatic triglyceride content (34). By contrast, mice lacking both isoforms of the adiponectin receptors display enhanced hepatic triglyceride accumulation. In sum, either lowered plasma adiponectin or lowered AdipoR2 expression in liver can sufficiently induce the development of hepatic steatosis.

Importantly, the actions of adiponectin receptors critically rely on adiponectin for their functional lowering of ceramides, and subsequent improvements in glucose and lipid homeostasis. This study adds strong *in vivo* genetic support that AdipoRs are indeed the cognate receptors that convey adiponectin actions. This challenges our previous notion that these receptors indeed have a strong basal activity, and rather, suggest that it is very difficult to eliminate adiponectin from culture systems where it is present in FBS containing medium, which is enriched in bovine adiponectin.

These studies provide strong preclinical evidence that adiponectin receptor agonism may be a powerful therapeutic tool. We show here for the first time, that AdipoRon stimulates a ceramidase activity and can activate the adiponectin receptors to induce its metabolic beneficial effects when adiponectin is not present.

Collectively, our data suggest that the lowering of ceramides is a critical player in adiponectin-induced improvements in non-alcoholic fatty liver disease and hepatic insulin resistance in mice with diet-induced obesity. Our data also demonstrate that the induction of AC activity is insufficient to rescue metabolic syndrome in ob/ob mice, while AdipoR2 overexpression is sufficient. Several key differences in these two approaches have been noted. First, adiponectin receptors lower more chain lengths of ceramides with diet induced obesity, suggesting that it is a potential novel therapeutic target. Recent reports show that the PAQR family of receptors, which includes AdipoRs, share homology with alkaline ceramidase (2). Furthermore, in mammalian cells, it remains unclear whether the adiponectin receptors themselves can catalyze ceramide hydrolysis or whether they sequester and induce a ceramidase upon induction. Our data using the R2-KO model suggests the latter seems to be the case. Unlike AC overexpression in the liver, AdipoR2 overexpression results in a significant increase in hepatic S1P levels. S1P has been shown in the past to induce AMPK, a major downstream effector of adiponectin (35). Thus, a possible explanation of why AdipoR2 overexpression is capable of rescuing ob/ob phenotype is that it is an essential initiator of the broad spectrum of adiponectin action. Thus, orally active small-molecule adiponectin receptor agonists, such as AdipoRon, could potentially be an important therapeutic agent for patients with non-alcoholic fatty liver disease and other obesity related metabolic syndrome (9).

Methods and Materials

Animals

All animal experimental protocols were approved by the Institutional Animal Care and Use Committee of University of Texas Southwestern Medical Center at Dallas. TRE-AC mice were generated by subcloning the human AC gene into a plasmid containing the TetO element. Following linearization, the construct was injected into C57/Bl6-derived blastocysts. Transgene-positive offspring were genotyped using PCR with the following primer sets: TRE-AC, 5'-GACTGTATTCAACCTTGATG and 5'-CATCTTCCCATTCTAAACAAC.

The *Rosa26-loxP-stop-loxP-rtTA* and *Albumin-Cre* mice were lines were obtained from Jackson Laboratories. *Albumin-Cre* mice were bred with the *Rosa26-loxP-stop-loxP-rtTA* mice to achieve liver-specific expression of rtTA. This mouse was subsequently crossed to the TRE-AC transgenic mice. The resulting triple transgenic mice expressed AC in liver only after exposure to doxycycline (Dox). All overexpression experiments were performed in a pure C57/Bl6 background. All experiments were conducted using littermate-controlled male mice. All Dox-chow diet (200 mg/kg Dox) or HFD-Dox (200 mg/kg Dox) experiments were initiated at approximately 6-12 weeks of age.

Neutral ceramidase activity assay

Acid ceramidase activity was determined by a fluorimetric assay using the substrate Rbm 14-12, a synthetic ceramide analog that possess a 12-carbon fatty acid chain length, at 20 uM after incubation for 3 hours with tissue lysates (20 ug protein) of both wild-type mice (WT) and Alb-AC mice after 8 weeks of HFD-dox (36).

Systemic tests

For OGTTs, mice were fasted for 3 hours prior to administration of glucose (2.5 g/kg body-weight by gastric gavage). At the indicated time-points, venous blood samples were collected in heparin-coated capillary tubes from the tail-vein. Glucose levels were measured using an oxidase-peroxidase assay (Sigma-Aldrich). Mice did not have access to food throughout the experiment. Glucose levels were determined using an oxidase-peroxidase assay (Sigma-Aldrich). Insulin levels were measured using commercial ELISA kits (Millipore Linco Research). For triglyceride clearance, mice were fasted overnight (~15 h), then gavaged with 15 ul/g body weight of 20% intralipid (Fresenius Kabi Clyton, L.P.). Blood was collected hourly and then assayed for triglyceride (Infinity, Thermo Fisher Scientific). In the hepatic VLDL-TG production assay, mice were fasted for 5 hours, followed by intravenous injection of 10% tyloxapol (Sigma-Aldrich) at 500 mg/kg body weight. Blood was collected hourly and then assayed for plasma triglyceride. The lipolysis suppression assay was initiated by i.p. injection of bovine insulin (0.1 mU/g) and serum was collected at 0, 15, 30, 60, and 120 mins for glycerol assays.

Hyperinsulinemic-euglycemic clamps

Hyperinsulinemic-euglycemic clamps were performed on conscious, unrestrained male C57 black WT and Alb-AC mice, as previously described (19, 37).

³H-triolein uptake and β -oxidation

For measurements of endogenous triolein clearance rates, tissue-specific lipid uptake and β -oxidation rates in transgenic tissues, methodologies were adapted from

previously detailed studies. Briefly, ^3H -triolein was tail-vein injected (2 uCi per mouse in 100 ul of 5% intralipid) into mice after a 5-hour fast. Briefly, blood samples (10 ul) were then collected at 1, 2, 5, 10 and 15 min after injection. At 20 minutes following injection, mice were euthanized, blood samples were taken and tissues were quickly excised, weighed and frozen at $-80\text{ }^\circ\text{C}$ until processing. Lipids were then extracted using a chloroform-to-methanol based extraction method. The radioactivity content of tissues, including blood samples, was quantified as described previously (19).

Quantitative real-time PCR

Tissues were excised from mice and snap-frozen in liquid nitrogen. Total RNA was isolated following tissue homogenization in Trizol (Invitrogen, Carlsbad, CA) using a TissueLyser (MagNA Lyser, Roche), then isolated using an RNeasy RNA extraction kit (Qiagen). The quality and quantity of the RNA was determined by absorbance at 260/280 nm. cDNA was prepared by reverse transcribing 1 ug of RNA with an iScript cDNA Synthesis Kit (BioRad). Results were calculated using the threshold cycle method (38), with β -actin used for normalization.

Histology, immunohistochemistry (IHC) and immunofluorescence (IF)

The relevant adipose and liver tissues were excised and fixed in 10% PBS-buffered formalin for 24 h. Following paraffin embedding and sectioning (5 μm), tissues were stained with H&E or a Masson's trichrome stain. For IHC, paraffin-embedded sections were stained using monoclonal antibodies to Mac2 (1:500, CL8942AP, CEDARLANE Laboratories USA Inc.). For IF, cells were grown on glass bottom culture dishes (MatTek Corporation) and were stained with polyclonal antibodies to CD36 (1:200, Novus Biologicals, USA).

Immunoblotting

Frozen tissue was homogenized in TNET buffer (50 mM Tris-HCl, pH 7.6, 150 mM NaCl, 5 mM EDTA, phosphatase inhibitors (Sigma-Aldrich) and protease inhibitors (Roche) and then centrifuged to remove any adipose layer present. After the addition of Triton X-100 (final concentration of 1%), protein concentrations were determined using a bicinchoninic acid assay (BCA) kit (Pierce). Proteins were resolved on 4–20% TGX gel (Bio-Rad) then transferred to nitrocellulose membranes (Protran). pAkt (Ser473, 4060) and total Akt (2920) (Cell Signaling Technology, Inc.) were used (1:1,000) for insulin signaling studies. Anti-CD36 (Novus Biologicals, USA) and anti-PKC ζ (Santa Cruz, USA) polyclonal antibodies were used (1:1000) for Westerns and Immunoprecipitations. Primary antibodies were detected using secondary IgG labeled with infrared dyes emitting at 700 nm (926-32220) or 800 nm (926-32211) (both at 1:5,000 dilutions) (Li-Cor Bioscience) and then visualized on a Li-Cor Odyssey infrared scanner (Li-Cor Bioscience). The scanned data were analyzed and quantitated using Odyssey Version 2.1 software (Li-Cor Bioscience).

Lipid quantifications

Sphingolipid were quantified as described previously by LC/ESI/MS/MS using a TSQ Quantum Ultra-triple quadrupole mass spectrometer (Thermo Fisher) equipped with an electrospray ionization (ESI) probe and interfaced with an Agilent 1100 HPLC (Agilent Technologies) (37). Diacylglycerol was quantified as previously described (37).

AdipoRon Treatment

Mice were injected IP with 5 mg/kg of AdipoRon (Sigma) as previously described (9). Serum glucose was monitored for 2 hours post-injection.

Statistics

All results are provided as means \pm s.e.m. All statistical analyses were performed using GraphPad Prism. Differences between the two groups over time (indicated in the relevant figure legends) were determined by a two-way analysis of variance for repeated measures. For comparisons between two independent groups, a Student's *t* test was used. Significance was accepted at $P < 0.05$.

Author contributions

JYX and WLH are co-first authors. WLH designed the studies, carried out the research, interpreted the results. JYX designed the studies, carried out the research, interpreted the results, and wrote the manuscript related to AC expression in the liver. JAJ, KS, MJP, AJS and RG assisted in study design, performed research, and reviewed the manuscript. PES designed the study, analysed the data, reviewed and revised the manuscript, and is responsible for the integrity of this work. All authors approved the final version of the manuscript

Acknowledgements

We thank Dr. Bob Hammer and the Transgenic Core Facility at UTSW for the generation of the transgenic lines, John Shelton and the Histology Core for assistance with histology and the UTSW Metabolic Core Unit for help in phenotyping. Supported by the National Institutes of Health (grants R01-DK55758, R01-DK099110 and P01DK088761-01 to PES). JYX is supported by a NIH fellowship 1F30-DK100095. WLH is supported by a R00-DK094973 and JDRF Award 5-CDA-2014-185-A-N. The authors declare no conflicts of interest.

References

1. Scherer PE, Williams S, Fogliano M, Baldini G, Lodish HF. A novel serum protein similar to C1q, produced exclusively in adipocytes. *The Journal of biological chemistry*. 1995;270(45):26746-9.
2. Villa NY, Kupchak BR, Garitaonandia I, Smith JL, Alonso E, Alford C, Cowart LA, Hannun YA, Lyons TJ. Sphingolipids function as downstream effectors of a fungal PAQR. *Molecular pharmacology*. 2009;75(4):866-75. doi: 10.1124/mol.108.049809. PubMed PMID: 19066337; PubMed Central PMCID: PMC2684929.
3. Kupchak BR, Garitaonandia I, Villa NY, Smith JL, Lyons TJ. Antagonism of human adiponectin receptors and their membrane progesterone receptor paralogs by TNFalpha and a ceramidase inhibitor. *Biochemistry*. 2009;48(24):5504-6. Epub 2009/05/21. doi: 10.1021/bi9006258. PubMed PMID: 19453184; PubMed Central PMCID: PMC2789275.
4. Holland WL, Summers SA. Sphingolipids, insulin resistance, and metabolic disease: new insights from in vivo manipulation of sphingolipid metabolism. *Endocr Rev*. 2008;29(4):381-402. PubMed PMID: 18451260.
5. Takabe K, Paugh SW, Milstien S, Spiegel S. "Inside-out" signaling of sphingosine-1-phosphate: therapeutic targets. *Pharmacol Rev*. 2008;60(2):181-95. Epub 2008/06/17. doi: pr.107.07113 [pii]10.1124/pr.107.07113. PubMed PMID: 18552276; PubMed Central PMCID: PMC2695666.
6. Spiegel S, Milstien S. Sphingosine-1-phosphate: an enigmatic signalling lipid. *Nat Rev Mol Cell Biol*. 2003;4(5):397-407. Epub 2003/05/03. doi: 10.1038/nrm1103nrm1103 [pii]. PubMed PMID: 12728273.
7. Turer AT, Browning JD, Ayers CR, Das SR, Khera A, Vega GL, Grundy SM, Scherer PE. Adiponectin as an independent predictor of the presence and degree of hepatic steatosis in the Dallas Heart Study. *The Journal of clinical endocrinology and metabolism*. 2012;97(6):E982-6. doi: 10.1210/jc.2011-3305. PubMed PMID: 22438228.
8. Nawrocki AR, Rajala MW, Tomas E, Pajvani UB, Saha AK, Trumbauer ME, Pang Z, Chen AS, Ruderman NB, Chen H, Rossetti L, Scherer PE. Mice lacking adiponectin show decreased hepatic insulin sensitivity and reduced responsiveness to peroxisome proliferator-activated receptor gamma agonists. *The Journal of biological chemistry*. 2006;281(5):2654-60. doi: 10.1074/jbc.M505311200. PubMed PMID: 16326714.
9. Okada-Iwabu M, Yamauchi T, Iwabu M, Honma T, Hamagami K, Matsuda K, Yamaguchi M, Tanabe H, Kimura-Someya T, Shirouzu M, Ogata H, Tokuyama K, Ueki K, Nagano T, Tanaka A, Yokoyama S, Kadowaki T. A small-molecule AdipoR agonist for type 2 diabetes and short life in obesity. *Nature*. 2013;503(7477):493-9. doi: 10.1038/nature12656. PubMed PMID: 24172895.
10. Tsuchida A, Yamauchi T, Ito Y, Hada Y, Maki T, Takekawa S, Kamon J, Kobayashi M, Suzuki R, Hara K, Kubota N, Terauchi Y, Froguel P, Nakae J, Kasuga M, Accili D, Tobe K, Ueki K, Nagai R, Kadowaki T. Insulin/Foxo1 pathway regulates expression levels of adiponectin receptors and adiponectin sensitivity. *The Journal of biological chemistry*. 2004;279(29):30817-22. doi: 10.1074/jbc.M402367200. PubMed PMID: 15123605.
11. Turpin SM, Nicholls HT, Willmes DM, Mourier A, Brodesser S, Wunderlich CM, Mauer J, Xu E, Hammerschmidt P, Bronneke HS, Trifunovic A, LoSasso G, Wunderlich FT, Kornfeld JW, Bluher M, Kronke M, Bruning JC. Obesity-Induced CerS6-Dependent C16:0 Ceramide Production Promotes Weight Gain and Glucose Intolerance. *Cell metabolism*. 2014;20(4):678-86. doi: 10.1016/j.cmet.2014.08.002. PubMed PMID: 25295788.

12. Raichur S, Wang ST, Chan PW, Li Y, Ching J, Chaurasia B, Dogra S, Ohman MK, Takeda K, Sugii S, Pewzner-Jung Y, Futerman AH, Summers SA. CerS2 Haploinsufficiency Inhibits beta-Oxidation and Confers Susceptibility to Diet-Induced Steatohepatitis and Insulin Resistance. *Cell metabolism*. 2014;20(4):687-95. doi: 10.1016/j.cmet.2014.09.015. PubMed PMID: 25295789.
13. Asano T, Watanabe K, Kubota N, Gunji T, Omata M, Kadowaki T, Ohnishi S. Adiponectin knockout mice on high fat diet develop fibrosing steatohepatitis. *Journal of gastroenterology and hepatology*. 2009;24(10):1669-76. doi: 10.1111/j.1440-1746.2009.06039.x. PubMed PMID: 19788607.
14. Yano W, Kubota N, Itoh S, Kubota T, Awazawa M, Moroi M, Sugi K, Takamoto I, Ogata H, Tokuyama K, Noda T, Terauchi Y, Ueki K, Kadowaki T. Molecular mechanism of moderate insulin resistance in adiponectin-knockout mice. *Endocrine journal*. 2008;55(3):515-22. PubMed PMID: 18446001.
15. Liu Q, Yuan B, Lo KA, Patterson HC, Sun Y, Lodish HF. Adiponectin regulates expression of hepatic genes critical for glucose and lipid metabolism. *Proceedings of the National Academy of Sciences of the United States of America*. 2012;109(36):14568-73. doi: 10.1073/pnas.1211611109. PubMed PMID: 22904186; PubMed Central PMCID: PMC3437840.
16. Holland WL, Adams AC, Brozinick JT, Bui HH, Miyauchi Y, Kusminski CM, Bauer SM, Wade M, Singhal E, Cheng CC, Volk K, Kuo MS, Gordillo R, Kharitonov A, Scherer PE. An FGF21-Adiponectin-Ceramide Axis Controls Energy Expenditure and Insulin Action in Mice. *Cell metabolism*. 2013;17(5):790-7. doi: 10.1016/j.cmet.2013.03.019. PubMed PMID: 23663742; PubMed Central PMCID: PMC3667496.
17. Kim JY, van de Wall E, Laplante M, Azzara A, Trujillo ME, Hofmann SM, Schraw T, Durand JL, Li H, Li G, Jelicks LA, Mehler MF, Hui DY, Deshaies Y, Shulman GI, Schwartz GJ, Scherer PE. Obesity-associated improvements in metabolic profile through expansion of adipose tissue. *J Clin Invest*. 2007;117(9):2621-37. PubMed PMID: 17717599.
18. Holland WL, Brozinick JT, Wang LP, Hawkins ED, Sargent KM, Liu Y, Narra K, Hoehn KL, Knotts TA, Siesky A, Nelson DH, Karathanasis SK, Fontenot GK, Birnbaum MJ, Summers SA. Inhibition of ceramide synthesis ameliorates glucocorticoid-, saturated-fat-, and obesity-induced insulin resistance. *Cell metabolism*. 2007;5(3):167-79. doi: 10.1016/j.cmet.2007.01.002. PubMed PMID: 17339025.
19. Kusminski CM, Holland WL, Sun K, Park J, Spurgin SB, Lin Y, Askew GR, Simcox JA, McClain DA, Li C, Scherer PE. MitoNEET-driven alterations in adipocyte mitochondrial activity reveal a crucial adaptive process that preserves insulin sensitivity in obesity. *Nature medicine*. 2012;18(10):1539-49. doi: 10.1038/nm.2899. PubMed PMID: 22961109; PubMed Central PMCID: PMC3745511.
20. Yamauchi T, Kamon J, Waki H, Terauchi Y, Kubota N, Hara K, Mori Y, Ide T, Murakami K, Tsuboyama-Kasaoka N, Ezaki O, Akanuma Y, Gavrilova O, Vinson C, Reitman ML, Kagechika H, Shudo K, Yoda M, Nakano Y, Tobe K, Nagai R, Kimura S, Tomita M, Froguel P, Kadowaki T. The fat-derived hormone adiponectin reverses insulin resistance associated with both lipodystrophy and obesity. *Nat Med*. 2001;7(8):941-6.
21. Xu A, Wang Y, Keshaw H, Xu LY, Lam KS, Cooper GJ. The fat-derived hormone adiponectin alleviates alcoholic and nonalcoholic fatty liver diseases in mice. *J Clin Invest*. 2003;112(1):91-100. PubMed PMID: 12840063.
22. Rogers CQ, Ajmo JM, You M. Adiponectin and alcoholic fatty liver disease. *IUBMB Life*. 2008;60(12):790-7. doi: 10.1002/iub.124.
23. Xu A, Wang Y, Keshaw H, Xu LY, Lam KSL, Cooper GJS. The fat-derived hormone adiponectin alleviates alcoholic and nonalcoholic fatty liver diseases in mice. *The Journal of Clinical Investigation*. 2003;112(1):91-100. doi: 10.1172/jci17797.

24. You M, Considine RV, Leone TC, Kelly DP, Crabb DW. Role of adiponectin in the protective action of dietary saturated fat against alcoholic fatty liver in mice. *Hepatology*. 2005;42(3):568-77. doi: 10.1002/hep.20821.
25. Buechler C, Wanninger J, Neumeier M. Adiponectin, a key adipokine in obesity related liver diseases. *World J Gastroenterol*. 2011;17(23):2801-11. Epub 2011 June 21. doi: 10.3748/wjg.v17.i23.2801.
26. Kotronen A, Yki-Jarvinen H, Aminoff A, Bergholm R, Pietilainen KH, Westerbacka J, Talmud PJ, Humphries SE, Hamsten A, Isomaa B, Groop L, Orho-Melander M, Ehrenborg E, Fisher RM. Genetic variation in the ADIPOR2 gene is associated with liver fat content and its surrogate markers in three independent cohorts. *European journal of endocrinology / European Federation of Endocrine Societies*. 2009;160(4):593-602. doi: 10.1530/EJE-08-0900. PubMed PMID: 19208777.
27. Stefan N, Machicao F, Staiger H, Machann J, Schick F, Tschritter O, Spieth C, Weigert C, Fritsche A, Stumvoll M, Haring HU. Polymorphisms in the gene encoding adiponectin receptor 1 are associated with insulin resistance and high liver fat. *Diabetologia*. 2005;48(11):2282-91. doi: 10.1007/s00125-005-1948-3. PubMed PMID: 16205883.
28. Namvaran F, Rahimi-Moghaddam P, Azarpira N, Nikeghbalian S. The association between adiponectin (+45T/G) and adiponectin receptor-2 (+795G/A) single nucleotide polymorphisms with cirrhosis in Iranian population. *Molecular biology reports*. 2012;39(3):3219-23. doi: 10.1007/s11033-011-1089-3. PubMed PMID: 21706165.
29. Buechler C, Wanninger J, Neumeier M. Adiponectin, a key adipokine in obesity related liver diseases. *World journal of gastroenterology : WJG*. 2011;17(23):2801-11. doi: 10.3748/wjg.v17.i23.2801. PubMed PMID: 21734787; PubMed Central PMCID: PMC3120939.
30. Shimizu A, Takamura T, Matsuzawa N, Nakamura S, Nabemoto S, Takeshita Y, Misu H, Kurita S, Sakurai M, Yokoyama M, Zen Y, Sasaki M, Nakanuma Y, Kaneko S. Regulation of adiponectin receptor expression in human liver and a hepatocyte cell line. *Metabolism: clinical and experimental*. 2007;56(11):1478-85. doi: 10.1016/j.metabol.2007.06.013. PubMed PMID: 17950097.
31. Kaser S, Moschen A, Cayon A, Kaser A, Crespo J, Pons-Romero F, Ebenbichler CF, Patsch JR, Tilg H. Adiponectin and its receptors in non-alcoholic steatohepatitis. *Gut*. 2005;54(1):117-21. doi: 10.1136/gut.2003.037010. PubMed PMID: 15591515; PubMed Central PMCID: PMC1774357.
32. Matsunami T, Sato Y, Ariga S, Sato T, Shimomura T, Kashimura H, Hasegawa Y, Yukawa M. Regulation of synthesis and oxidation of fatty acids by adiponectin receptors (AdipoR1/R2) and insulin receptor substrate isoforms (IRS-1/-2) of the liver in a nonalcoholic steatohepatitis animal model. *Metabolism: clinical and experimental*. 2011;60(6):805-14. doi: <http://dx.doi.org/10.1016/j.metabol.2010.07.032>.
33. Asterholm IW, Scherer PE. Enhanced metabolic flexibility associated with elevated adiponectin levels. *The American journal of pathology*. 2010;176(3):1364-76. doi: 10.2353/ajpath.2010.090647. PubMed PMID: 20093494; PubMed Central PMCID: PMC2832156.
34. Yamauchi T, Nio Y, Maki T, Kobayashi M, Takazawa T, Iwabu M, Okada-Iwabu M, Kawamoto S, Kubota N, Kubota T, Ito Y, Kamon J, Tsuchida A, Kumagai K, Kozono H, Hada Y, Ogata H, Tokuyama K, Tsunoda M, Ide T, Murakami K, Awazawa M, Takamoto I, Froguel P, Hara K, Tobe K, Nagai R, Ueki K, Kadowaki T. Targeted disruption of AdipoR1 and AdipoR2 causes abrogation of adiponectin binding and metabolic actions. *Nat Med*. 2007;13(3):332-9. doi: 10.1038/nm1557. PubMed PMID: 17268472.
35. Levine YC, Li GK, Michel T. Agonist-modulated regulation of AMP-activated protein kinase (AMPK) in endothelial cells. Evidence for an AMPK -> Rac1 -> Akt -> endothelial nitric-oxide

- synthase pathway. *The Journal of biological chemistry*. 2007;282(28):20351-64. doi: 10.1074/jbc.M702182200. PubMed PMID: 17519230.
36. Bedia C, Camacho L, Abad JL, Fabrias G, Levade T. A simple fluorogenic method for determination of acid ceramidase activity and diagnosis of Farber disease. *Journal of lipid research*. 2010;51(12):3542-7. doi: 10.1194/jlr.D010033. PubMed PMID: 20871013; PubMed Central PMCID: PMC2975727.
 37. Holland WL, Miller RA, Wang ZV, Sun K, Barth BM, Bui HH, Davis KE, Bikman BT, Halberg N, Rutkowski JM, Wade MR, Tenorio VM, Kuo MS, Brozinick JT, Zhang BB, Birnbaum MJ, Summers SA, Scherer PE. Receptor-mediated activation of ceramidase activity initiates the pleiotropic actions of adiponectin. *Nature medicine*. 2011;17(1):55-63. doi: 10.1038/nm.2277. PubMed PMID: 21186369; PubMed Central PMCID: PMC3134999.
 38. Livak KJ, Schmittgen TD. Analysis of relative gene expression data using real-time quantitative PCR and the 2⁻($\Delta\Delta C_T$) Method. *Methods*. 2001;25(4):402-8. Epub 2002/02/16. doi: 10.1006/meth.2001.1262. PubMed PMID: 11846609.

Figure 1

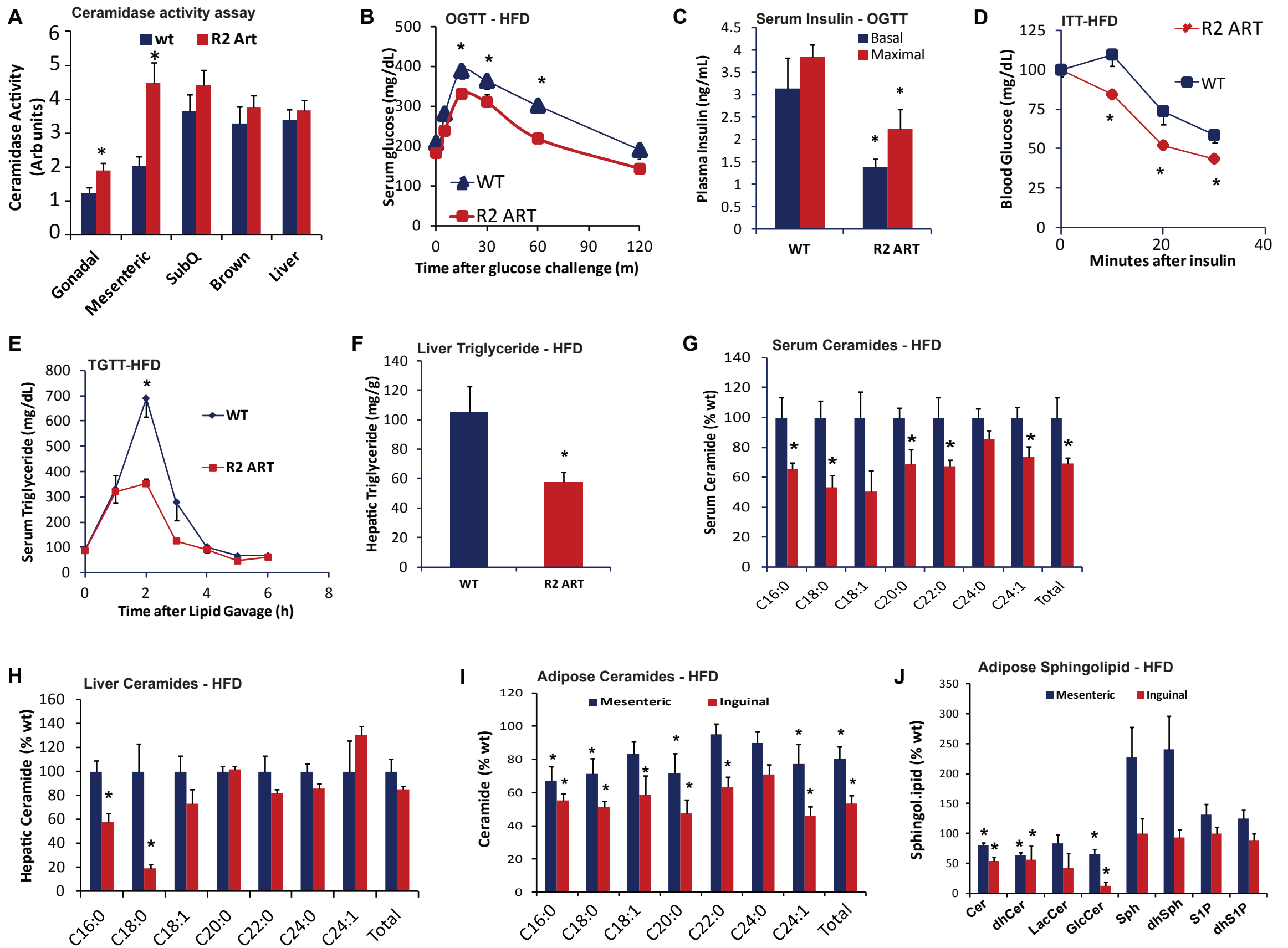


Fig 1. Inducible Adipose-specific overexpression of AdipoR2 result in systemic improvements in glucose and lipid homeostasis. **A)** Analysis of neutral ceramidase activity from adipose depots and liver Art-R2 mice and WT littermates after 10 days of dox-Chow. **B-J)** After 8 weeks of HFD, mice were switched to HFD-dox. Circulating glucose levels were measured during an oral glucose tolerance test (OGTT, 2.5g/kg glucose per oral gavage) 7 days after dox. **C)** Serum insulin levels during the OGTT were quantified via ELISA. **D)** Circulating glucose levels measured during an insulin tolerance test (ITT) (0.75 U/kg, IP). **E)** Circulating triglyceride (TG) levels were measured during an oral TG clearance test (20% intralipid, 15 uL/g body weight; single gavage) in Alb-AC mice and WT littermate controls. **F)** Hepatic TG content was enzymatically quantified. **G-I)** Ceramide species of the indicated chain lengths were quantified in serum (G), liver (H) and mesenteric and inguinal adipose depots (I) were quantified and expressed as % of wildtype. **J)** Total abundance of distinct sphingolipid species were quantified from inguinal and mesenteric adipose (n = 6-8/group). * $P < 0.05$.

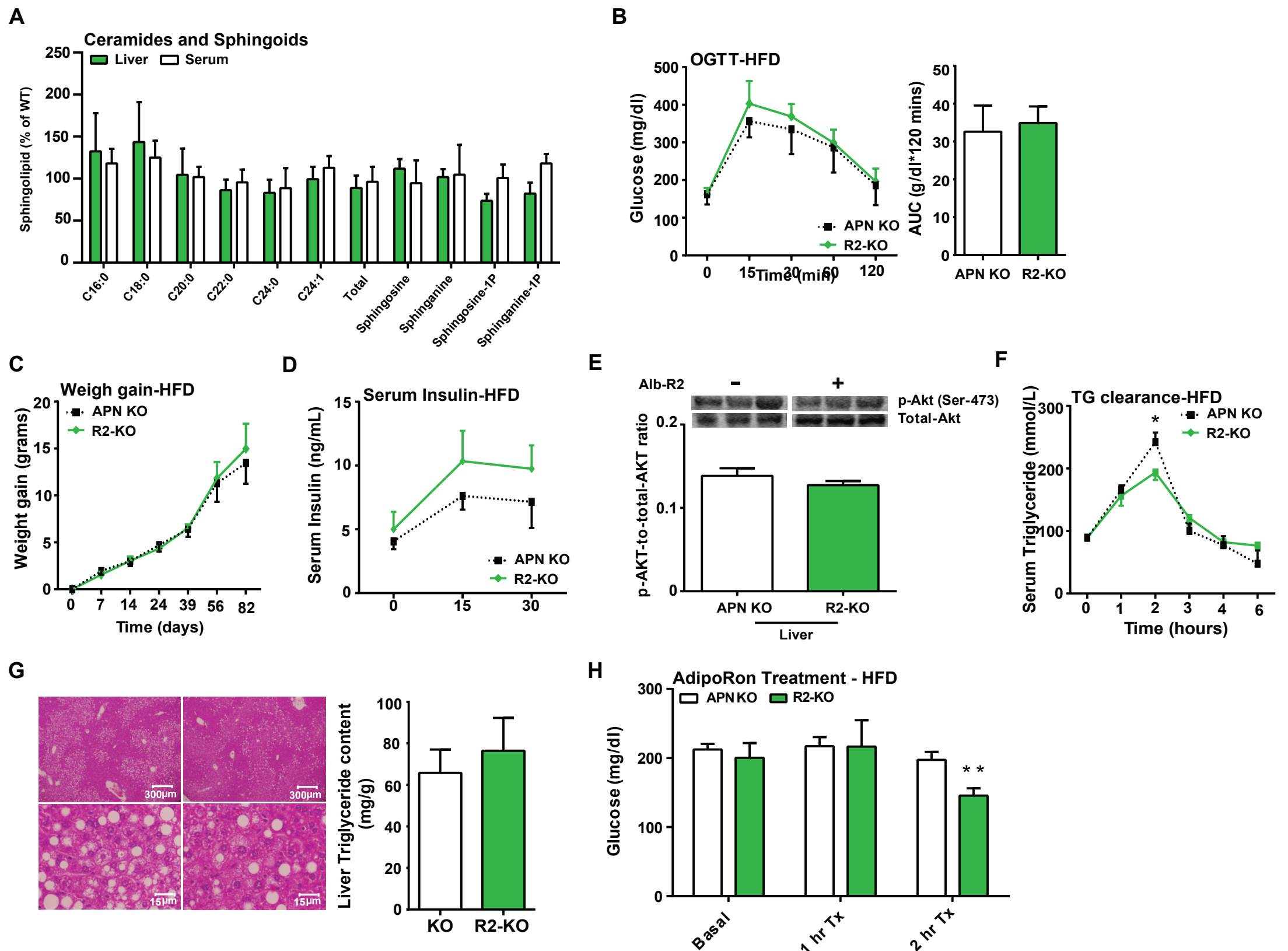
Figure 3

Fig. 3. The metabolic improvements of adiponectin receptor overexpression in the liver are adiponectin dependent. **A)** Analysis of liver and serum ceramide and sphingoid species from R2-KO mice and APN KO littermates. **B)** Circulating glucose levels were measured during an oral glucose tolerance test (OGTT) for R2-KO and APN KO mice (2.5g/kg glucose per oral gavage). **C)** Weight gain in R2-KO mice and APN KO littermates during 10 weeks of HFD-dox. **D)** Serum insulin levels during the OGTT were quantified via ELISA for R2-KO mice. **E)** Representative immunoblots of phosphorylated and total Akt of insulin stimulated R2-KO and APN KO shown in triplicate. **F)** Circulating triglyceride (TG) levels were measured during an oral TG clearance test (20% intralipid, 15 uL/g body weight; single gavage) in R2-KO and APN KO littermate controls. **G)** Representative H&E stained images of R2-KO and WT livers. Bar graphs on the right represent quantification of liver triglyceride levels. All samples are from R2-KO mice and APN KO littermates after 10 weeks of HFD-dox challenge (n = 6), unless specified otherwise. **H)** Serum glucose levels were measured before and after IP injection of AdipoRon (5mg/kg) in APN KO and R2-KO mice after 10 weeks of HFD-dox challenge. * $P < 0.05$, ** $P < 0.01$ by Student's *t* test.

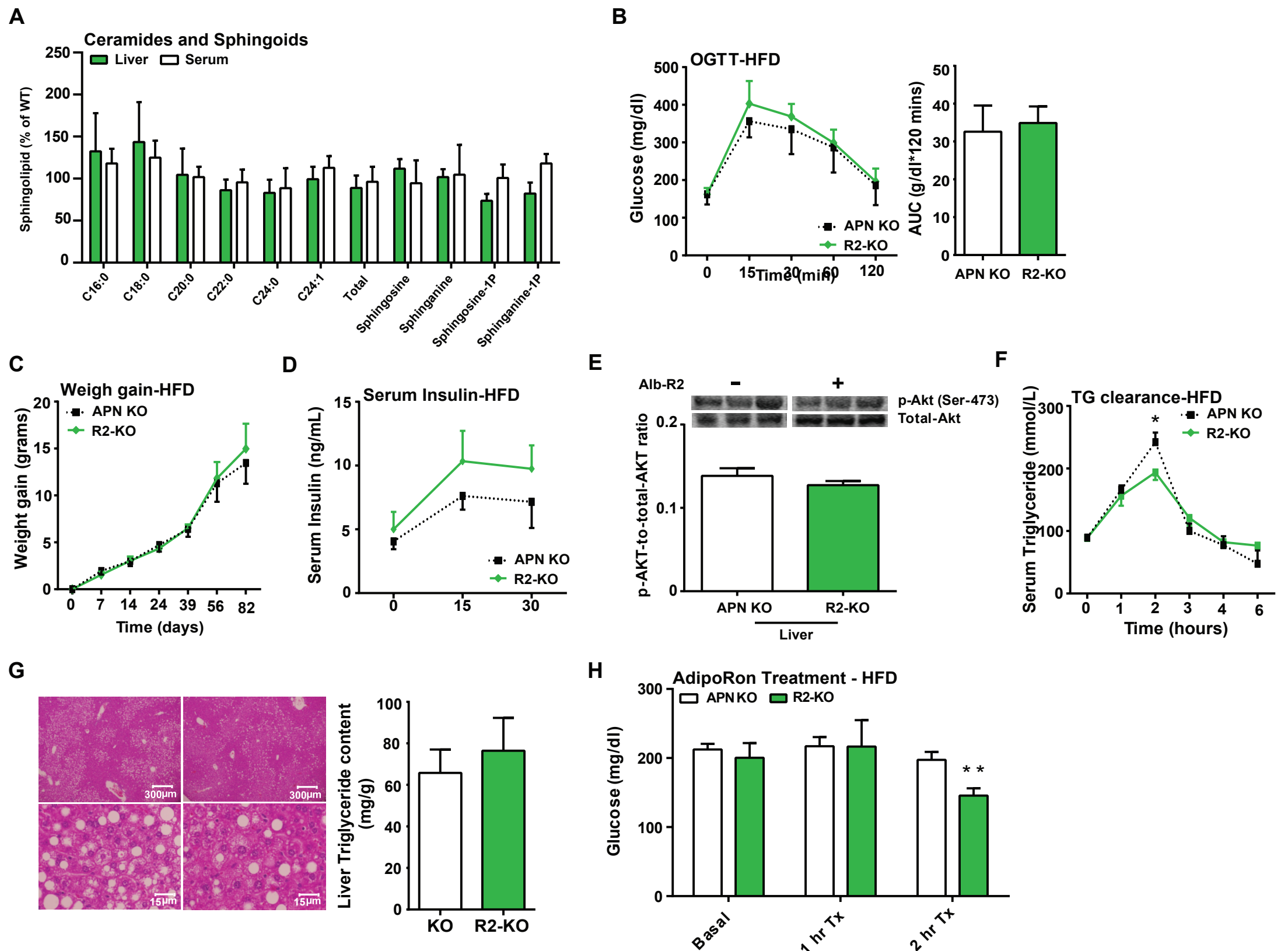
Figure 3

Fig. 3. The metabolic improvements of adiponectin receptor overexpression in the liver are adiponectin dependent. **A)** Analysis of liver and serum ceramide and sphingoid species from R2-KO mice and APN KO littermates. **B)** Circulating glucose levels were measured during an oral glucose tolerance test (OGTT) for R2-KO and APN KO mice (2.5g/kg glucose per oral gavage). **C)** Weight gain in R2-KO mice and APN KO littermates during 10 weeks of HFD-dox. **D)** Serum insulin levels during the OGTT were quantified via ELISA for R2-KO mice. **E)** Representative immunoblots of phosphorylated and total Akt of insulin stimulated R2-KO and APN KO shown in triplicate. **F)** Circulating triglyceride (TG) levels were measured during an oral TG clearance test (20% intralipid, 15 uL/g body weight; single gavage) in R2-KO and APN KO littermate controls. **G)** Representative H&E stained images of R2-KO and WT livers. Bar graphs on the right represent quantification of liver triglyceride levels. All samples are from R2-KO mice and APN KO littermates after 10 weeks of HFD-dox challenge (n = 6), unless specified otherwise. **H)** Serum glucose levels were measured before and after IP injection of AdipoRon (5mg/kg) in APN KO and R2-KO mice after 10 weeks of HFD-dox challenge. * $P < 0.05$, ** $P < 0.01$ by Student's *t* test.

Figure 4

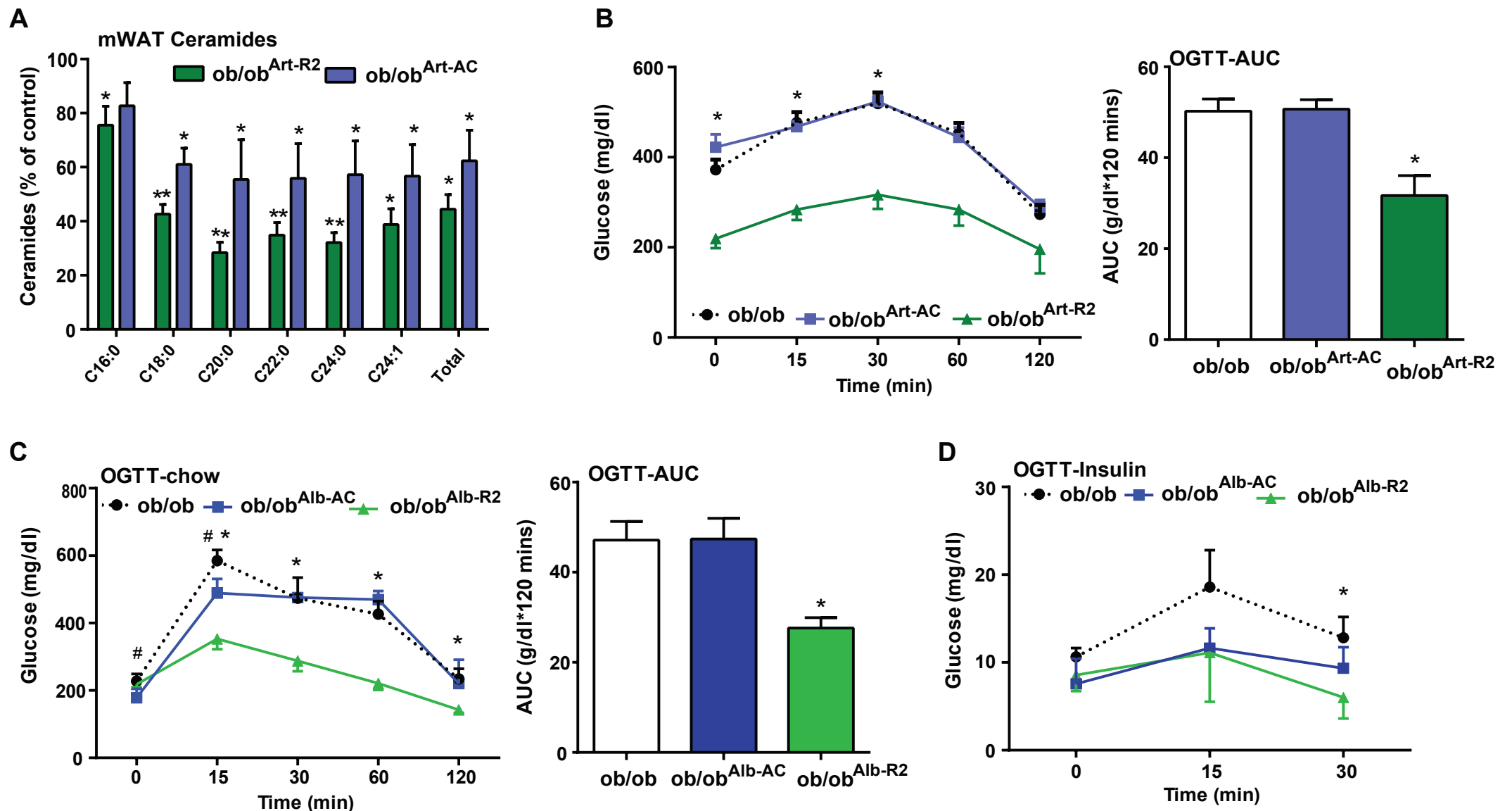
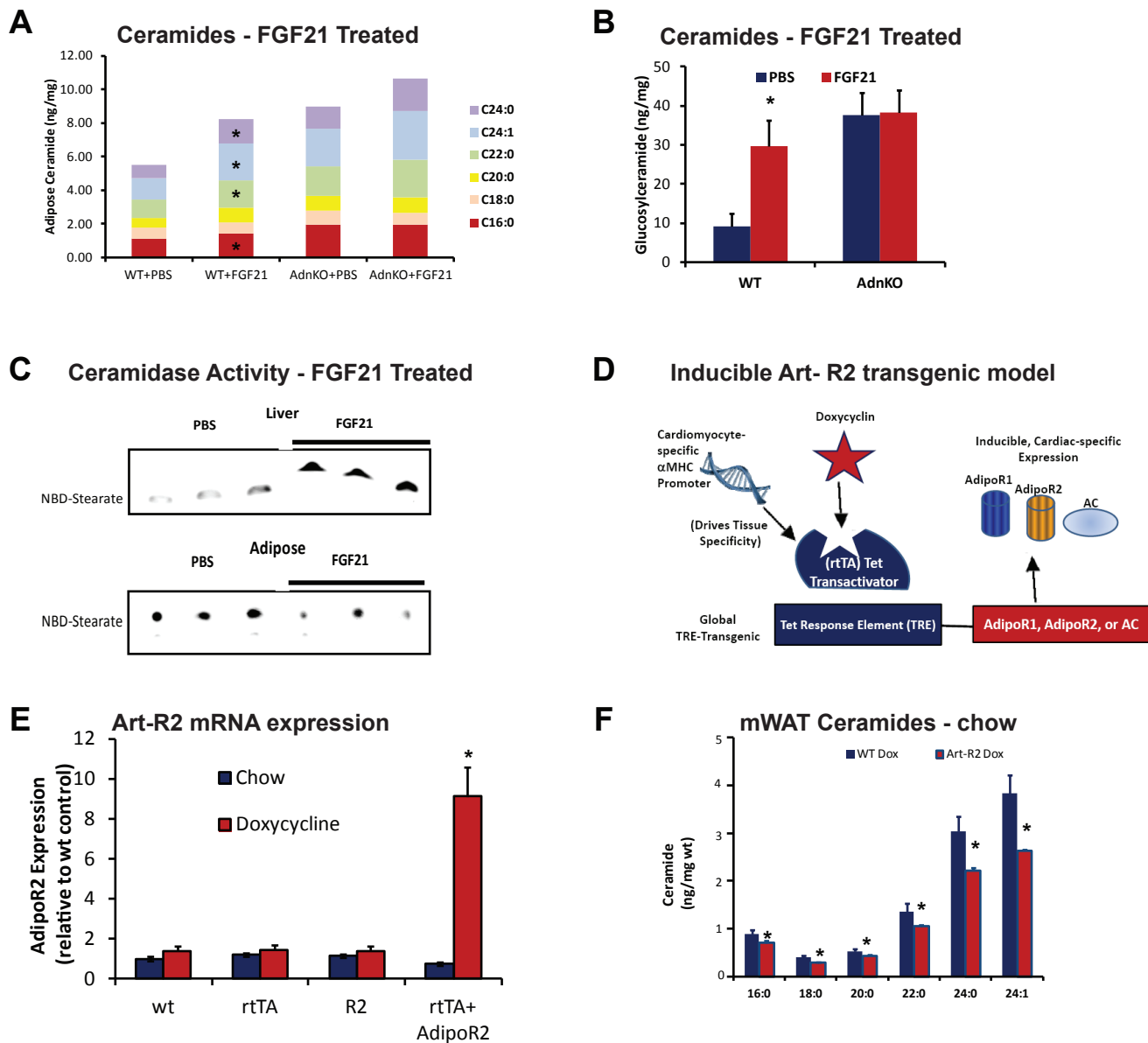


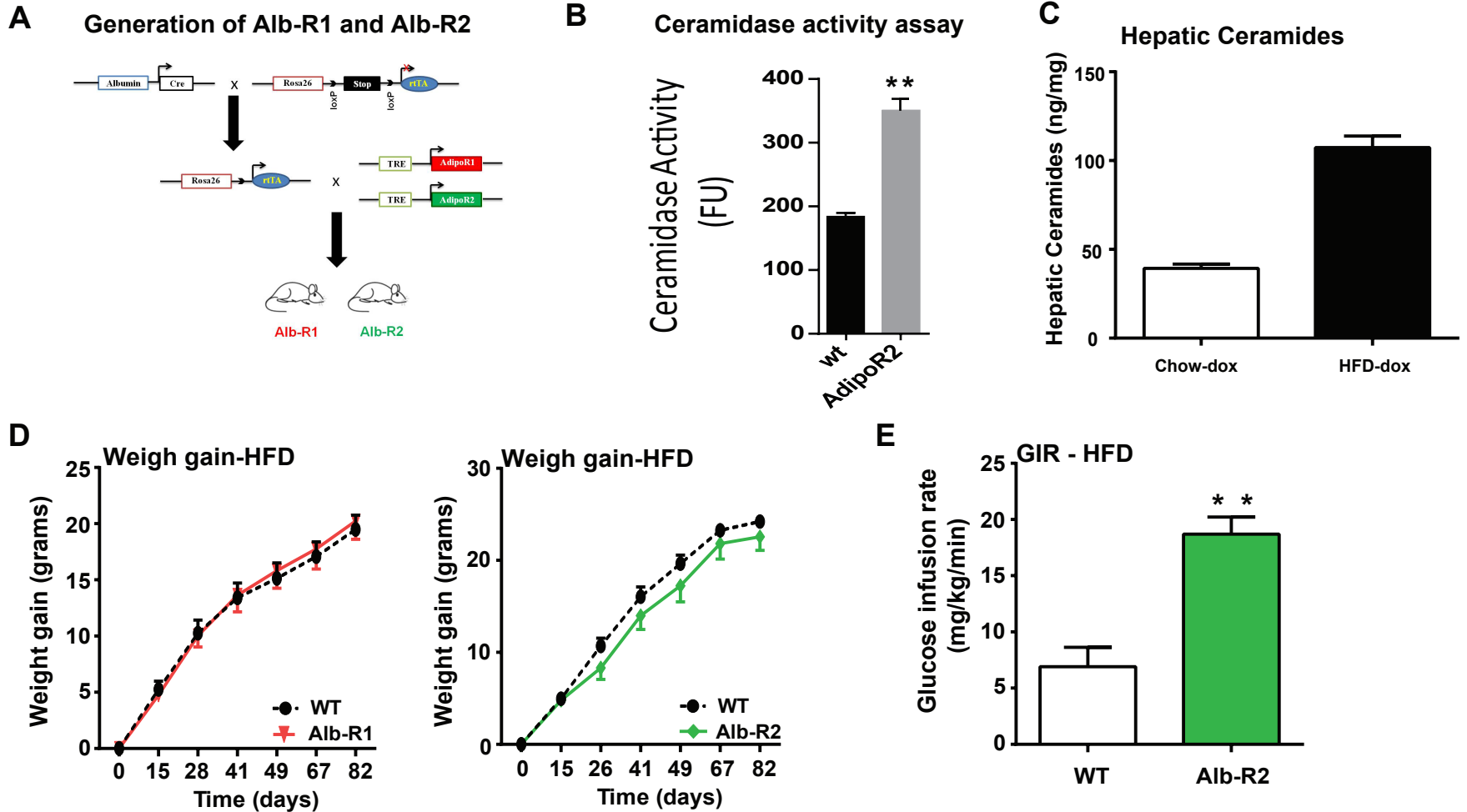
Fig 4. Overexpression of adiponectin receptors, but not acid ceramidase rescues glucose homeostasis in ob/ob mice **A**) Ceramide species of the indicated chain lengths were quantified in mesenteric and inguinal adipose depots from ob/ob mice following 2 weeks of dox-induced overexpression to drive Art-AdipoR2 or Art-Acid Ceramidase (AC). Data were quantified and expressed as % of wildtype ob/ob control. **B**) Circulating glucose levels were measured during an oral glucose tolerance test (OGTT) (2.5 g/kg glucose per oral gavage) in ob/ob, ob/ob Art-AC, and ob/ob Art-AdipoR2 transgenic mice **C**) Circulating glucose levels were measured during an oral glucose tolerance test (OGTT) (2.5 g/kg glucose per oral gavage) after 10 days of dox-induced expression of AdipoR2 or Acid Ceramidase in the liver of ob/ob mice (* depicts ob/ob vs ob/ob^{Alb-R2}, # depicts ob/ob vs ob/ob^{Alb-AC}). **D**) Insulin levels before and during the OGTT were measured by ELISA. *,#P<0.05 by Student's *t* test.

Supplemental Figure 1



Supplemental Figure 1 in support of Fig. 1: A&B FGF21 (1 mg/kg/d, sc minipump) promotes elevated ceramides (**A**) and glucosylceramides (**B**) in subcutaneous adipose tissue. **C** 2 hours after injection of FGF21 (1 mg/kg, IP) neutral ceramidase activity was measured by the formation of NBD Stearate cleavage from NBD-Ceramide. Fluorescent bands are shown in triplicate after resolving stearate from ceramide via thin layer chromatography. **D** The schematic diagram depicts our adipose specific transgenic model, which utilizes a doxycycline transactivator which is expressed under the control of an adiponectin promoter to limit doxycycline induced transcription of TRE-AdipoR, selectively within the mature adipocyte. **E** AdipoR2 expression in mesenteric adipose was evaluated by qPCR in mice expressing TRE-AdipoR2 in the presence or absence of the ART transactivator or doxycycline. **F** Ceramides were measured from mesenteric AdipoR2 after 10 days of dox chow. *P<0.05.

Supplemental Figure 2



Supplemental Fig. 2 in support of Fig. 2: Inducible liver-specific overexpression of either AdipoR1 or AdipoR2 results in significantly reduced C_{16:0} ceramide species in the liver and improved total body glucose homeostasis and reduced hepatic lipid accumulation under HFD feeding. A) Strategy of generating mice with liver-specific inducible expression of AC (Acid Ceramidase). B) Neutral ceramidase activity was measured by the formation of NBD Stearate cleavage from NBD-Ceramide. Fluorescent bands are shown in triplicate after resolving stearate from ceramide via thin layer chromatography and quantified by densitometry. C) Liver ceramide content of mice fed either of chow or HFD. D) Weight gain in Alb-R1, Alb-R2 mice and APN KO littermates during 10 weeks of HFD-dox. E) Glucose infusion rate during hyperinsulinemic-euglycemic clamp of Alb-R2 and WT mice fed a HFD-dox diet for 8 weeks. *P<0.05, **P<0.01 by students *t*test.

Chapter 4

CONCLUSIONS AND FUTURE DIRECTION

4:1 Conclusions

The understanding of adipose tissue function has changed dramatically in the past 20 years. Once viewed simply as a passive reservoir for energy storage, adipose tissue is now recognized as an endocrine organ that plays an important role in metabolism (1). As obesity ascends to epidemic levels in the United States, understanding obesity in terms of adipose tissue dysfunction becomes increasingly important. Adipose tissue secretes a wide array of unique factors, adipokines, which allow it to act on target organs in an autocrine, paracrine, and endocrine manner. Adipokines have been widely highlighted in the literature to function in regulating whole-body energy homeostasis. Furthermore, altered adipokine levels lead to profound changes in insulin sensitivity and alterations of metabolites that are widely observed in individuals suffering from obesity and other forms of metabolic syndromes (2). Among these adipokines, adiponectin is one of the most potent metabolic regulators due to its anti-inflammatory, anti-apoptotic, and insulin sensitizing actions (3). Unlike the vast majority of adipokines, adiponectin's expression level is inversely correlated with adipose tissue expansion (4). In addition, it has been established that circulating adiponectin promotes insulin sensitivity by acting on peripheral tissues such as liver and muscle to decrease gluconeogenesis and enhance glucose uptake respectively (5, 6).

Although there is a vast amount of literature on the systemic effects of adiponectin, no unifying mechanism has yet explained how adiponectin can exert such

a variety of beneficial systemic effects at the cellular level. Yamauchi *et al* in 2003 discovered that adiponectin's actions are mediated through seven transmembrane G-protein coupled receptor-like receptors, named adiponectin receptors 1 and 2 (7). Studies in myocytes have shown that adiponectin, by acting through the adiponectin receptors, can activate AMP-activated protein kinase (AMPK) and increase expression and decrease acetylation of peroxisome proliferator-activated receptor gamma coactivator-1alpha (PGC-1alpha), a protein important for mitochondrial biogenesis (8, 9). Recently, our lab demonstrated that these receptors confer ceramidase activity that can be enhanced by adiponectin. Ceramide promotes apoptosis by aiding death receptor clustering, apoptosome formation, Bcl-2-associated X protein (Bax) translocation, and impairing activation of Akt via activation of protein kinase C or protein phosphatase 2A (PP2A). Our studies therefore linked the pleiotropic effects of adiponectin to the changes of intracellular ceramides and their metabolites (10). Interestingly, adiponectin receptors are also expressed in adipocytes (11). This discovery seems to advocate the idea that adiponectin is able to act locally in an autocrine or paracrine manner to augment adipose tissue function.

The objectives of this dissertation were to identify the effects of acute catabolism of ceramides on systemic metabolism. We studied this using a series of targeted cell-specific and inducible transgenic models. These were the first ever inducible and tissue specific models to be used to study the ceramide/sphingolipid axis *in vivo*. The most salient findings include (Fig. 1):

1. Liver specific overexpression of acid ceramidase results in a significant reduction of C16 and C18 ceramides species in both liver and serum in mice

challenged with a HFD. This reduction corresponds with significant improvements in systemic glucose homeostasis and insulin sensitivity and at the same time slows the development of NAFLD in mice challenged with HFD.

2. Adipose specific overexpression of acid ceramidase also results in a significant reduction of C16 and C18 ceramides in the adipose while lowering total ceramide levels in the adipose and serum in mice fed a HFD. This corresponds with significant improvements in systemic glucose homeostasis and insulin sensitivity and slows the development of NAFLD in mice challenged with HFD.
3. Liver specific overexpression of acid ceramidase results in modulations in sphingolipid levels in adipose tissue. Conversely, adipose specific overexpression of acid ceramidase results in changes in liver sphingolipid levels. This highlights the existence of a “cross-talk” between the two tissues as they shuttle a common pool of sphingolipids back and forth through circulation.
4. Both the overexpression of acid ceramidase in adipose or liver is capable of rescuing the NAFLD phenotype in mice with existing fatty livers. This confirms, unambiguously, that ceramide accumulation plays an important role in the development of NAFLD *in vivo*.
5. Targeted manipulation of ceramide alters atypical PKC activation in the liver, which can critically influence uptake and lipogenic programs.

6. Liver specific overexpression of AdipoR1 and AdipoR2 results in significant reductions in hepatic accumulation of C16 and C18 ceramides. Overexpression of AdipoR2 also results in significant increases in S1P in the liver. This corresponds to improvements in systemic glucose homeostasis and insulin sensitivity and amelioration of NAFLD in mice challenged with a HFD.
7. Adipose specific overexpression of AdipoR2 results in lowering of C16 and C18 ceramides in adipose tissue and lowered circulating ceramide levels. This not only corresponds to improvements in total body glucose homeostasis and insulin sensitivity but also reduction in hepatic lipid accumulation in mice challenged with HFD.
8. The effects of adiponectin receptor overexpression are rely on adiponectin for their functional lowering of ceramides. When AdipoR2 is overexpressed in the liver in adiponectin knockout mice, it fails to lower hepatic or serum ceramides and does not result in any beneficial metabolically effects. This adds strong *in vivo* evidence that AdipoRs are indeed the cognate receptors that convey adiponectin actions.
9. Liver specific overexpression of AdipoR2 but not acid ceramidase is capable of rescuing mice in the Lep^{ob/ob} background. This suggests that AdipoR2 initiates intracellular processes that are independent of ceramide degradation to promote the broad spectrum adiponectin functions.

4:2 Ongoing studies and future directions

We pioneered work demonstrating that diminishing sphingolipids via targeted-disruption of their catabolic enzymes in the liver or adipose tissue improves insulin sensitivity, glucose homeostasis, and prevents the onset of frank diabetes in genetically disposed models. Previous work has shown that ceramide accumulation in both peripheral and central tissues can result in the failed insulin action and ensuing metabolic syndrome (12-14).

Sphingolipids and central regulation of metabolism

Several previous reports highlight the potential for ceramides to alter hypothalamic regulation of energy balance. Our initial insights which suggested a role for sphingolipids in hypothalamic signaling stemmed from the observation that myriocin, an inhibitor of serine palmitoyltransferase (SPT-the rate limiting enzyme in *de novo* ceramide synthesis), decreases body weight gain in diet-induced obese mice(15, 16), but not ZDF rats, Zucker fa/fa rats or ob/ob mice(17). Collectively, these studies suggested that leptin function is needed to see the effects of a ceramide synthesis inhibitor on body weight regulation. Though circulating leptin levels are lower, mirroring the degree of adiposity (16), enhanced leptin-mediated effects on energy expenditure appear to be present in myriocin treated mice (15). Together these findings suggest enhanced sensitivity to leptin-induced energy expenditure. The Lopaschuk group has shown that intracerebroventricular (ICV) infusion of myriocin enhances leptin-induced suppression of food intake in icv leptin tolerance tests (18). By contrast, ICV administration of the short chain ceramide analog C2 ceramide impairs leptin-mediated suppression of food intake. More recently, ICV delivery of another soluble analog, C6

ceramide, was shown to increase body weight gain by altering energy expenditure (12). Insulin sensitivity was impaired, as measured by insulin tolerance tests; however, confounds of greater body mass existed in these studies. We now know that endogenous ceramides increase within the hypothalamus during administration of high fat diets (19) or lipid emulsions enriched in saturated fatty acids (20). Furthermore, glial cells, particularly mature oligodendrocytes, play critical roles in supplying the lipids used in myelination, including cholesterol and sphingolipid (21, 22). Recent observations suggest that glia are activated, particularly in the arcuate nucleus of the hypothalamus, by high-fat feeding and may play critical roles in the development of obesity and abnormal glucose homeostasis (23, 24). Notably, Krabbe's disease, a lysosomal storage disease caused by impaired degradation of glucosylceramides causes enhanced gliosis, which is prevented by inhibition of *de novo* sphingolipid (25)

Given the emergence of central regulation of glucose control (26), these studies prompted us to develop the genetic tools required to definitively evaluate the contributions of endogenous hypothalamic ceramides to alterations in glucose homeostasis. Using our doxycycline inducible system, we made transgenic mice that overexpress acid ceramidase in glial cells (GFAP-AC) and POMC neurons (POMC-AC). In the GFAP-AC, we found that prior to doxycycline induction, the mice have similar body weight and glucose tolerance compared to WT. However, when placed on HFD-dox, body weights of GFAP-AC and WT mice begin to diverge (data not shown). Consistent with the lowering of body weight, glucose tolerance is significantly improved in GFAP-AC mice compared to its littermate controls (data not shown). This phenomenon was also observed in Contreras *et al's* study where they ICV injected C6

ceramides in mice and reported a increase in weight gain and reduced glucose tolerance. Furthermore, similar to Contreras *et al's* study, lowering of central ceramide levels, in this case in glial cells, also enhanced mitochondrial biogenesis and increased mitochondrial respiration in brown adipose tissue (data not shown) (12). Furthermore, BAT in GFAP-AC mice showed reduced whitening compared to WT littermates when challenged with HFD (data not shown). In the future, we will evaluate the importance of glial sphingolipid production to both the *initiation* and *reversal* of obesity, insulin resistance, and glucose intolerance. We will further evaluate changes in signaling and neuronal excitability within the POMC neurons of GFAP-AC mice; crossing the GFAP-AC with mice constitutively expressing GFP under the POMC promoter aids in easy identification of POMC positive cells for electrophysiological assessments and co-localization of signaling intermediates (pAkt, pStat3). We will additionally assess the propensity for gliosis, a common histological finding in HFD fed rodents (27), in GFAP-AC mice. The intensity, size, morphology, and abundance of GFAP positive cells will be assessed in a double-blind manner and scored using previously established scoring methods (23). Overall, this preliminary data point to the idea that sphingolipids play an important role in central regulation of body weight and glucose homeostasis and further investigation is necessary to dissect the specific mechanisms on how this phenomenon occurs.

Adiponectin has been shown to be present in the cerebrospinal fluid of humans and adiponectin receptors were also found to be expressed in the hypothalamus (28-30). Past studies in rodents found that ICV administration of adiponectin decreased body weight mainly by stimulating energy expenditure and was able to rescue the

Lep^{ob/ob} phenotype (31). Considering our preliminary data showing that lowering glial ceramides is capable of increasing BAT mitochondrial respiration and lowering body weight, the mechanism of how ICV administration of adiponectin conferring improvements in systemic metabolism is by lowering central ceramide levels. With the development of small molecule agonists of adiponectin receptors, perhaps finding methods of central delivery will be an important therapeutic agent for treating obesity and metabolic syndrome in the future.

References:

1. Kershaw EE, Flier JS. Adipose tissue as an endocrine organ. *The Journal of clinical endocrinology and metabolism*. 2004;89(6):2548-56. doi: 10.1210/jc.2004-0395. PubMed PMID: 15181022.
2. Hauner H. Secretory factors from human adipose tissue and their functional role. *The Proceedings of the Nutrition Society*. 2005;64(2):163-9. PubMed PMID: 15960861.
3. Turer AT, Scherer PE. Adiponectin: mechanistic insights and clinical implications. *Diabetologia*. 2012;55(9):2319-26. doi: 10.1007/s00125-012-2598-x. PubMed PMID: 22688349.
4. Hotta K, Funahashi T, Bodkin NL, Ortmeier HK, Arita Y, Hansen BC, Matsuzawa Y. Circulating concentrations of the adipocyte protein adiponectin are decreased in parallel with reduced insulin sensitivity during the progression to type 2 diabetes in rhesus monkeys. *Diabetes*. 2001;50(5):1126-33. PubMed PMID: 11334417.
5. Berg AH, Combs TP, Scherer PE. ACRP30/adiponectin: an adipokine regulating glucose and lipid metabolism. *Trends in endocrinology and metabolism: TEM*. 2002;13(2):84-9. PubMed PMID: 11854024.
6. Combs TP, Berg AH, Obici S, Scherer PE, Rossetti L. Endogenous glucose production is inhibited by the adipose-derived protein Acrp30. *The Journal of clinical investigation*. 2001;108(12):1875-81. doi: 10.1172/JCI14120. PubMed PMID: 11748271; PubMed Central PMCID: PMC209474.
7. Yamauchi T, Kamon J, Ito Y, Tsuchida A, Yokomizo T, Kita S, Sugiyama T, Miyagishi M, Hara K, Tsunoda M, Murakami K, Ohteki T, Uchida S, Takekawa S, Waki H, Tsuno NH, Shibata Y, Terauchi Y, Froguel P, Tobe K, Koyasu S, Taira K, Kitamura T, Shimizu T, Nagai R, Kadowaki T. Cloning of adiponectin receptors that mediate antidiabetic metabolic effects. *Nature*. 2003;423(6941):762-9. doi: 10.1038/nature01705. PubMed PMID: 12802337.
8. Yamauchi T, Kamon J, Minokoshi Y, Ito Y, Waki H, Uchida S, Yamashita S, Noda M, Kita S, Ueki K, Eto K, Akanuma Y, Froguel P, Foufelle F, Ferre P, Carling D, Kimura S, Nagai R, Kahn BB, Kadowaki T. Adiponectin stimulates glucose utilization and fatty-acid oxidation by activating AMP-activated protein kinase. *Nature medicine*. 2002;8(11):1288-95. doi: 10.1038/nm788. PubMed PMID: 12368907.
9. Iwabuchi M, Yamauchi T, Okada-Iwabuchi M, Sato K, Nakagawa T, Funata M, Yamaguchi M, Namiki S, Nakayama R, Tabata M, Ogata H, Kubota N, Takamoto I, Hayashi YK, Yamauchi N, Waki H, Fukayama M, Nishino I, Tokuyama K, Ueki K, Oike Y, Ishii S, Hirose K, Shimizu T, Touhara K, Kadowaki T. Adiponectin and AdipoR1 regulate PGC-1alpha and mitochondria by Ca(2+) and AMPK/SIRT1. *Nature*. 2010;464(7293):1313-9. doi: 10.1038/nature08991. PubMed PMID: 20357764.
10. Holland WL, Miller RA, Wang ZV, Sun K, Barth BM, Bui HH, Davis KE, Bikman BT, Halberg N, Rutkowski JM, Wade MR, Tenorio VM, Kuo MS, Brozinick JT, Zhang BB, Birnbaum MJ, Summers SA, Scherer PE. Receptor-mediated activation of ceramidase activity initiates the pleiotropic actions of adiponectin. *Nature medicine*. 2011;17(1):55-63. doi: 10.1038/nm.2277. PubMed PMID: 21186369; PubMed Central PMCID: PMC3134999.
11. Rasmussen MS, Lihn AS, Pedersen SB, Bruun JM, Rasmussen M, Richelsen B. Adiponectin receptors in human adipose tissue: effects of obesity, weight loss, and fat depots. *Obesity*. 2006;14(1):28-35. doi: 10.1038/oby.2006.5. PubMed PMID: 16493120.
12. Contreras C, Gonzalez-Garcia I, Martinez-Sanchez N, Seoane-Collazo P, Jacas J, Morgan DA, Serra D, Gallego R, Gonzalez F, Casals N, Nogueiras R, Rahmouni K, Dieguez C, Lopez M. Central ceramide-induced hypothalamic lipotoxicity and ER stress

- regulate energy balance. *Cell reports*. 2014;9(1):366-77. doi: 10.1016/j.celrep.2014.08.057. PubMed PMID: 25284795.
13. Chavez JA, Holland WL, Bar J, Sandhoff K, Summers SA. Acid ceramidase overexpression prevents the inhibitory effects of saturated fatty acids on insulin signaling. *The Journal of biological chemistry*. 2005;280(20):20148-53. doi: 10.1074/jbc.M412769200. PubMed PMID: 15774472.
 14. Xia JY, Morley TS, Scherer PE. The adipokine/ceramide axis: key aspects of insulin sensitization. *Biochimie*. 2014;96:130-9. doi: 10.1016/j.biochi.2013.08.013. PubMed PMID: 23969158; PubMed Central PMCID: PMC3859861.
 15. Yang G, Badeanlou L, Bielawski J, Roberts AJ, Hannun YA, Samad F. Central role of ceramide biosynthesis in body weight regulation, energy metabolism, and the metabolic syndrome. *American journal of physiology Endocrinology and metabolism*. 2009;297(1):E211-24. doi: 10.1152/ajpendo.91014.2008. PubMed PMID: 19435851; PubMed Central PMCID: PMC2711669.
 16. Zhang QJ, Holland WL, Wilson L, Tanner JM, Kearns D, Cahoon JM, Pettey D, Losee J, Duncan B, Gale D, Kowalski CA, Deeter N, Nichols A, Deesing M, Arrant C, Ruan T, Boehme C, McCamey DR, Rou J, Ambal K, Narra KK, Summers SA, Abel ED, Symons JD. Ceramide mediates vascular dysfunction in diet-induced obesity by PP2A-mediated dephosphorylation of the eNOS-Akt complex. *Diabetes*. 2012;61(7):1848-59. doi: 10.2337/db11-1399. PubMed PMID: 22586587; PubMed Central PMCID: PMC3379648.
 17. Holland WL, Brozinick JT, Wang LP, Hawkins ED, Sargent KM, Liu Y, Narra K, Hoehn KL, Knotts TA, Siesky A, Nelson DH, Karathanasis SK, Fontenot GK, Birnbaum MJ, Summers SA. Inhibition of ceramide synthesis ameliorates glucocorticoid-, saturated-fat-, and obesity-induced insulin resistance. *Cell metabolism*. 2007;5(3):167-79. doi: 10.1016/j.cmet.2007.01.002. PubMed PMID: 17339025.
 18. Gao S, Zhu G, Gao X, Wu D, Carrasco P, Casals N, Hegardt FG, Moran TH, Lopaschuk GD. Important roles of brain-specific carnitine palmitoyltransferase and ceramide metabolism in leptin hypothalamic control of feeding. *Proceedings of the National Academy of Sciences of the United States of America*. 2011;108(23):9691-6. doi: 10.1073/pnas.1103267108. PubMed PMID: 21593415; PubMed Central PMCID: PMC3111271.
 19. Morselli E, Fuente-Martin E, Finan B, Kim M, Frank A, Garcia-Caceres C, Navas CR, Gordillo R, Neinast M, Kalainayakan SP, Li DL, Gao Y, Yi CX, Hahner L, Palmer BF, Tschop MH, Clegg DJ. Hypothalamic PGC-1alpha protects against high-fat diet exposure by regulating ERalpha. *Cell reports*. 2014;9(2):633-45. doi: 10.1016/j.celrep.2014.09.025. PubMed PMID: 25373903; PubMed Central PMCID: PMC4223650.
 20. Holland WL, Bikman BT, Wang LP, Yuguang G, Sargent KM, Bulchand S, Knotts TA, Shui G, Clegg DJ, Wenk MR, Pagliassotti MJ, Scherer PE, Summers SA. Lipid-induced insulin resistance mediated by the proinflammatory receptor TLR4 requires saturated fatty acid-induced ceramide biosynthesis in mice. *The Journal of clinical investigation*. 2011;121(5):1858-70. doi: 10.1172/JCI43378. PubMed PMID: 21490391; PubMed Central PMCID: PMC3083776.
 21. Chrast R, Saher G, Nave KA, Verheijen MH. Lipid metabolism in myelinating glial cells: lessons from human inherited disorders and mouse models. *Journal of lipid research*. 2011;52(3):419-34. doi: 10.1194/jlr.R009761. PubMed PMID: 21062955; PubMed Central PMCID: PMC3035679.
 22. Goritz C, Mauch DH, Nagler K, Pfriederger FW. Role of glia-derived cholesterol in synaptogenesis: new revelations in the synapse-glia affair. *Journal of physiology, Paris*. 2002;96(3-4):257-63. PubMed PMID: 12445904.

23. Berkseth KE, Guyenet SJ, Melhorn SJ, Lee D, Thaler JP, Schur EA, Schwartz MW. Hypothalamic gliosis associated with high-fat diet feeding is reversible in mice: a combined immunohistochemical and magnetic resonance imaging study. *Endocrinology*. 2014;155(8):2858-67. doi: 10.1210/en.2014-1121. PubMed PMID: 24914942; PubMed Central PMCID: PMC4098007.
24. Yi CX, Habegger KM, Chowen JA, Stern J, Tschop MH. A role for astrocytes in the central control of metabolism. *Neuroendocrinology*. 2011;93(3):143-9. doi: 10.1159/000324888. PubMed PMID: 21372559.
25. LeVine SM, Pedchenko TV, Bronshteyn IG, Pinson DM. L-cycloserine slows the clinical and pathological course in mice with globoid cell leukodystrophy (twitcher mice). *Journal of neuroscience research*. 2000;60(2):231-6. PubMed PMID: 10740228.
26. Gautron L, Elmquist JK, Williams KW. Neural Control of Energy Balance: Translating Circuits to Therapies. *Cell*. 2015;161(1):133-45. doi: 10.1016/j.cell.2015.02.023. PubMed PMID: 25815991.
27. Thaler JP, Yi CX, Schur EA, Guyenet SJ, Hwang BH, Dietrich MO, Zhao X, Sarruf DA, Izgur V, Maravilla KR, Nguyen HT, Fischer JD, Matsen ME, Wisse BE, Morton GJ, Horvath TL, Baskin DG, Tschop MH, Schwartz MW. Obesity is associated with hypothalamic injury in rodents and humans. *The Journal of clinical investigation*. 2012;122(1):153-62. doi: 10.1172/JCI59660. PubMed PMID: 22201683; PubMed Central PMCID: PMC3248304.
28. Kusminski CM, McTernan PG, Schraw T, Kos K, O'Hare JP, Ahima R, Kumar S, Scherer PE. Adiponectin complexes in human cerebrospinal fluid: distinct complex distribution from serum. *Diabetologia*. 2007;50(3):634-42. doi: 10.1007/s00125-006-0577-9. PubMed PMID: 17242917.
29. Neumeier M, Weigert J, Buettner R, Wanninger J, Schaffler A, Muller AM, Killian S, Sauerbruch S, Schlachetzki F, Steinbrecher A, Aslanidis C, Scholmerich J, Buechler C. Detection of adiponectin in cerebrospinal fluid in humans. *American journal of physiology Endocrinology and metabolism*. 2007;293(4):E965-9. doi: 10.1152/ajpendo.00119.2007. PubMed PMID: 17623750.
30. Une K, Takei YA, Tomita N, Asamura T, Ohru T, Furukawa K, Arai H. Adiponectin in plasma and cerebrospinal fluid in MCI and Alzheimer's disease. *European journal of neurology : the official journal of the European Federation of Neurological Societies*. 2011;18(7):1006-9. doi: 10.1111/j.1468-1331.2010.03194.x. PubMed PMID: 20727007.
31. Qi Y, Takahashi N, Hileman SM, Patel HR, Berg AH, Pajvani UB, Scherer PE, Ahima RS. Adiponectin acts in the brain to decrease body weight. *Nature medicine*. 2004;10(5):524-9. doi: 10.1038/nm1029. PubMed PMID: 15077108.

Figure 1

↓ Ceramides → Insulin Sensitivity ↑
Rich Sources of Circulating Ceramides

Rapid Equilibration

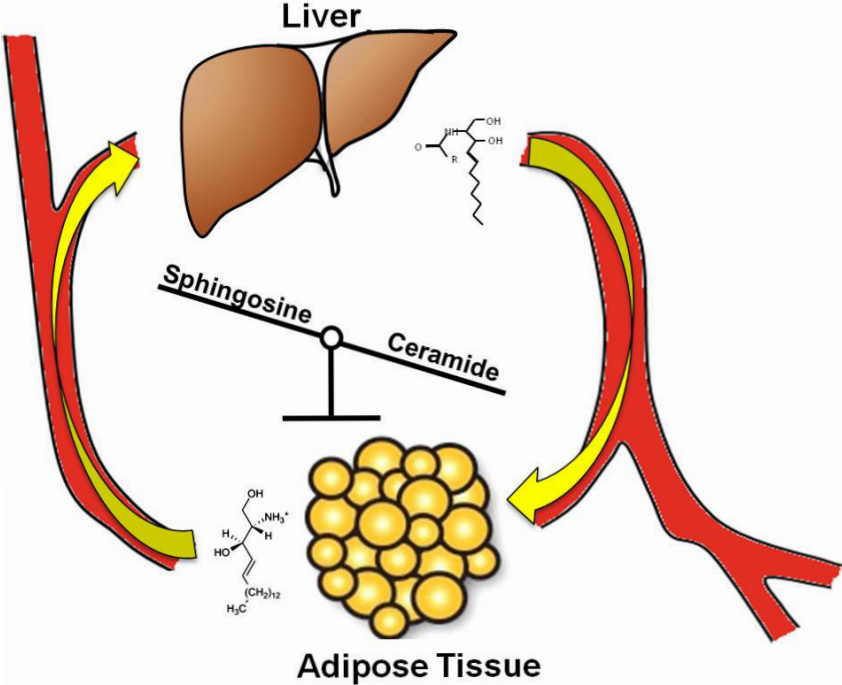


Figure 2

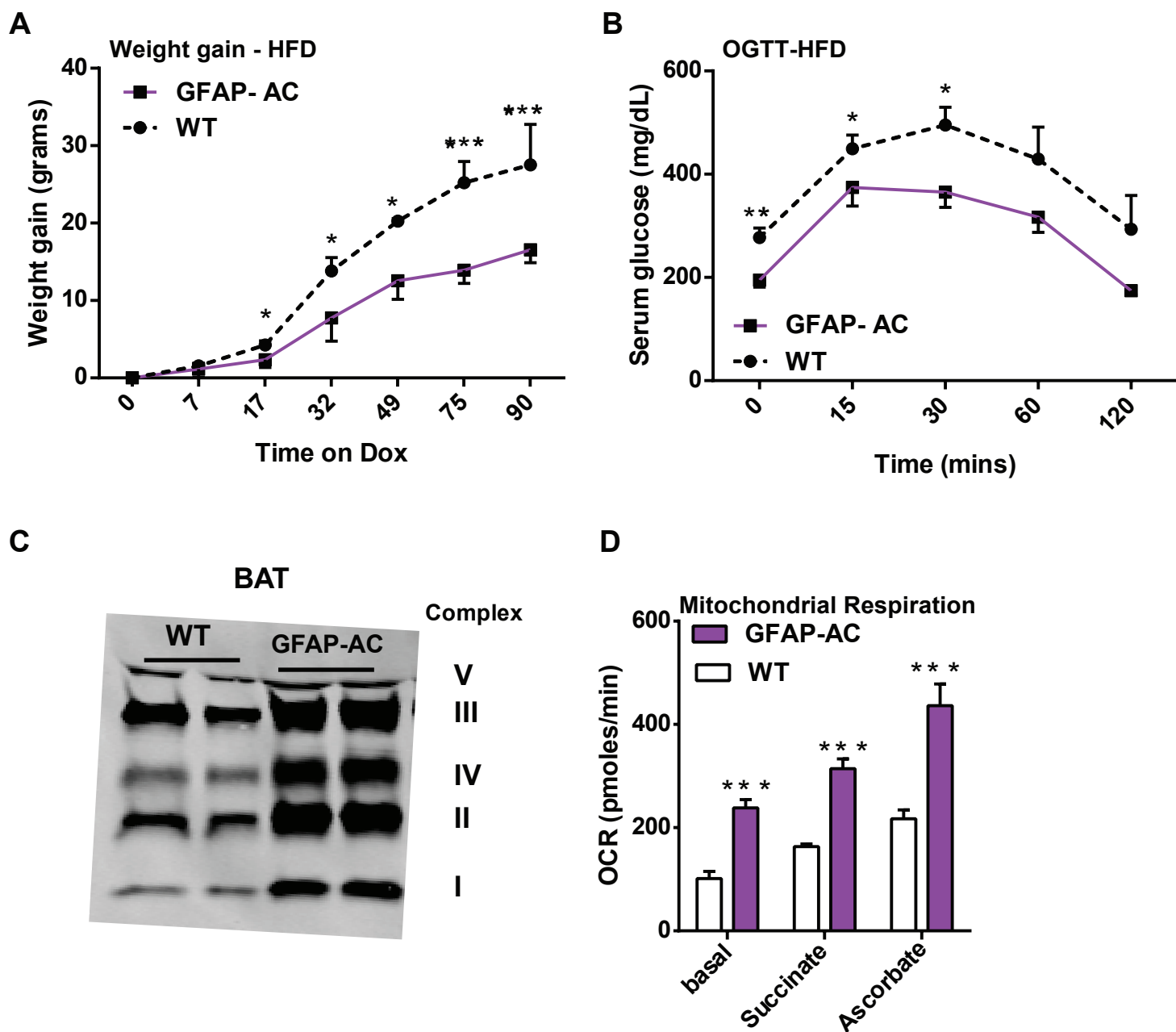


Fig. 2: Overexpression of acid ceramidase in glial cells reduces weight gain and improves glucose homeostasis in mice fed HFD. A) Weight gain in GFAP-AC mice and WT littermates during 3 months of HFD-dox. **B)** Circulating glucose levels were measured during an oral glucose tolerance test (OGTT) (2.5 g/kg glucose per oral gavage) in GFAP AC and WT mice. **C)** Representative immunoblots of mitochondrial complexes in BAT of GFAP-AC and WT mice after 3 months of HFD-Dox. **D)** Oxygen consumption rate of mitochondrias isolated from BAT of GFAP-AC and WT mice after 3 months of HFD-Dox. * $P < 0.05$, ** $P < 0.01$, *** $P < 0.001$ by students t test.